


1-1-2011

The Role Of Zip Superfamily Of Metal Transporters In Chronic Diseases, Purification & Characterization Of A Bacterial Zip Transporter: Zupt.

Iryna King
Wayne State University

Follow this and additional works at: http://digitalcommons.wayne.edu/oa_theses

 Part of the [Biochemistry Commons](#), and the [Molecular Biology Commons](#)

Recommended Citation

King, Iryna, "The Role Of Zip Superfamily Of Metal Transporters In Chronic Diseases, Purification & Characterization Of A Bacterial Zip Transporter: Zupt." (2011). *Wayne State University Theses*. Paper 63.

This Open Access Thesis is brought to you for free and open access by DigitalCommons@WayneState. It has been accepted for inclusion in Wayne State University Theses by an authorized administrator of DigitalCommons@WayneState.

**THE ROLE OF ZIP SUPERFAMILY OF METAL TRANSPORTERS
IN CHRONIC DISEASES,
PURIFICATION & CHARACTERIZATION
OF A BACTERIAL ZIP TRANSPORTER:
ZUPT**

by

IRYNA KING

THESIS

Submitted to the Graduate School

of Wayne State University,

Detroit, Michigan

in partial fulfillment of the requirements

for the degree of

MASTER OF SCIENCE

2011

**MAJOR: BIOCHEMISTRY &
MOLECULAR BIOLOGY**

Approved by:

Advisor

Date

© COPYRIGHT BY

IRYNA KING

2011

All Rights Reserved

DEDICATION

I dedicate this work to my father,

Julian Banas,

whose footsteps I indisputably followed into science

&

my every day inspiration, my son, William Peter King

ACKNOWLEDGMENTS

First and foremost I would like to thank the department of Biochemistry & Molecular Biology at Wayne State University School of Medicine for giving me an opportunity to conduct my research and be a part of their family. I would like to thank my advisor Dr. Bharati Mitra for taking me into the program and nurturing a biochemist in me. Majority of what I have learned about protein purification and characterization came from you and being a part of your lab. I will forever be grateful. I would like to thank Dr. Jianjun Wang and Dr. Timothy L. Stemmler for being a part of my committee and guiding my research to the finish line. I am grateful to all of the professors whom I have encountered during my time at Wayne State: thank you all for sharing your knowledge and expertise and contributing to the individual and scientist that I have become over the last few years.

I would like to thank Dr. David Oupicky for admitting me to the Department of Pharmaceutical Sciences of Wayne State University and allowing me to start my M.S. career at his lab. You are one of the few who have always supported your students' ideas and personal aspirations. I have always admired that about you. I would also like to thank everyone who has supported me financially throughout this degree. Starting with Dr. Xiangyi Lu, at the Institute of Environmental Health Sciences of Wayne State University, who insisted that I join department of Biochemistry and Molecular Biology. From the bottom of my heart I would like to thank Dr. Kezhong Zhang, at the Center for Molecular Medicine and Genetics of Wayne State University School of Medicine, who employed me during my last semester here. Your lab is one of the most result-driven, peaceful, and learning environments I have ever been a member of. I wish all the best of research luck to both of the labs and all the people who work there.

I would like to thank and hug all of my past and current lab members from my BMB, PSC, and CMMG families who have stood by me throughout my time at Wayne State University. Special thanks go to Dr. Ashoka Shyamalee Kandegedara and Dr. Sandhya Muralidharan for teaching me all the practical knowledge and helping me start this project. Many thanks to Dr. Dhaval Joshi who has not only been my friend but also my right hand around the lab. I would like to thank Sara Jaleel, Gargi Mahapatra, Anamika Chaudhary and Walid Ali Hammoud for their friendships and help around the lab. I would like to thank Sudipa Ghimire, who has been working on her M.S. along-side with me at BMB, for suggesting the protein expression optimization protocol and Victoria Murray and Dr. Wang's lab for developing it. Special thanks to Dr. Maik Hüttemann, at the Center for Molecular Medicine and Genetics of Wayne State University School of Medicine, for his inspirational teachings and encouragement. I wish you all the best of success in your careers. Hopefully our paths will cross again one day.

I would like to thank all my family and friends who have always pointed out the light at the end of the tunnel. Roberto Mendez, for being a great friend and helping me during the last stages of this project. Mark Andrew Johnson, for studying for the GRE, for the friendship, and for holding me emotionally grounded throughout the years. I wish you both the best of luck in pursuing your Ph.D.s. I would like to thank my dad for the emotional and financial support throughout my university career. I would like to thank everyone at my dad's house for helping care for my son while science had me by my ears. Finally, I would like to thank my husband, Richard Daniel King Jr., who stood by me through thick and thin, took care of our son days and nights without end, and allowed me to pursue my career. I forever owe you.

As someone dear to me said, “it’s not always about the destination, it’s about the journey...” and thanks to you all I had one hell of a journey.

TABLE OF CONTENTS

Dedication.....	ii
Acknowledgments.....	iii
List of Tables.....	ix
List of Figures.....	x
Chapter 1: Introduction.....	1
1.1 What are <i>ZIP</i> transporters?	3
1.2 <i>ZIPs</i> vs. <i>ZnTs</i>	4
1.3 Importance of <i>ZIP</i> family in plants.....	5
1.4 Roles of <i>ZIPs</i> in bacterial infections.....	12
1.5 Expression of <i>ZIPs</i> and <i>ZnTs</i> in human body with respect to Zn imbalance.....	17
1.5.1 Asthma linked to Zn deficiency.....	17
1.5.2 The role of Zn deficiency in Diabetes.....	20
1.5.3 Link between Zn & Alzheimer's disease.....	24
1.6 <i>ZIP</i> 's structures & their metal-binding implications.....	26
1.6.1 Biochemical Characteristics of the <i>ZIP</i> family.....	28
1.7 What is known about ZupT?.....	39
Chapter 2: Experiments, Results & Discussion.....	44
2.1 Goal.....	44
2.2 Materials.....	44
2.3 Methods.....	45

2.3.1	Construction of ZupT/pBAD/mycHis-P with a Precision Protease site.....	45
2.3.2	Creation of ZupT/pBAD/mycHis-C mutants.....	46
2.3.3	Optimization of ZupT expression.....	48
2.3.4	Purification of ZupT.....	49
2.3.5	Characterization of ZupT using Fluorescence Spectroscopy.....	50
2.3.6	Characterization of ZupT with UV-Visible spectroscopy.....	51
2.3.7	Obtaining metal binding stoichiometry with ICP-MS.....	51
2.4	Results.....	52
2.4.1	ZupT sequence analysis.....	52
2.4.2	Optimizing ZupT expression.....	53
2.4.3	ZupT purification.....	55
2.4.4	ZupT characterization.....	56
2.4.4.1	Titration of fluorescence emission of ZupT with Cd.....	56
2.4.4.2	Titration of fluorescence emission of ZupT with Fe.....	59
2.4.4.3	UV-Visible spectroscopy study with Fe.....	63
2.4.4.4	Titration of fluorescence emission of ZupT with Pb.....	66
2.4.4.5	Titration of fluorescence emission of ZupT with Zn.....	69
2.4.4.6	ICP-MS metal binding stoichiometries.....	72
2.5	Discussion.....	73
2.6	Future Direction.....	77
	Appendix A: ZupT purification procedure.....	79
	Appendix B: ZupT characterization with Fluorescence spectroscopy.....	83

Appendix C: ZupT characterization with UV-Visible spectroscopy.....	84
Appendix D: Obtaining metal binding stoichiometry with ICP-MS.....	85
References.....	86
Abstract.....	106
Autobiographical Statement.....	108

LIST OF TABLES

1.1	Proposed specificity and location of <i>ZIP</i> family metal transporters in plants.....	7
1.2	Expression of <i>ZIPs</i> and <i>ZnTs</i> in disease pathologies due to Zn imbalance.....	19
1.3	Comparison between mouse and human Slc39A8, (<i>ZIP8</i>), and Slc39A14, (<i>ZIP14</i>), genes.....	37
1.4	Properties of the mouse <i>ZIP8</i> and <i>ZIP14</i> proteins.....	38
2.1	ZupT Site-Directed Mutagenesis Primers.....	47
2.2	ICP-MS ZupT/pBAD/mycHis-P metal binding stoichiometries.....	72

LIST OF FIGURES

1.1	Summary of proposed transition metal transporters identified in plants thus far.....	8
1.2	The battle for transition metals between the host and bacteria.....	16
1.3	Zinquin staining of a section of mouse pancreas.....	21
1.4	The outcome of the interaction between diet and allelic variations of genes controlling Zn fluxes on the balance between health and disease.....	23
1.5	Topological model of SLC39 proteins.....	28
1.6A	Sequence alignment of the mouse and human <i>ZIP1</i> transmembrane domains 1-8.....	30
1.6B	Sequence alignment of the mouse and human <i>ZIP2</i> transmembrane domains 1-8.....	31
1.6C	Sequence alignment of the mouse and human <i>ZIP3</i> transmembrane domains 1-8.....	32
1.7	Conservation within the fourth transmembrane domain revealed a subfamily of mammalian <i>ZIP</i> proteins.....	33
1.8	Phylogenetic tree of the 14 mouse <i>ZIP</i> domains of the Slc39 gene-encoded proteins.....	34
2.1	ZupT subcloned from pBAD/mycHis-C into pBAD/mycHis-P with an addition of a Precision Protease site.....	45
2.2	Two homologically-conserved regions in ZupT.....	52
2.3	Western blot comparison of ZupT expression before 1 st selection.....	53
2.4	Resulting colonies from 1 st and 2 nd selections compared on a 12% SDS gel.....	54
2.5	SDS gels with fractions obtained during ZupT/pBAD/mycHis-P purification: (A) a 12% SDS gel and (B) a 15% SDS gel.....	55
2.6	300-500 nm emission spectrum of ZupT/pBAD/mycHis-P with Cd.....	56
2.7	300-400 nm emission spectrum of ZupT/pBAD/mycHis-P with Cd.....	57
2.8	Fluorescence study 330.9 nm peak analysis: Fluorescence vs. [Cd] (uM).....	58
2.9	300-500 nm emission spectrum of ZupT/pBAD/mycHis-P with Fe.....	59

2.10A	300-400 nm emission spectrum of ZupT/pBAD/mycHis-P with ↓ [Fe].....	60
2.10B	300-400 nm emission spectrum of ZupT/pBAD/mycHis-P with ↑ [Fe].....	61
2.11	Fluorescence study 330.9 nm peak analysis: Fluorescence vs. [Fe] (uM).....	62
2.12	10uM ZupT/pBAD/mycHis-P UV-Vis absorbance peak.....	63
2.13	Fe UV-Vis peak minus the ZupT/pBAD/mycHis-P absorbance peak.....	64
2.14	UV-Vis 329.6 nm peak analysis: Absorbance vs. [Fe] (uM).....	65
2.15	300-500 nm emission spectrum of ZupT/pBAD/mycHis-P with Pb.....	66
2.16	300-400 nm emission spectrum of ZupT/pBAD/mycHis-P with Pb.....	67
2.17	Fluorescence study 330.9 nm peak analysis: Fluorescence vs. [Pb] (uM).....	68
2.18	300-500 nm emission spectrum of ZupT/pBAD/mycHis-P with Zn.....	69
2.19	300-400 nm emission spectrum of ZupT/pBAD/mycHis-P with Zn.....	70
2.20	Fluorescence study 330.9 nm peak analysis: Fluorescence vs. [Zn] (uM).....	71

CHAPTER 1

INTRODUCTION

Zinc (Zn) is ubiquitous. It is an essential micronutrient in all living cells. In mammals Zn is the second most abundant essential trace metal. This transition metal is a component of many metalloproteins and thus functions either as a co-factor for many metallo-enzymes or as a structural element for Zn-finger or ring-finger proteins (10, 91). Since Zn^{2+} is a small, hydrophilic, and a highly charged ion, it cannot be transported across the plasma or intracellular organelle membrane by passive diffusion. In excess Zn can be toxic and its regulation is vital in any organism. Zn is regulated with the help of chelators and a number of different Zn transporter proteins which help uptake and distribute it around the cell (26, 35, 77). Different types of cells require a different constant concentration of Zn at all times. Presence of excess free Zn ions can be toxic to the cell. All cells must have tightly regulated homeostatic mechanisms in order to preserve healthy levels and proper compartmentalization of Zn. This is accomplished through the actions of specialized proteins that facilitate Zn uptake, efflux and compartmentalization (28, 125). If the integrity of genes responsible for maintenance of Zn homeostasis is compromised by mutations or polymorphisms, this will likely result in complex genetic variations and even sensitivity to dietary Zn in health and disease.

Zn plays fundamental housekeeping role in physiology, cellular metabolism and gene expression. It is necessary for stabilization of thousands of protein domains and is required as a catalytic cofactor of more than 300 enzymes (145, 11, 10). Recent global searches within the human genome estimated that about 10% of the human proteome consists of potential Zn-binding proteins (3). Thus, it is clear why a large number of biological processes are dependent

on Zn homeostasis. Finally, an imbalance of Zn homeostasis has complex implications in a human body and can ultimately contribute to the onset of chronic pathologies (157, 118).

By consumption of meat and other sources of animal proteins, humans can obtain their Recommended Daily Allowance (RDA) of Zn, which is 12–15 mg/day. Animal proteins have high Zn content and the metal is already bound to ligands, which facilitate its absorption. Alternative sources of Zn include sea-foods, dairy products, cereals and even nuts (73). Unfortunately, majority of vegetables are not ready sources of Zn because of the presence of phytate, abundant in legumes and cereals. Phytate is known to chelate metal ions and inhibit their absorption (78). Therefore, diets low in animal proteins but rich in phytate contribute to the high incidence of mild–moderate Zn deficiency in developing countries (33). Although, even individuals feeding on a balanced diet may also undergo suboptimal intake of Zn as result of specific physiological status. This could be evident during pregnancy or acute inflammation (Table 1.2) (33). Human brain, being a mystery that it is, still has not been fully investigated for expression of all known members of *ZIP* and *ZnT* families.

Based on their structural and functional features human Zn transporter proteins have been grouped into two families: Solute Carrier Family 39A (SLC39A), which includes mammalian ZRT/IRT-related proteins (*ZIPs*), and Solute Carrier Family 30A (SLC30A), which comprises mammalian *ZnTs* (28, 125, 28). These two transmembrane families of Zn transporters are believed to have opposite roles in cellular Zn homeostasis. Both *ZIPs* and *ZnTs* contain a high content of lipophilic amino acids (33). While *ZnT* transporters reduce the cytoplasmic Zn by promoting export of Zn out of the cell or sequestration of Zn into subcellular compartments during cellular Zn abundance, *Zip* transporters' function is to increase the cytoplasmic Zn

concentration by enhancing Zn uptake or release of the stored Zn from subcellular compartments to the cytoplasm of the cell when Zn is deficient (19, 27, 47, 69, 70, 81, 82, 94, 95, 104, 121, 122, 126, 134, 136, 137, 151, 152). Thus far, fourteen members of *Zip* family and ten members of the *ZnT* family have been identified through mouse and human genome analyses (68, 33). The fourteen *ZIP*-encoding genes that have been identified in the human genome have been grouped into four sub-families according to the molecular features of the encoded proteins. Furthermore, amongst these Zn transporters, seven *Zip* proteins (*Zip*1-7) and eight *ZnT* proteins (*ZnT*1-8) have been functionally characterized. Even though the role of *ZIP* transporters in humans, mice, and bacteria, including their contribution to overall metal-homeostasis and their mechanism of action, is not well understood, this defect in metal transport has been associated with numerous diseases (130, 146, 104). For instance, mutations in two Zn transporters have been linked to the Zn deficiency diseases acrodermatitis enteropathica (*ZIP*4) in humans and lethal milk syndrome (*ZnT*4) in mice (146, 104).

In *E.coli*, the uptake of Zn is mediated by two major types of transporters: *ZnuACB*, which belongs to the cluster C9 family of (TroA-like) ATP-binding cassette (ABC) transporters, and *ZupT*, which is a member of the *ZIP* family of transporters (80, 84). *ZupT* is a broad substrate spectrum metal permease whose exact mechanism of action is currently unknown, but it has been proposed that it may involve a chemiosmotic transmembrane gradient (55).

1.1 What are *ZIP* transporters?

Maintaining metal homeostasis is one of the primary goals for organisms found throughout biology. In eukaryotes this is partly achieved by *ZRT/IRT*-like protein (*ZIP*) superfamily of metal transporters (30, 115). This superfamily has derived its name from some of

its first identified members (*ZRT*, *IRT*-like protein) (115). It was originally believed that these transporters only transported iron or zinc (115). They were also shown to transport cadmium and manganese (42, 43, 90, 129). In fact, the first identified member of this family, which was Iron-regulated transporter-1 (*Irt1*), from *Arabidopsis*, while selectively binding and importing iron was also able to mediate transport of cadmium, manganese, and zinc (42, 43, 91, 129). Two other members of this family were identified in yeast. These were Zn-regulated transporter-1 (*Zrt1*) and *Zrt2*, which are involved in yeast's Zn uptake (72, 71). Altogether, around 85 *ZIP* family members have been identified from bacteria, archaea and different eukaryotes, plus 15 genes in *Arabidopsis* (113). Amino acid sequences alignment groups *ZIPs* into four sub-families, even though all of the higher plant genes seem to fall into a single group (113).

1.2 *ZIPs* vs. *ZnTs*

In order to maintain a healthy homeostasis of such essential metals like Zn, mammals have been equipped with the Zn transporter (*ZnT*) family of proteins. *ZnT* family of proteins is believed to have an opposite role on Zn homeostasis when compared to the *ZIP* family. While all of the *ZIP* proteins mediate Zn uptake from the extracellular environment or intracellular vesicles into the cytoplasm, proteins belonging to the *ZnT* family are accountable for Zn efflux from the cytoplasm towards either intracellular vesicles or/and the extracellular space, as well as for Zn delivery to precise metalloproteins (81, 76). *ZnT* family of proteins is unique in a way that its members function in a tissue-, cell-, and organelle-specific manner in order to maintain the levels of Zn in check (94). Due to the importance of these metal transporters, it is no wonder that there have been ten of the members of *Znt* family identified in mammals. Unlike *ZIP* family proteins, which have eight transmembrane domains, these encompass six predicted

transmembrane domains and thus are believed to function as multimers. Finally, Zn is the key regulator to the gene expression of *Znt1*, while dietary Zn controls the mRNA levels of *Znt1* and *Znt2* in liver, intestines, and kidneys (97, 108).

1.3 Importance of ZIP family in plants

For healthy growth and development plants require transition metals like Zn, Fe, Cu, and Mn. These are acquired from the soil and distributed around the plant depending on their needed concentrations within the different cells and organelles. In excess, the same metals can be toxic to the cell if proper regulatory mechanisms are not in place to regulate their concentrations (5). The membrane transport systems responsible for regulation of metal concentrations in plants include the ZIP family, the heavy metal (or CPx-type) ATPases (HMAs), the natural resistance-associated macrophage proteins (Nramps), the cation diffusion facilitator (CDF) family, and the cation antiporters (115, 155, 51). In the last decade our knowledge of these transporter families has increased drastically. A summary of ZIP family members contributing to plants' metal homeostasis, their metal specificity and tissue localization is outlined in Table 1.1. Their proposed membrane localization on the other hand can be found in Figure 1.1. Overall, possible transporters of all essential metals, besides Mo, have been proposed thus far (79).

Not surprisingly, as seen in Table 1.1, ZIPs are for the most part expressed within the roots of the plants and their metal specificity encompasses such metals like Zn, Fe, Cd, and Mn. Two of them, LeIRT1 and LeIRT2, are proposed to have a broad range of metal specificity. Even though IRT1 preferentially transports Fe, it has also been shown to transport Mn, Cd, and Zn (42, 43, 90, 129). Interestingly, most essential metals have at least two gene families with specificity for its transport. For instance, Fe can be transported by ZIPs and Nramps, while Zn is a substrate

for *ZIPs* and *CDFs*. Furthermore, when compared to yeast that only has 3 *ZIP* genes, *Arabidopsis* has a shocking 15 *ZIP* genes. Some of these transporters are possibly involved in active efflux while others in influx (153). This also contributes to the differences apparent in their affinities for different metals. Whereas majority of *ZIP* proteins transport Zn, another reason for existence of multiple *zip* genes in any given organism could be that they may differ in the metals that they transport in the biological context of a given organism (94). To cope with varying metal availabilities both high and low affinity mechanisms are needed, which is the case in yeast (34, 147). As seen in Figure 1.1, it takes a large number of different genes, including *ZIPs*, to facilitate both uptake and efflux mechanisms in plants in order to provide responses to a variety of environmental stress conditions.

Table 1.1 Proposed specificity and location of *ZIP* family metal transporters in plants (79)

Name	Family members in <i>A. thaliana</i>	Proposed specificity	Cellular location	Main tissue expression
ZIP	15			
IRT1		Fe, Zn, Mn, Cd	PM	Roots
IRT2		Fe, Zn		Roots
OsIRT1		Fe		Roots
LeIRT1		Fe (broad?)		Roots
LeIRT2		broad?		Roots
TcZNT1		Zn, Cd		Roots, shoots
TcZNT2		–		Roots
ZIPs1-3		Zn		Roots
ZIP4		Zn	Plastids	Roots, shoots
GmZIP1		Zn	Peribacteroid membrane	Root nodules

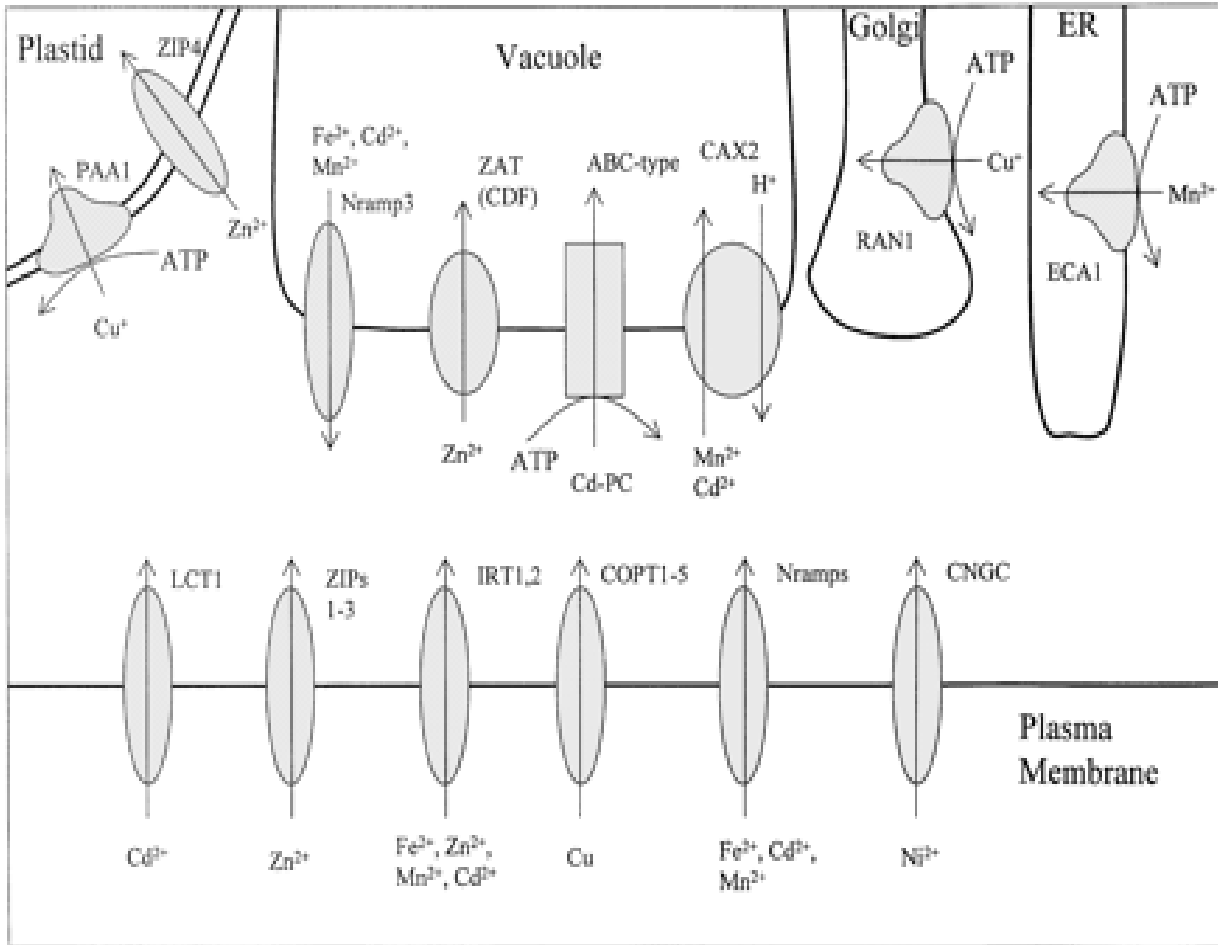


Figure 1.1

Summary of proposed transition metal transporters identified in plants thus far

Membrane localization of some of these transporters, especially those at the plasma membrane is yet to be confirmed (79).

Plants require Fe for their normal growth and development. Unfortunately, Fe is often difficult to obtain from the soil due to its low solubility. Therefore, plants have evolved two mechanisms to conquer this problem (65, 138). Strategy II is utilized by grasses, which secrete phytosiderophores that chelate Fe^{3+} after which the complex is absorbed through the roots. Though, majority of plants depend on Strategy I that involves using reductive mechanism in order to mobilize Fe^{3+} . By acidifying the soil, plants reduce ferric ions through a plasma membrane-located Fe^{3+} chelate reductase. Roots then absorb the ferrous ions with the help of a Fe^{2+} transporter.

As mentioned earlier, AtIRT1, the first member of the ZIP family to be identified, was cloned from *Arabidopsis* via functional complementation of an iron-uptake-deficient yeast mutant (*fet3 fet4*) (42, 79). In roots, *IRT1* is believed to be the main transporter for high affinity Fe uptake (21, 150). At Fe-deficient conditions, after 24 hours *IRT1* mRNA is detectable (21). In addition, *IRT1* mRNA and protein levels peak after 72 hours, while its mRNA and protein remain undetectable 12 hours after shifting back to Fe-adequate conditions (21). Interestingly, under Fe-scarce conditions, plants overexpressing *AtIRT1* are also found to accumulate elevated concentrations of Cd and Zn than their wild type counterparts (21). This discovery was also supported by transport studies done in yeast (42, 90). Also, as seen in the *T. caerulescens* ecotype Ganges, the uptake of Cd but not Zn was drastically improved by Fe deficiency, and this might have resulted due to an increase of *TcIRT1-G* mRNA in root tissues (110).

A knockout of *IRT1*, created in *Arabidopsis*, showed severe growth defects and was chlorotic, although application of exogenous Fe was able to rescue the condition (150). The protein was found to localize to the plasma membrane, and during Fe-deficient conditions it was

mainly expressed in the root's external layers. In addition, *IRT1* mutants showed major changes in their photosynthetic efficiency and developmental defects were noted which were believed to be consistent with Fe transport/deficiency (62, 148). Surprisingly, during Fe deficiency *AtIRT2* is also expressed in root epidermal cells (12). Yet, it was unable to substitute the loss of *IRT1* (120). It also seems to have a higher specificity for its substrates: while it was reported to complement Fe and Zn uptake mutants it was unable to transport Cd or Mn in yeast (149). Overall, these two transporters might have different functions in *Arabidopsis*.

These *ZIP* family transporters have also been identified and studied in tomatoes. Here, for the most part, they are expressed in roots (40). Also as seen before, *LeIRT1*, but not *LeIRT2*, was robustly enhanced by Fe deficiency and it was up-regulated by P and K deficiencies in the root medium (153). In rice, *OsIRT1*, with a high homology to the *AtIRT1* gene of *Arabidopsis*, just like in tomatoes was also highly expressed in roots and was induced by Fe-deficiency and additionally by Cu-deficiency (12). These results have an implication of a possible co-regulatory mechanism for some essential minerals' transporter genes.

Yeast complementation studies have contributed greatly to our understanding of the functional properties of plant *ZIP* transporters. It was reported that *ZIP* transporters 1–3 from *Arabidopsis* are able to restore Zn uptake to yeast Zn uptake mutants *zrt1 zrt2*; and thus were projected to influence transport of Zn (58, 115). In Zn-deficient plants, *ZIPs* 1, 3 and 4 were expressed in the roots, while *ZIP4* was additionally found in the shoots and is expected to have a chloroplast-targeting sequence (58, 115). In yeast, *ZRT1* was reported to be a high affinity Zn transporter, which is glycosylated and expressed at the plasma membrane (34). *ZRT2*, on the other hand, was reported to be a low affinity Zn transporter (115). Furthermore, another *ZIP*

homologue found in yeast, ZRT3 was reported to be involved in the mobilization of stored Zn from the vacuole (112). Similarly, *TcZNT1*, from the Zn/Cd-hyperaccumulating plant, *Thlaspi caerulescens* was shown to facilitate high-affinity Zn uptake and low-affinity Cd uptake after expression in yeast (123). High levels of *TcZNT1* were expressed in root and shoot of *T. caerulescens*, meanwhile overexpression of this transporter due to a change in Zn concentration resulted in amplified Zn influx in the roots (6). Finally, it was reported that *TcZNT1* and *TcZNT2* were mostly expressed in roots, but their expression was not associated with Zn availability (6). Unlike in *T. caerulescens*, in the non-hyperaccumulator *T. arvense*, *TcZNT1* and *TcZNT2* were shown to be exclusively expressed during Zn deficiency (6).

One of the members of the *ZIP* family, *GmZIP1*, has now been identified in soybean (117). According to functional complementation studies, of the *zrt1 zrt2* yeast cells, *GmZIP1* is greatly selective for Zn (117). It was also reported that yeast Zn uptake was inhibited by Cd (118). Unlike the previously mentioned *ZIP* genes, *GmZIP1* was specifically expressed in the nodules and not in roots, stems or leaves (117). Moreover, its protein was localized to the peribacteroid membrane, which implicates a possible role in the symbiosis (117).

Overall, the proposed role of *ZIP* transporters in Zn nutrition is well supported by the characterization of homologues from different species (37). Studying the above discussed metal transporter families in plants is crucial to humans. The knowledge elucidated can be useful in genetic modification of certain species, either to improve the metal quality of crops for human and animal nutrition or for the purposes of phytoremediation, which is a technology that uses plants to remove toxic elements from soil.

1.4 Roles of ZIPs in bacterial infections

Integrity of the bacterial cell envelope is crucial for a large number of fundamental physiological processes. These include nutrient uptake, cell wall synthesis, signal transduction, motility, energy generation, protein folding and secretion. It has been shown that all of the *ZIP* proteins mediate Zn uptake from the extracellular environment or intracellular vesicles into the cytoplasm (28). It has also been shown that in mammals Zn has an important immunomodulatory function and is absolutely critical for innate and acquired immunity (111). Furthermore, after exposure to lipopolysaccharide (LPS) Zn levels decrease in the serum and Zn accumulates in the liver (109). Even though Zn concentrations are estimated to be in the millimolar concentrations within host cells, available Zn might be unattainable to bacterial pathogens and/or significantly reduced after activation of innate immune defenses (2, 111). Unfortunately, *Znu*, the high-affinity Zn uptake system tends to mask the action of ZupT (132, 130). According to the recent studies, a role in pathogen fitness for ZupT, along with ZnuABC, during urinary tract infection was found in mice (130).

In order to protect themselves from intracellular pathogens, infected vertebrates perform sequestration of extracellular Zn, but they also decrease their cellular Zn concentrations (22, 111). The bacteria are engulfed into phagosomes, by phagocytic and antigen presenting cells of the immune system, which unite with lysosomes that contain antimicrobial factors. Macrophages and IFN- γ stimulated T cells are known to express *ZIP8* (8, 7). When T cells are stimulated, *ZIP8* associates with the lysosomal protein Lamp1, which suggests a possible association with the lysosome (7). Additionally, it was shown that in transfected human embryonic kidney cells *ZIP8* is also found associated with lysosomes (8). Since *ZIP8* is a member of ZRT/IRT family it

was no surprise that the initial studies showed that it is possibly capable of transporting Zn (8). Furthermore, it has been determined that T cells decrease lysosomal Zn levels upon activation of cells overexpressing *ZIP8*, while there is an increase of cytosolic Zn levels (8, 7). The above suggests that *ZIP8* is positioned to transport Zn from the lysosome into the cytoplasm, which in turn disrupts zinc-dependent bacterial processes.

Decreasing lysosomal Zn levels is not sufficient, thus vertebrates also reduce their cytoplasmic Zn levels in order to combat a bacterial infection. When dendritic cells are stimulated with lipopolysaccharide, a decreased expression of *ZIP* importers is observed along with subsequently an increased expression of *ZnT* Zn exporters (116, 87). As a result, cytosolic Zn levels are decreased (111, 116, 87). It is unknown if this alteration of Zn concentration affects the invasive pathogens. It has been shown that alteration of Zn levels has an impact on dendritic cell maturation and activation, as well as on T-cell development (156, 7, 116, 87). This makes it rather impossible to determine the role of modified Zn concentrations on virulence and microbial growth.

It is for certain that a decreased level of Zn can lead to a disruption of a large number of bacterial processes which would impact the pathogen's ability to infect the host. Bacteria incorporate Zn into approximately 4–6% of all proteins (4). This essential metal is exploited in control of bacterial gene expression, for cellular metabolism, and as a cofactor of bacterial virulence factors. For instance, the iron responsive regulator Fur, alcohol dehydrogenases, lyases, hydrolases, and Cu/Zn superoxide dismutases are all bacterial proteins that utilize Zn (88, 11). In order to overcome Zn sequestration, bacteria express high affinity Zn transporters. At the minimum there are two kinds of Zn uptake systems that are used by bacteria. Most common one

is homologous to the high affinity ZnuABC transport systems, which are found in *E. coli* (84). In general, these Znu-like systems have been associated in a number of Gram-negative and Gram-positive bacteria (84). Additional system of Zn transporters resembles the eukaryotic ZIP family transporters, even though its homologs have only been found in *E. coli* (84).

Worthy of mention is that bacterial Zn and Mn transporters are both a part of the cluster 9 family of ABC transporters (84). This similarity complicated the identification of a transported substrate. Examples of this include the metal binding protein PsaA from *Streptococcus pneumonia* that has been shown to transport Mn in vivo although it contains Zn-coordinating histidine and aspartic acid residues, which are highly conserved between Zn transporters (84, 98). Additional example is TroA, a component of the *Treponema pallidum* TroABC transport system, which is homologous to the Mn binding protein MntA from *Bacillus subtilis* and therefore was expected to transport Mn. Unfortunately, crystallographic studies along with heterologous expression in *E. coli* propose that TroA is a Zn transporter instead (84, 101, 59). It is sometimes difficult to predict a correct substrate for a given transporter, thus only careful biochemical studies could show the true colors for all of these metal transporters.

On the other hand, inactivation of ZnuABC transport systems in quite a few bacterial pathogens, including *Campylobacter jejuni*, *Salmonella enterica*, *Haemophilus ducreyi*, *Uropathogenic E. coli*, *Brucella abortus*, and *Streptococcus pyogenes* results in decreased virulence/colonization of bacteria (29, 2, 103, 130, 13, 154, 86). Other mechanisms for overcoming Zn sequestration could exist. At the end, more studies need to be conducted in order to characterize Zn acquisition systems in bacteria as well as to understand the role of Zn sequestration of the host and its impact on bacteria.

In addition to sequestering Zn, as a defense mechanism against bacterial invaders, vertebrates also sequester Fe and Mn (41, 144, 22). Figure 1.2 below depicts the proposed current model for the battle between invertebrates and bacterial pathogens for non-iron nutrient metals. New discoveries show a possibility that nutritional immunity might include other essential transition metals like copper or nickel. Along with high affinity transport systems, bacterial pathogens might express siderophore-like molecules to mediate the acquisition of non-iron transition metals. This was observed in methanotrophs in which methanobactin assists copper acquisition through mechanisms similar to siderophore-mediated iron capture (124). Just like with Zn sequestration, further investigation is needed to entirely understand the battle for transition metals between the host and bacteria. Furthermore, studying acquisition of non-iron transition metals could provide useful information about the bacterial physiology which in turn could be useful in development of new therapeutics.

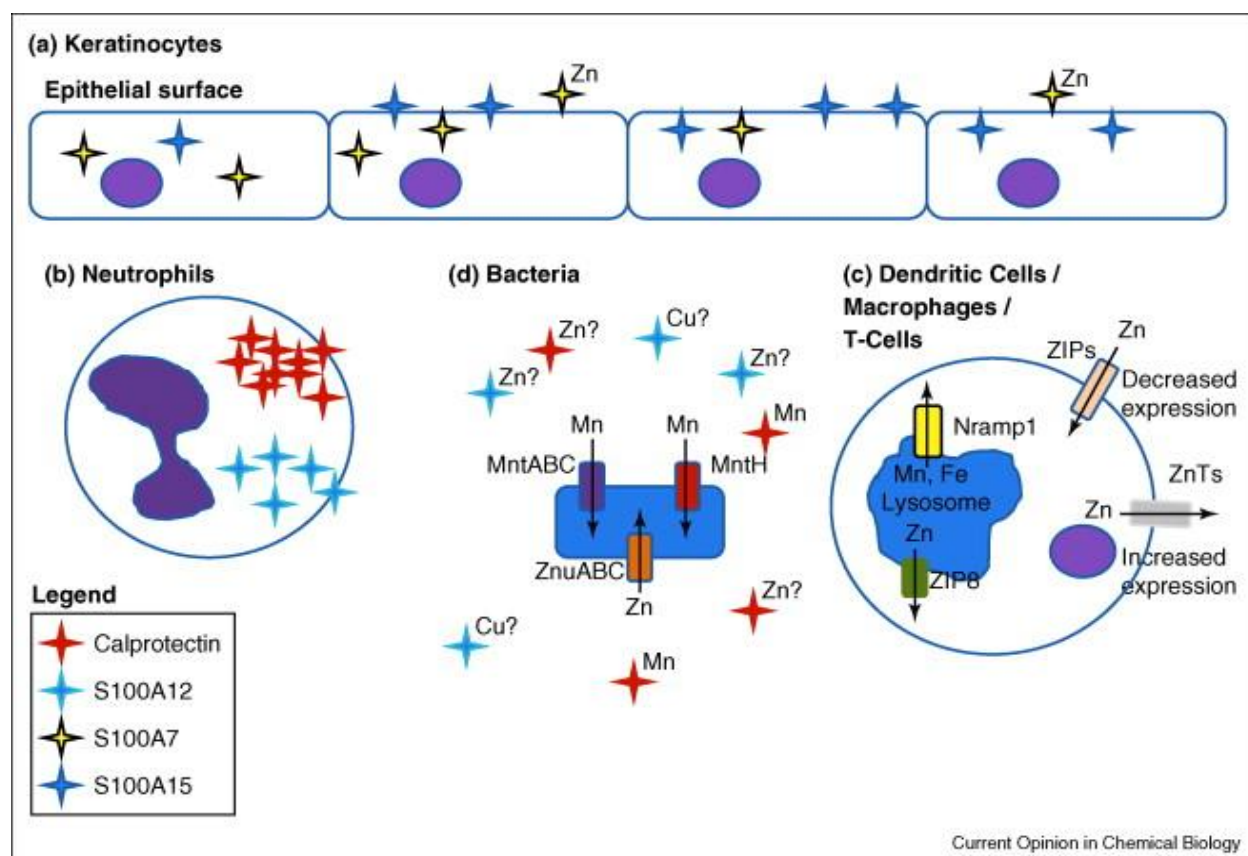


Figure 1.2

The battle for transition metals between the host and bacteria

(a) Keratinocytes express the antimicrobial compounds S100A7 and S100A15 that in turn sequester metals and prevent infection. After microbial infection, (b) the neutrophil proteins S100A8/S100A9 (calprotectin) and S100A12 bind Mn/Zn and Cu/Zn, respectively. (c) Activated dendritic cells alter the expression of *ZIP* importers and *ZnT* exporters, which results in reduced cytoplasmic levels of Zn. Expression of ZIP8 by macrophages, dendritic cells, and T cells results in decline of lysosomal Zn concentrations. Nrp1, widely expressed by phagocytic cells, transports Mn out of the lysosome. (d) In order to compete with host-mediated Zn and Mn sequestration bacteria express high affinity metal transporters (140).

1.5 Expression of *ZIPs* and *ZnTs* in human body with respect to Zn imbalance

1.5.1 Asthma linked to Zn deficiency

Asthma is a clear example of the importance of Zn homeostasis. This disease is characterized as a chronic airways inflammatory disease, which results from environmental factors in already genetically predisposed individuals (36). Hallmarks of asthma include recurring incidents of wheezing, breathlessness and chest tightness triggered by airway inflammation. Furthermore, an increasing number of studies have been linking asthma to Zn deficiency (31, 135).

Expression of *ZIPs* and *ZnTs* in disease pathology of asthma due to Zn imbalance is summarized in Table 1.2 below. According to one of the studies, individuals with low Zn consumption displayed a four- to five-fold higher combined risk of bronchial reactivity, atopy, and allergic-type symptoms than individuals with higher Zn consumption (31, 135). Additionally, in a 5-year follow up study, it was shown that Zn intake during pregnancy is negatively associated with asthma and shortness of breath in children later on in life (32). In a different study, Zn levels were measured in the hair of wheezy infants as well in healthy controls to show that Zn levels were significantly lower in infants suffering from wheezing (118). This sparked a theory that Zn levels, its deficiency, might contribute to the wheezing during early childhood (50).



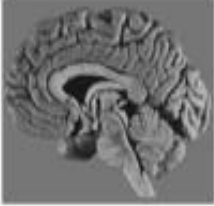
Stainings of airway epithelium from different species had one thing in common: an intense Zinquin staining. Zinquin is a Zn-specific fluorescent probe, and its staining here was completely quenched in the presence of the Zn chelator TPEN (N,N,N',N'-tetrakis-(2-pyridylmethyl)-ethylenediamine) (142). Labile Zn is a more dynamic, free or loosely bound form

of Zn that is more readily exchangeable. Here, labile Zn pools were for the most part found associated with apical structures, which were in the proximity of cilia basal bodies (143, 15). Furthermore, it has been shown that a deficit of Zn results in airway epithelial cells becoming highly susceptible to apoptosis, which is induced by oxidants or by the FAS death receptor pathway (15). It was proposed that programmed cell death may be responsible for acute lung injury due in part to epithelial cell loss. Exhaustion of labile Zn along with tumor necrosis factor alpha (TNF), interferon gamma (IFN) and FAS receptor stimulation quickens caspase-3 activation, proteolysis of E-cadherin and β -catenin, as well as cellular apoptosis. This results in amplified paracellular leak through monolayers of both upper airway and alveolar lung epithelial cultures. Surprisingly, supplementation with Zn successfully inhibited both apoptosis and paracellular leak (131).

Animal models can be utilized to mimic human asthma condition. This is achieved by facilitating allergic airway inflammation using Balb/c mice. Following sensitizing, these mice are aerochallenged with ovalbumin (OVA) which leads to development of airway eosinophilia that is correlated with airway hyper-responsiveness, damage of airway epithelium, mucous hyperplasia and collagen deposition (45). The resulting airway inflammation leads to depletion of stainable Zn. Furthermore, when mice are fed varying diets, those with Zn limited diets (ZL, 14 mg/kg Zn) after exposure to the allergen OVA displayed higher airways hyper-responsiveness, along with elevated mucus cell hyperplasia and eosinophilia, when compared to mice fed a Zn sufficient diet (ZN, 50 mg/kg Zn) (143). After attaining airway inflammation in mice null for the MT-I and MT-II gene functions, the animals demonstrated significantly elevated eosinophils and neutrophils in broncho-alveolar fluid when compared to wild type

controls. Additionally, there were increased expressions of interleukin1 β , 8-oxy-deoxyguanoside and nitrotyrosine (74). All of the above findings indicate that Zn and MT provide a protective role against antigen-induced airway inflammation (160). Finally, supplementation with Zn decreases infiltration of inflammatory cells after acute airways inflammation, here induced by OVA (161).

Table 1.2 Expression of ZIPs and ZnTs in disease pathologies due to Zn imbalance (33)

	Lung Epithelium 	Endocrine Pancreas 	Brain* 
Zn imbalance in the associated pathologies	Asthma (Zn deficiency)	Diabetes (Zn deficiency)	Alzheimer's disease (Zn accumulation)
Zn localization	Apical cytoplasm [31,32]	Secretory vesicles [42]	Synaptic vesicles [68]
Zn function	Antioxidant?	Insulin/glucagone secretion [43,52]	Synaptic transmission [69]
Expressed ZIPs	ZIP1, 6, 7, 8, 14 [37]	ZIP3, 4, 6, 7, 8, 14 [51]	ZIP6, 7* [74]
Expressed ZnTs	ZnT1, 2, 4, 5, 7 [37]	ZnT1, 4, 5, 6, 7, 8 [51]	ZnT1, 3, 4, 5, 6, 7 [74]
Human genes containing SNPs associated with disease	ADAM33 (Zn-dependent metalloprotease)[37]	MT2A promoter [10]	?
Effects of Zn deficiency	↑ disease risk ↑ apoptosis [33]	↑ disease risk ↑ Islet cell damage [39,40]	
Effects of Zn supplementation	↓ inflammation [37]	Protection from chemically-induced diabetes ↑ MT gene expression [61]	
Effects of Zn chelation			↓ A β plaque deposition [64]

In mice supplemented with Zn, enhanced expressions of ZIP1 and ZIP14 were observed, while a decline was evident in ZIP4 and ZnT4 expressions. The observed alterations in gene expressions of these Zn transporters, during airways inflammation, resulted as an attempt to achieve intracellular Zn homeostasis (96). Overall, this study showed that proteins that are responsible for regulating Zn fluxes are crucial in maintaining airways physiology and are important during the onset of inflammatory diseases.

1.5.2 The role of Zn deficiency in Diabetes

Disturbed glucose homeostasis and varying degrees of hyperglycemia are hallmarks of diabetes. Pancreas has a very intricate architecture, which is for the most part composed of exocrine acinar cells that synthesize and secrete the components of pancreatic juice. Also, the islets of Langerhans, which are scattered within the exocrine tissue, comprise the endocrine component of the pancreas (33). Zn, on the other hand, is found throughout the pancreas (33). Expression of *ZIPs* and *ZnTs* in disease pathology of diabetes due to Zn imbalance was summarized in Table 1.2 earlier.

This essential metal is a vital part of pancreatic juice (33). Additionally, Zn is found to be more concentrated in endocrine islet cells, and even more so in the secretory vesicles of β -cells where it is known to stabilize the structure of insulin granules (Figure 1.3) (17, 92). Using Zinquin, coupled with digital image analysis, it was possible to visualize labile Zn, as well as measure it in intact islets and dissociated islet cells (33). Labile Zn was found to be concentrated in secretory vesicles (33). A scattered cytoplasmic fluorescence signal was due to an extragranular pool of labile Zn, which in turn could be used by the newly formed secretory granules (159).

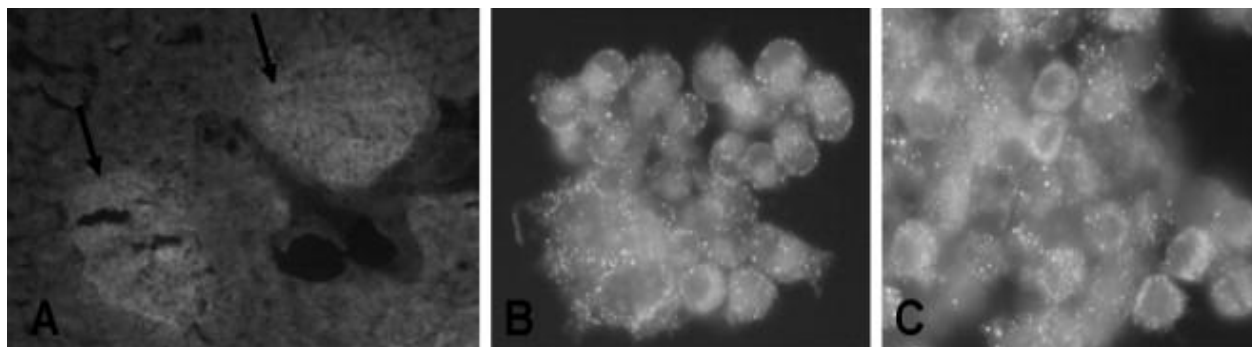


Figure 1.3

Zinquin staining of a section of mouse pancreas (A), mouse glucagonoma α -TC1 cells (B) and mouse insulinoma β -TC6 cells (C). Arrows indicate two islets of Langherans surrounded by acinar exocrine cells (33).

External stimuli like an increase in glucose concentration results in a change of intracellular free Zn concentration. Interestingly, it was shown *in vitro* that presence of 25.6mM glucose diminishes Zinquin staining (159). Presence of Zn ions in beta cells facilitates more than stabilization of insulin hexamers: it has been postulated that released Zn ions might provide a paracrine effect in promoting glucagon secretion, mediated by alpha cells (75). In contradiction, a different study reported Zn to have an inhibitory effect on glucagon secretion in isolated pancreata and dissociated alpha cells (46). Finally, it was also shown that Zn ions released by beta cells might add to their own destruction during insulin hypersecretion (85).

It has been predicted that Zn homeostasis might be significant in the onset and/or progression of diabetes. This claim has been strengthened by results from studies conducted in man and rodent models (1, 17). In mice, it was shown that supplementation with dietary Zn protected the rodents against chemically induced diabetes (66). Meanwhile, in human patients, a

lower serum Zn concentration was observed in Type 1 diabetes when compared with healthy controls (139). In summary, Zn deficiency might be responsible for the decreased ability of the pancreas to respond to glucose, which ultimately leads to islet cell damage (1). Tyrosine phosphatase 1B, an enzyme which is a key regulator of the phosphorylation state of the insulin receptor is targeted by Zn ions that are known to display insulinomimetic effects. In addition, according to the recent studies local Zn deficiencies might play an important role in the development of insulin resistance by activation of stress pathways, with a loss of tyrosine phosphatase control as an end result (64, 63).

Recently, the mouse pancreas was used to investigate the correlation between dietary Zn and the expression of Zn transporters (33). As a result, 16 *ZIP* and *ZnT* transporters were revealed to be expressed (33). Also, a human genetic study identified a SNP in the promoter region of the *MT2A* gene that is closely associated with Type 2 diabetes (52). Unfortunately, there is no information available on the incidence of SNPs in Zn transporter genes, as well as on their possible involvement in the development of pancreas-related pathologies. Disruption of Zn homeostasis can result from improper dietary intake of Zn, but also from impaired activity of proteins controlling Zn metabolism (Figure 1.4) (33).

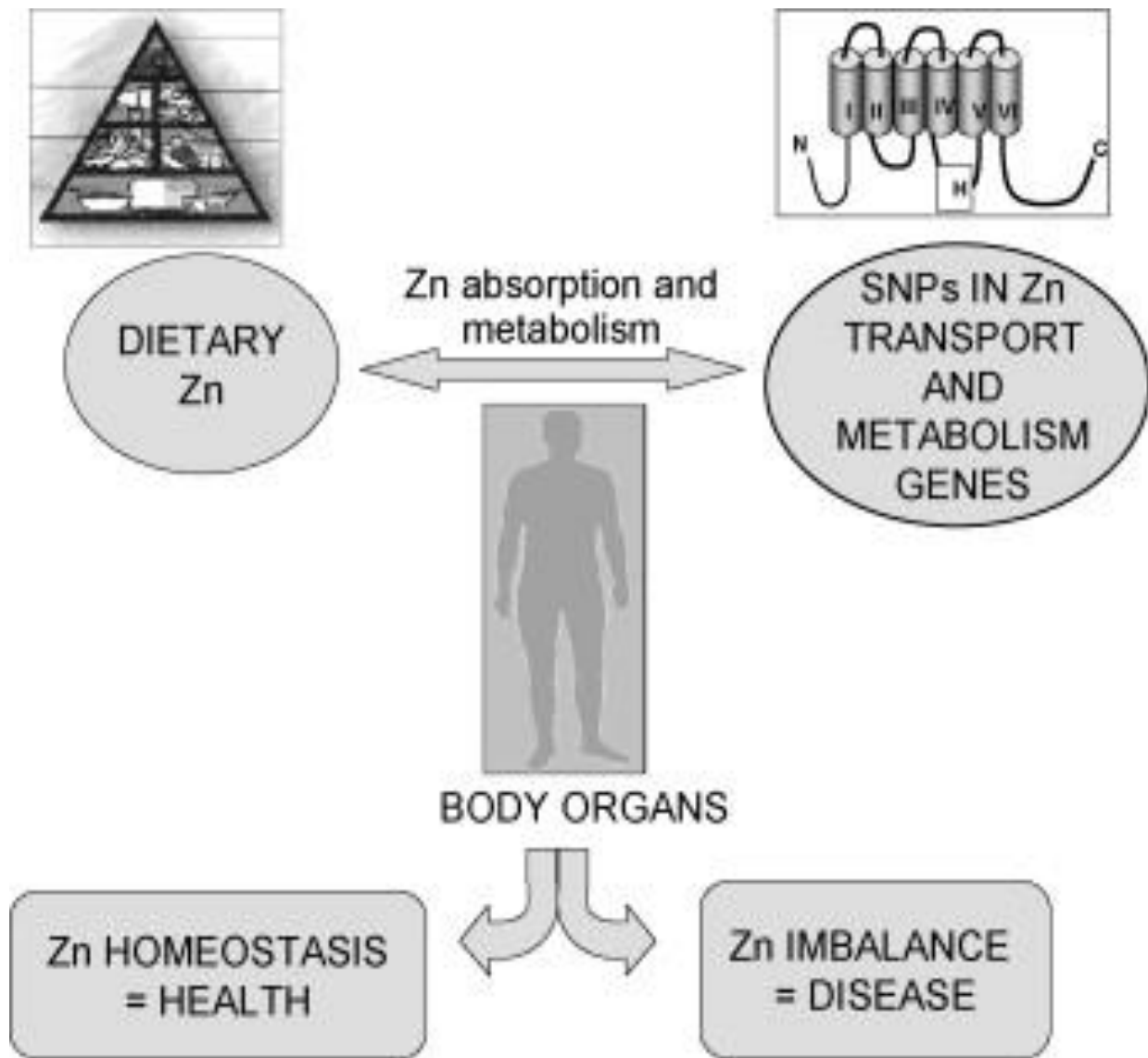


Figure 1.4

The outcome of the interaction between diet and allelic variations of genes controlling Zn fluxes on the balance between health and disease (33)

1.5.3 Link between Zn & Alzheimer's disease

Alzheimer's disease (AD) is a polygenic neurodegenerative disorder linked to aging. Its hallmarks include progressive impairment of memory and cognitive abilities. The onset of AD is believed to be due to the abnormal accumulation and deposition of extracellular senile plaques, which are made up of Cu-Zn aggregates of the amyloid β -peptide ($A\beta$). In turn, $A\beta$ results from proteolytic cleavage of the precursor APP (amyloid β -protein precursor), which is a member of an integral membrane glycoprotein family. There is a cysteine-rich specific domain which is conserved in all APP superfamily members (67). Zn ions are known to bind this domain (33).

Numerous studies are pointing to Zn's involvement in AD pathogenesis, as well as its distorted metabolism in AD's pathology (67). Expression of *ZIPs* and *ZnTs* in disease pathology of Alzheimer's due to Zn imbalance was summarized in Table 1.2 earlier. Excess Zn, in particular, was found associated with amyloid plaques (67). Also, the interaction of $A\beta$ with Zn and other biometals was found to promote amyloid plaque aggregation and decrease its solubility in vitro (67). Since proper AD diagnosis can only be done post-mortem, one of the greatest tools to study AD is to use the transgenic mouse model Tg2576. These transgenic mice overexpress an isoform of human APP, which contains the K670N, and the M671L mutations (157, 141). At 3 months these animals have normal learning and memory in spatial reference, but by 10 months both parameters are impaired (67). This is characteristic of $A\beta$ plaque deposition (67). When these animals were treated with clioquinol, an orally bioavailable metal chelator, a significant inhibition of cortical amyloid accumulation was observed (18). Besides, even early-phase clinical trials suggested that $A\beta$ plaque deposition can be inhibited by Zn chelation (128, 49).

Due to high Zn concentrations in the brain, its transport and regulation here are crucial.

Zn is mainly accumulated in the glutamate synaptic vesicles of presynaptic nerve terminals. Furthermore, Zn ions inhibit postsynaptic glutamate receptors. Excitation with glutamate leads to a quick uptake of Zn via a saturable transport system. Following Zn uptake, Zn along with glutamate is resealed during neurotransmission and has been reported to reach concentrations as high as 300 μM in the synapse (49). Excess Zn must be removed in order to protect adjacent neurons: excess of extracellular Zn is toxic and could contribute to brain damage, as seen in transient cerebral ischemia (141, 89).

On the contrary, Zn deficiency can also have devastating consequences in human physiology. It has been shown to drastically affect behavior of infants and children. Fortunately, there is a very tight regulation of Zn homeostasis in our brain, since brain Zn concentration is found to remain within a narrow range. Moreover, one study in mice, fed with a Zn-limiting diet, showed a decline in the expression of MT-I and ZnT1, meanwhile a Zn importer ZIP6 was found to be upregulated (20). This finding could suggest a possible mechanism that brain employs in order to preserve Zn during Zn deficiency (20).

Overall, Zn homeostasis in the brain is maintained by the actions of metallothioneins, ZnTs and ZIP proteins. Similarly to other cell types, in neurons Zn is mainly found tightly bound to metallo-proteins. In the brain, just as seen earlier during bacterial infections, Zn is sequestered but into synaptic vesicles of glutamatergic neurons (122). In order to transport high concentrations of labile Zn, from the cell bodies to the axon terminals where it's packaged into synaptic vesicles, this cell type utilizes the ZnT3 transporter (122). Interestingly, when a ZnT3(-/-) genotype was introduced into Tg2576 mice brain development and learning abilities were not affected, instead it resulted in an approximately 50% reduction in amyloid burden (99). It was

found that ZnT3 expression was regulated by estrogen. This was no surprise, since both in humans and rodents there is a higher occurrence of AD in postmenopausal females when compared to males of equal age. Additionally, in comparison with males, in aging Tg2576:ZnT3(+/+) female mice there were increased levels of synaptic Zn, insoluble amyloid beta, along with plaques (99, 100). The above physiological attributes, which were clearly sex-linked, were not present in Tg2576:ZnT3(-/-) (99, 100). While more studies are necessary to elucidate the true roles of metal transporters in the brain, their importance in the onset and progression of neurodegenerative diseases, like AD, is undeniable.

In a nutshell, many factors contribute to the onset and progression of multifactorial diseases. As described above, these include genetic and environmental factors, such as diet. Using mutation screens along with linkage studies, scientists have been able to identify a number of mutations in several genes attributing to chronic diseases. Furthermore, numerous reports are singling out Zn, as well as its metabolism, as the key player in the onset of a rising number of chronic diseases. Therefore, research of Zn's metabolism and regulation, by metal transporters like those belonging to the *ZIP* family, will illuminate the influence of dietary Zn on disease risk.

1.6 *ZIP*'s structures & their metal-binding implications

Searches of human and mouse genomes revealed numerous members of *ZIP* superfamily, including as many as 14 in humans. Additionally, there was a conserved subfamily that was identified in mice and humans. It includes three *zip* genes: *zip1*, *zip2*, and *zip3*. Furthermore, human *ZIP1* (SLC39A1) along with *ZIP2* (SLC39A2) have been shown to act as Zn transporters (94, 95). In these studies, Zn transport was measured in mammalian cells which were transiently transfected with an empty vector or a vector containing hZip1 or hZip2 cDNAs (94, 95). To

determine the role of these genes in Zn transport transfected K562 erythroleukemia cells expressing these genes were utilized (94, 95). Cells expressing hZip1 were shown to accumulate more Zn than control cells because of increased Zn influx (95). These cells also showed a Zn-uptake profile that was biochemically indistinguishable from the endogenous activity (95). On the other hand, it was observed in cells expressing hZip2 that Zn transport was time-, temperature-, and concentration-dependent and saturable with an apparent K_m of 3 μ M (94). While hZip1's activity was not energy-dependent, nor did it require K^+ or Na^+ gradients, it was stimulated by HCO_3^- treatment, suggesting a Zn- HCO_3^- -cotransport mechanism (94). Finally, both hZip1 and hZip2 were observed to localize in the plasma membrane (94, 95). Furthermore, a mutation in the human *ZIP4* gene (SLC39A4) was found in the genetic Zn metabolism disorder acrodermatitis enteropathica (152). Also, that it is responsible for encoding a Zn-regulated Zn transporter in mice. Since it is a conserved gene, it further underlines the fact that mammalian *ZIP* genes are vital components of the Zn homeostasis mechanism (38).

Thus far there hasn't been a study conducted *in vivo* in order to assess the three *zip* gene systemic expression and regulations. While *ZIP1* mRNA has been reported to be present in most human tissues as well as in cultured human cell lines, *zip1* mRNA was present in majority of adult rat and embryonic mouse tissues (95, 105). Unlike *ZIP1*, *ZIP2* mRNA was not detected in human tissue RNAs (94). *ZIP3*'s expression is yet to be determined in any system, and *zip1* and *zip2* are still in need of characterization in adult mouse tissues. It was reported that in cultured prostate cell lines there is a mild hormonal regulation of *ZIP1* mRNA (23). Also, in THP-1 cells treated with a Zn chelator, and in human monocytes, *ZIP2* mRNA abundance was significantly elevated, while *ZIP1*, *ZIP3*, and *ZIP4* mRNA abundance remained the same (25, 14).

1.6.1 Biochemical Characteristics of the ZIP family

Several of the *ZIP* proteins have been functionally characterized and as a result are believed to have similar membrane topologies. This includes eight transmembrane domains, as well as the amino- and carboxy-terminal ends found on the outside of the plasma membrane (Figure 1.5) (28).

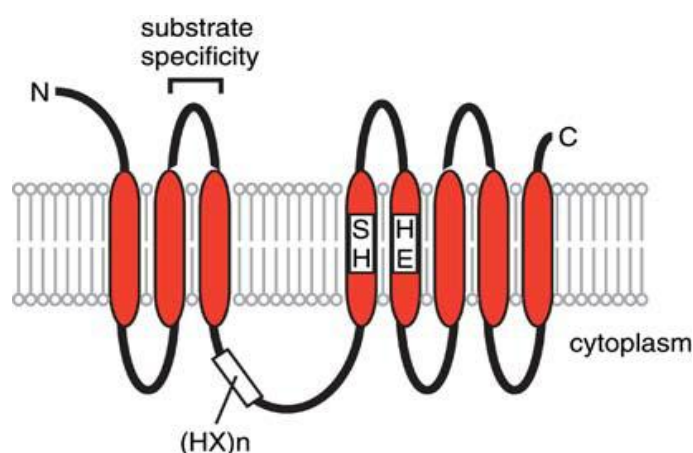


Figure 1.5

Topological model of SLC39 proteins

8 transmembrane (TM) domains are indicated in red. The histidine-rich region in the cytoplasmic loop between TM III and IV, conserved histidines and charged/polar residues in TM IV and V, and the location of substrate specificity determinants mapped in Irt1 are also shown above (28).

These domains contain conserved histidine, serine, and glycine residues within the fourth transmembrane domain (37). *ZIP* proteins are known to have a variable region, which is likely to contain a possible metal-binding domain that is rich in His residues (56, 28). *Arabidopsis ZIP* proteins, for instance, have a varying amino acid range, from 326 to 425 (115). This is all due to the variable region that is speculated to be found in cytoplasm between transmembranes III and IV (115). Furthermore, motifs that are found to be conserved in *ZIP* proteins are believed to be involved in metal transport or its regulation. One example of this would include a motif like HAGHVHIHTHASHGHTH that is a part of ZIP1, and is also conserved in a number of *ZIP* proteins (115). These proteins also contain a histidine-rich loop, which is found between third and fourth transmembrane domains (37, 28). Finally, there was a predicted amino acid conservancy of 83-93% found between all 8 transmembrane domains of the mouse and human *ZIP1*, *ZIP2*, and *ZIP3* genes (Figure 1.6A, B, C) (37).

A

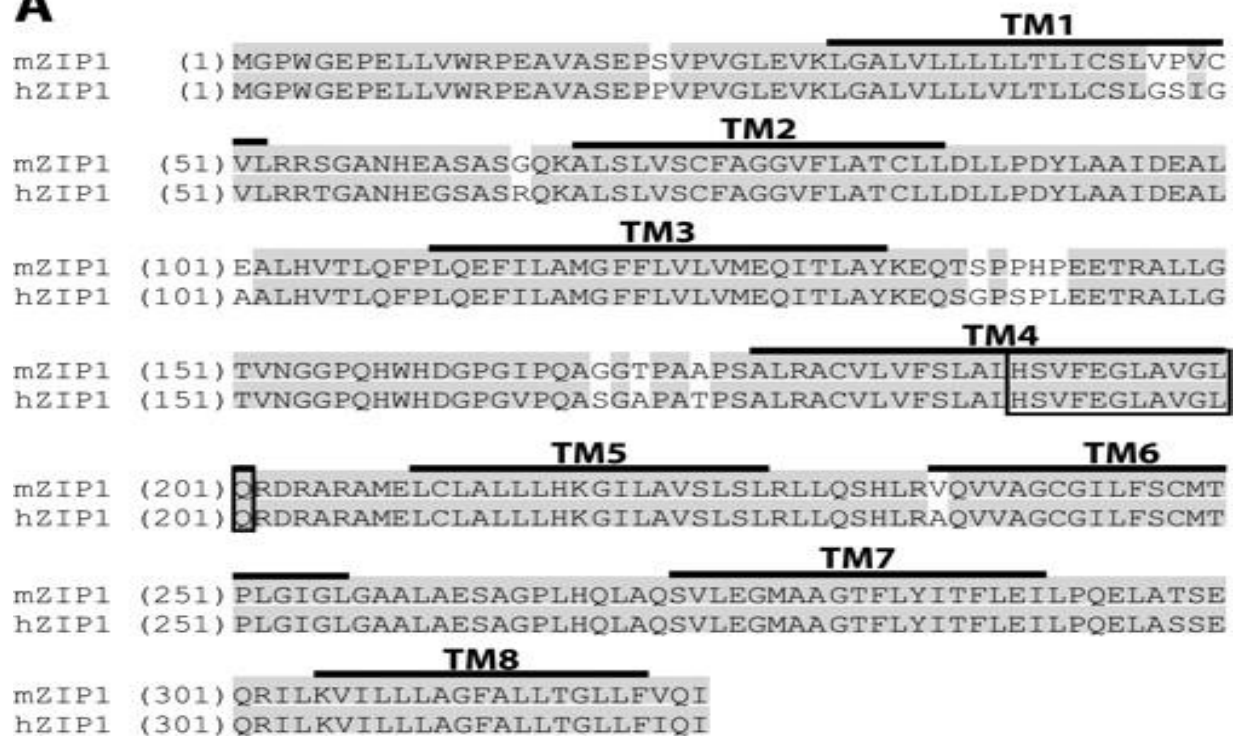


Figure 1.6A

Sequence alignment of the mouse and human *ZIP1* transmembrane domains 1-8 (37)

In these figures the shaded regions depict conserved sequences, and the 8 putative transmembrane domains (*TM*) are highlighted with a solid line above the mouse sequences. The conserved 12-amino acid signature sequence that is characteristic of this subfamily is boxed for each *ZIP*.

B

		TM1	
mZIP2	(1)	MEVLLGVKIGCLLALLVLTLCGLTPITYVKWFQMDAATGHHHRVLSLLGC	
hZIP2	(1)	MEQLLGIGKLGCLFALLALTLCGLTPICFKWFQIDAARGHHRVLRLLGC	
		TM2	
mZIP2	(51)	TSAGVFLGAGLMHMTAEALEGIESEIQKFVEQNSTGSKGNSSRDAASSYV	
hZIP2	(51)	ISAGVFLGAGFMHMTAEALEEIESQIQKFMVQNRASERNSSGDADSAHM	
		TM3	
mZIP2	(101)	EYPYGELVISLGFFFVFLLESALQCCHGAAGGSTVQEEEWGGTHAFGFH	
hZIP2	(101)	EYPYGEIISLGFFLVFFLESALQCCPGAAGGSTVQDEEWGGAHIFELH	
		TM4	TM5
mZIP2	(151)	KHPAVPSPSRGPLRALVLLLSLSFHSVFEGGLAVGLQATVAATIQLCVAVL	
hZIP2	(151)	SHGHLPSPSKGPLRALVLLLSLSFHSVFEGGLAVGLQPTVAATVQLCLAVL	
		TM6	
mZIP2	(201)	AHKGLVVFSVGLRLGKIGTGPRWATFCILSLALMSPVGLALGLTVAGGAS	
hZIP2	(201)	AHKGLVVFGVGMRLVHLGTSSRWAVFSILLALMSPGLGLAVGLAVTGGDS	
		TM7	
mZIP2	(251)	GQTQGLAQAVLEGIAAGTFLYVTFLEILPRELACPEAPLAKYSCVAAGFA	
hZIP2	(251)	EGGRGLAQAVLEGVAAGTFLYVTFLEILPRELASPEAPLAKWSCVAAGFA	
		TM8	
mZIP2	(301)	FMALIALWA	
hZIP2	(301)	FMAFIALWA	

Figure 1.6B

Sequence alignment of the mouse and human *ZIP2* transmembrane domains 1-8 (37)

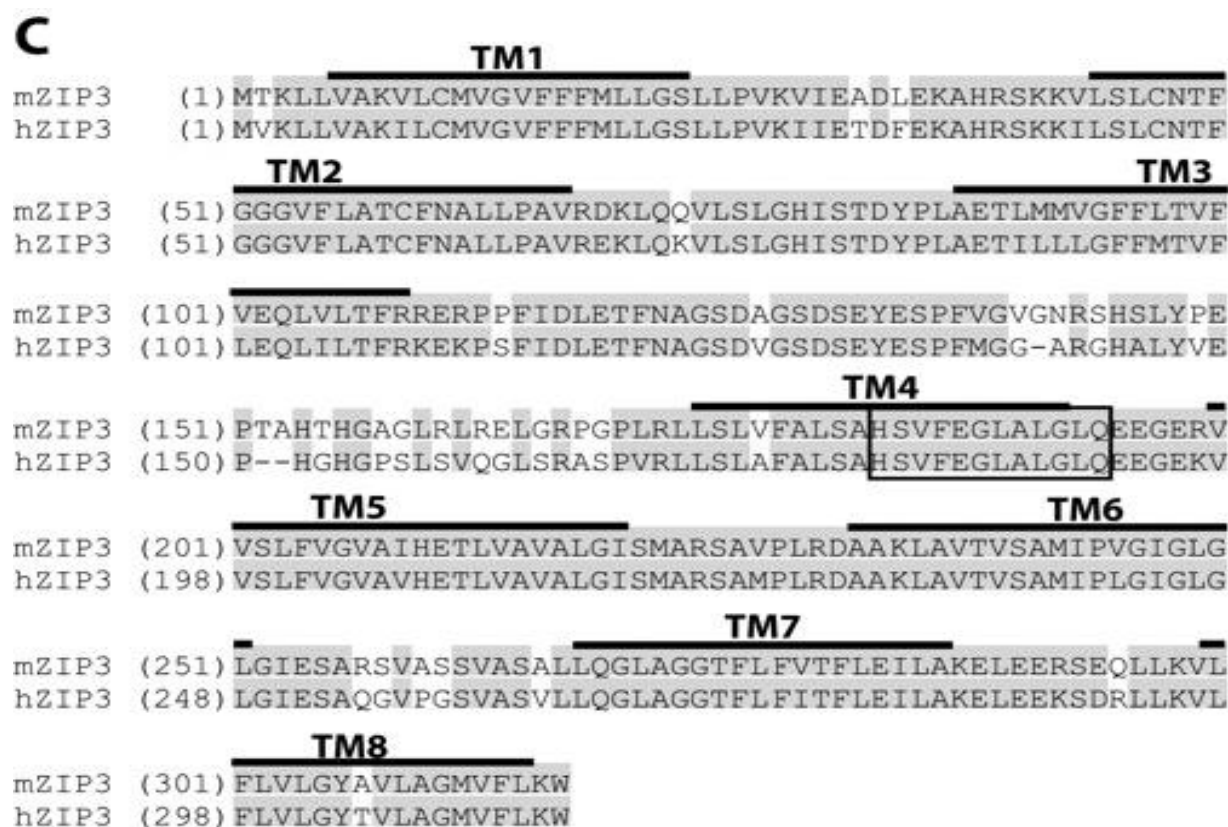


Figure 1.6C

Sequence alignment of the mouse and human *ZIP3* transmembrane domains 1-8 (37)

12-amino acid sequences, with a conserved motif: HSVFEGLAVGLQ from the human *ZIP1*, *ZIP2*, and *ZIP3* proteins, were used to search the mouse translated high throughput genome sequences data base on the NCBI Protein Database server (37). The result yielded three different BAC entries that were derived from the C57/B6 strain of mice. The alignment of these, depicted in Figure 1.7 below, provided the identity of the mouse *zip1*, *zip2*, and *zip3* genes (37). Here, the fourth transmembrane domain was aligned with a few known *ZIP* proteins from *Arabidopses*, yeast, and human. Conservation within the human sequences revealed the three

mouse *ZIP* proteins belonging to a subfamily. As seen with other members of the *ZIP* family, these sequences contain the conserved histidine, serine, and glycine residues (*boldface*). In addition, human and mouse *ZIP1*, *ZIP2*, and *ZIP3* are a part of a smaller subfamily that shares an extended 12-amino acid sequence (*underlined*). The only exception is the one conserved amino acid substitution that is seen in *ZIP3* (37).

Arabidopsis	{	IRT1	ELGI I V HSVVIGLSLGATSDT
		ZIP1	EI GI V V HSV I IGI SLGASQSI
		ZIP2	I FAL CF HS IFEGIAI GLSDTK
		ZIP3	ELGI I V HSVVIGISLGASQSP
Yeast	{	ZRT1	EFGVI F HSVMI GLNLGSVGD
		ZRT2	EFG I I F HSVFVGLSLSVAGE
Human	{	ZIP1	VFSLAL <u>HSVF</u> EGLAVGLQRDR
		ZIP2	LLSL SF <u>HSVF</u> EGLAVGLQPTV
		ZIP3	AFALSA <u>HSVF</u> EGLALGLQEEG
Mouse	{	ZIP1	VFSLAL <u>HSVF</u> EGLAVGLQRDR
		ZIP2	LL SLSF <u>HSVF</u> EGLAVGLQATV
		ZIP3	VFALSA <u>HSVF</u> EGLALGLQEEG

Figure 1.7

Conservation within the fourth transmembrane domain revealed a subfamily of mammalian *ZIP* proteins (37)

Earlier mentioned, SLC39 gene family has 14 greatly conserved members in the human and mouse genomes (53). As depicted in Figure 1.8, when compared to the other 12 family members, evolutionarily mouse ZIP14's closest neighbor is ZIP8 (61). Noteworthy, the human and mouse SLC39A14 genes both contain two exons 4, which give rise to ZIP14A and ZIP14B alternatively-spliced variants. It is believed, that ~425 million years ago ZIP8 and ZIP14 diverged from one another sometime following the land animal–sea animal split (53). This theory is based on the fact that the puffer fish, *Takefugu rubripes*, genome includes one gene that is practically identical to both mouse genes (53). Not depicted here, the human SLC39A14 and SLC39A8 genes are homologous to the mouse orthologs.

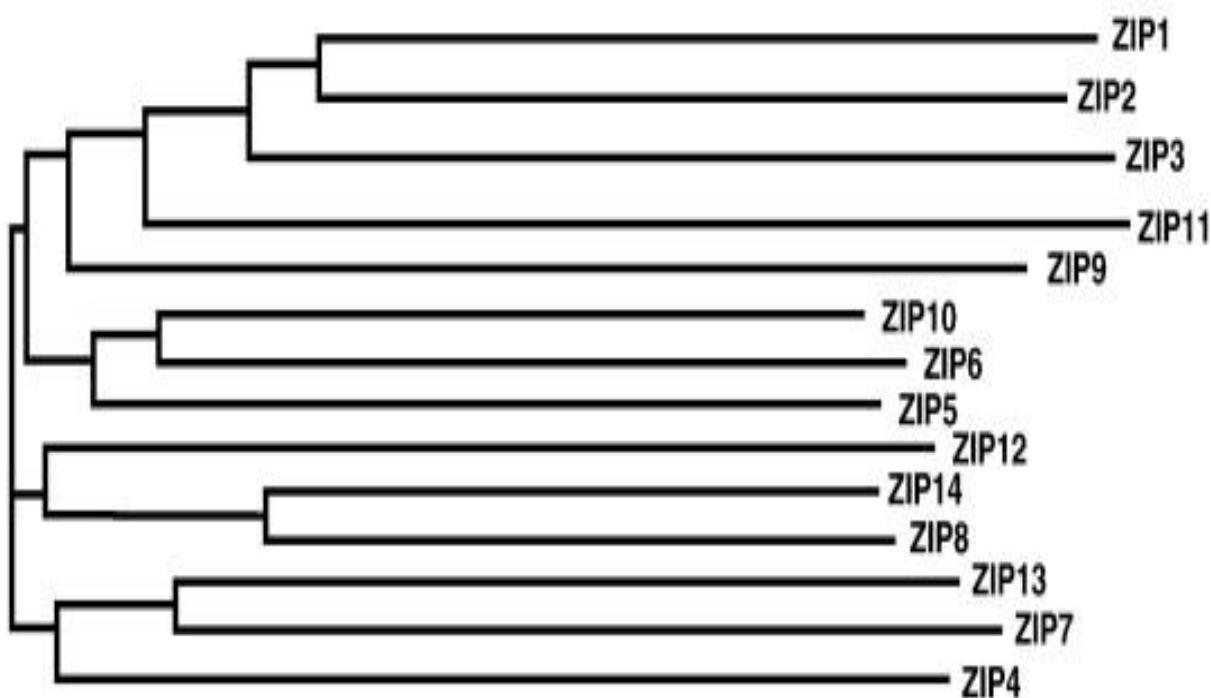


Figure 1.8

Phylogenetic tree of the 14 mouse *ZIP* domains of the *Slc39* gene-encoded proteins (nearest-neighbor joining (NNJ)-generated) (61)

Residues in or near transmembrane helices (TMH) IV and V are critical for efficient metal-uptake (129). Transmembrane domain IV is believed to contain the most conserved region of these proteins. It is also predicted to form an amphipathic helix, which contains a fully conserved histidine that may form part of an intramembranous metal binding site involved in transport (115, 113). Furthermore, it has been shown that the transport function after heterologous expression in yeast was eliminated after conserved histidines or some of the adjacent residues were mutated (129). A related study was done with human hZIP1 (SLC39A1), which indicated that histidines located within TMH and in connecting loop domains were essential for Zn transport (114). Although there have been a number of proposed mechanisms, the mechanism for ZIP-mediated metal ion transport is still unknown. One of them includes a bicarbonate stimulated hZIP2 and a Zn (II)/bicarbonate co-transport (94). Bicarbonate might also drive the metal-uptake in other ZIP-transporters, like ZIP8 (Slc39A8) and ZIP14 (Slc39A14) (60, 53).

While studying rvZIP14A and rvZIP14B cell lines, the Nebert lab revealed that ZIP14 transporters uptake Cd by a temperature- and energy-dependent method, while functioning optimally at pH = 7.2 (61). ZIP14 proteins, in particular the B isoform, displayed a high affinity for Cd. Furthermore, it was observed that ZIP14-mediated Cd uptake is most inhibited by Zn^{2+} , followed by Mn^{2+} and finally Cu^{2+} . ZIP8- and ZIP14-mediated Cd uptake is dependent on presence of extracellular HCO_3^- , characterizing ZIP14A and ZIP14B as $\text{M}^{2+}/\text{HCO}_3^-$ symporters, where $\text{M}^{2+} = \text{Zn, Mn or Cd}$. Finally, ZIP14A and ZIP14B were found to be located on the apical surface of MDCK cells (53). In Table 1.3 below, one can find a comparison between the human

versus mouse SLC39A8 and SLC39A14 genes and in Table 1.4 the properties of the mouse ZIP8 and ZIP14 protein transporters (61).

It has been observed that Cd in the environment is capable of displacing either endogenous Zn or Mn and then entering the epithelial cell. By forming disulfide bonds, Cd can demolish countless enzymes/proteins via oxidative stress. Hand-in-hand with Cd, Hg and Pb are also able to cause renal proximal tubular acidosis and osteomalacia, additionally Hg and Pb have been reported to act as competitive inhibitors of ZIP8-mediated Cd and Zn uptake (9). Platinum and uranium are the only other metals known to cause this human condition.

Table 1.3 Comparison between mouse and human Slc39A8, (ZIP8), and Slc39A14, (ZIP14), genes (61)

	Mouse Slc39a8 gene	Mouse Slc39a14 gene
Chromosomal location	Chr 3; nt 135488243(+)	Chr 14; nt 70751231(-)
Transcript distance spanned#a	64,860 bp	92,502 bp
Size of mRNA	3.1–3.3 kb	2.0 kb
Molecular weight of protein	50,082 Da	53,754 versus 53,962 Da
Number of amino acids in protein	462	489
	Human SLC39A8 gene	Human SLC39A14 gene
Chromosomal location	4q22–q24	8p21.2
Transcript distance spanned	88,148 bp	57,942 bp
Size of mRNA	3.3–3.5 kb	4.6 kb
Molecular weight of protein	49,631 Da	54,056 versus 54,212 Da
Number of amino acids in protein	461	492

Table 1.4 Properties of the mouse ZIP8 and ZIP14 proteins (61)

Properties	ZIP8	ZIP14A	ZIP14B
Tissues in which gene is expressed most highly (assessed by Northern and qRT-PCR)	Lung = testis > > kidney >> liver > > brain > duodenum	Liver > duodenum> > kidney > testis> >brain = lung	Liver = duodenum > >brain = testis > >kidney = lung
Cations transported by mammalian cells in culture (always with HCO_3^-)	Zn, Mn, Cd	Zn, Mn, Cd	Zn, Mn, Cd
Km values for M^{2+} uptake in mammalian cell culture	Mn 2.2 μM ; Cd 0.62 μM	Mn 18 μM ; Cd 1.1 μM	Mn 4.4 μM ; Cd 0.14 μM
Cation inhibitors of Cd uptake in mammalian cell culture	Mn > Hg >> Pb = Cu = Zn = Cs	Zn >> Mn > Cu	Zn >> Mn > Cu
Cations transported by <i>Xenopus</i> oocytes	Zn, Cd	Zn, Cd	Zn, Cd
Km values for Cd uptake in <i>Xenopus</i> oocytes	Zn 0.26 μM ; Cd 0.48 μM	Zn 0.38 μM ; Cd 0.46 μM	Cd 0.30 μM
Cation inhibitors of Cd uptake in <i>Xenopus</i> oocytes	Zn > Cu = Pb = Hg	Hg = Pb > Zn > Cu > Fe > Mn	Hg = Pb > Zn > Fe > Cu > Mn

1.7 What is known about ZupT?

ZupT is a cytoplasmic membrane protein, which was the first characterized bacterial member of the *ZIP* family of metal ion transporters, previously only believed to be present in eukaryotes (57). Its gene was first discovered in *Escherichia coli*, and it formerly went by *ygiE* (93). Before 2002, it was believed that there were only three Zn transport systems available in *E.coli*: the efflux of Zn was mediated by the P-type ATPase ZntA and the cation diffusion facilitator ZitB, while during Zn deficiency Zn was taken up by the high-affinity ABC transporter ZnuABC (54, 127, 132). Grass *et. al* showed that ZupT was an additional Zn transporter system, which facilitated Zn's uptake in *E.coli* (57). Furthermore, as seen earlier with other *ZIP* family proteins, ZupT also plays an important role in a number of different diseases. For instance, during urinary tract infection (UTI) in mice, Znu and ZupT were essential for growth in Zn-limited conditions (130). It was also reported that Znu was the main Zn transporter, and that the loss of Znu and ZupT had a collective effect on fitness during UTI, which in turn could have resulted from reduced resistance to oxidative stress and motility (130).

Multiple reports have showed ZupT to be a transporter of broad substrate specificity (55, 119). Besides Zn, ZupT was reported to mediate uptake of $^{55}\text{Fe}^{2+}$ (55). It was reported that an *E. coli* strain, whose known Fe uptake systems were demolished, was able to grow in the presence of chelators only if *zupT* was expressed (55). Also, in the same strain, heterologous expression of *Arabidopsis thaliana* ZIP1 alleviated the Fe deficiency (55). Additionally, ZupT's expression resulted in *E. coli* cells' hypersensitivity to Co^{2+} and Mn^{2+} (55). Along with already mentioned uptake of Zn, Fe, and Co, phenotypic and transport analysis reported ZupT is also involved in transport of Mn, but also Cd^{2+} (119). According to competition experiments ZupT showed a

slight preference for Zn, which was supported by kinetic parameters for Zn, when compared to Co and Mn (119). ZupT was also observed to transport Cu^{2+} (119). Although, copper-uptake into *E. coli* cells, and the role of ZupT in it, is physiologically not relevant because there is no cytoplasmic protein known that requires a copper co-factor in *E. coli*. Interestingly, ZupT does not seem to be metal regulated: expression of a $\Phi(\text{zupT-lacZ})$ operon fusion showed that *zupT* is expressed constitutively at a low level (55).

In silico analysis suggested that most ZIP transporters including ZupT have a topology comprising of eight TMH along with an expanded loop domain between TMH III and IV (129, 114). Amino acid sequence analysis of different ZIPs revealed several conserved residues between eukaryotic and prokaryotic ZIP proteins, which are for the most part located in TMH VI and V (119). Site-directed mutagenesis has been done on a number of amino acid residues within the ZupT sequence with a goal to identify the residues contributing to its substrate specificities. It has been reported that ZupT with a H89A mutation has lost Co and Fe transport activity, while the S117V mutant could no longer transport Mn (119). E152D mutant, on the other hand, displayed general metal uptake impairment but completely lost its ability to mediate the transport of Zn and Mn (119). After four amino acid residues in IRT1 (H197, S198, H224, E228) were found to be vital for transport activity, similar residues were investigated in the shorter ZupT peptide at similar positions but not in conserved order (S117, H119, H148, E152) (129, 119). Here, only mutations H119 and H148 left the protein basically inactive (119). Furthermore, mutations of S117, and E152 residues also displayed distinguishing phenotypes. For instance, the S117V mutant lost its Mn-transport activity, along with a minor reduction in Co-uptake, while cells with E152D or E152A were unable to take up Zn and Cd or Zn, respectively (119). In

addition, mutation of E60 residue led to loss of Cd, and to some degree also Co, transport without having any effects on other substrates (119). In growth experiments, ZupT E60D mutant was similar to wild-type ZupT, but its uptake-activity was altered (119). Finally, even though the negative charge of this glutamate was retained, since it was mutated to aspartate, its transport abilities were impaired. Furthermore, this mutant's ZupT protein was synthesized in low quantity, as it was barely detectable by immuno-blotting (119).

One of the proposed mechanisms for metal uptake by ZupT included the proton motive force because the protonophores FCCP and CCCP were reported to inhibit the metal transport (119). Studies were conducted to address this issue. If metal transport by ZupT depended on proton force, its mechanism would be similar to that of MntH, where maximum transport is achieved at low pH (24). The opposite was observed for ZupT and other *ZIP* transporters. ZupT was shown to work best at physiological pH (119). Its metal uptake was independent of K^+ -, Na^+ - or Mg^{+} -ions, thus showing that it did not participate in a substrate co-transport with these cations (119). ZupT's affinity for its substrates might increase with increasing pH, and therefore its transport efficiency is reported to be higher at near neutral pH. Likewise, one can explain ZupT's increased transport of Zn at increasing pH levels. Finally, it could be due to the pH of the outside environment, which could be responsible for the protonation-state of the amino acid residues within ZupT, that ZupT's optimal activity was observed at pH 7.2 (119). Also, at neutral pH ZupT's metal uptake into the cells was inhibited by ionophores (119). Interesting to note, mammalian ZIP8's Cd-transport was energy-dependent but, similarly to ZupT, independent of K^+ -, Na^+ - or Cl^- -ions (60). ZupT also seems to be unlike its eukaryotic *ZIP* homologues due to its lack of stimulation by bicarbonate (119). Alternative mechanism proposed that metal-uptake by

ZupT might be driven just by the concentration gradient of labile transition metal cations found across the plasma membrane (16). If one were to change the pH gradient across the membrane by let's say two orders of magnitude: it would most likely be insufficient since the concentration gradient of Zn across the cytoplasmic membrane is at least 14 orders of magnitude (16).

There was a comparison conducted between ZupT and ZIP family members from eukaryotes. Through the means of retroviral infection of fetal mouse fibroblast cultures with ZIP8 cDNA, transport kinetics of ZIP8 for Cd^{2+} and Mn^{2+} were obtained with apparent K_m values as 2.2 and 0.69 μM as well as V_{\max} values of 73.8 and 92.1 $\text{pmol} \times \text{min}^{-1} \times \text{mg protein}^{-1}$, respectively (60). These results were similar to the reported results from metal transport study with ZupT and Mn^{2+} : K_m 1.16 \pm 0.29 μM Mn, with a V_{\max} 850 \pm 90 $\text{pmol} \times \text{g d.w.}^{-1} \times \text{min}^{-1}$ (119). The reported apparent affinity of ZupT for Zn^{2+} : 0.71 \pm 0.14 μM Zn^{2+} in *E. coli* was in the same order of magnitude to what was observed for ZIP8 and Zn^{2+} : K_m = 0.26 μM Zn^{2+} , and similar to what was measured for IRT1 expressed in yeast: K_m = 2.8 μM Zn^{2+} (119, 60, 90). Interesting to note, metal competition studies showed that ZIP8-mediated Cd^{2+} -transport was inhibited by other metal cations especially by Mn^{2+} , Hg^{2+} and Pb^{2+} but not by Fe^{2+} or Ni^{2+} (60). An additional study reported that Cd^{2+} transport into *Xenopus* oocytes through ZIP8 was well inhibited by Zn^{2+} but not by Mn^{2+} (107). ZupT transport of Zn^{2+} , on the other hand, was not inhibited but somewhat elevated by presence of Fe^{2+} , even though Fe^{2+} is one of its substrates (119). Similarly, in IRT1 Fe^{2+} but not Fe^{3+} also led to an increase in Zn^{2+} -uptake rate (90). Likewise, Zn^{2+} transport by ZIP8 and ZIP14 was increased in the presence of the alternative substrate Fe^{2+} (53). Therefore, transport by ZIP proteins ZIP8, ZIP14, IRT1 as well as ZupT follows typical Michaelis–Menten kinetics (53). If this was not the case and an allosteric

regulation by Fe^{2+} of ZupT-mediated Zn-transport was involved, in an inverse experiment, Fe^{2+} transport would be controlled by Zn. On the contrary, a 50-fold surplus of Zn over Fe^{2+} did not diminish Fe^{2+} -uptake by ZupT (119).

Without a purified ZupT protein its true biochemistry is difficult to characterize.

CHAPTER 2

EXPERIMENTS, RESULTS & DISCUSSION

2.1 Goal

As described in Chapter 1, *ZIP* family of metal transporters is expressed amongst different organisms in order to maintain their metal homeostasis and thus contribute greatly to their growth and development. *ZIPs* have also been found to play key roles in bacterial infections, as well as the onset and progression of chronic diseases in humans.

The goal of this study was to purify and characterize one of the bacterial *ZIP* transporters: *E.coli* ZupT. Studies conducted in *E.coli* can provide a great number of characteristic data for such transmembrane proteins like ZupT. In comparison with mammalian cells, *E.coli*'s lack of complex organelles, and ease of genetic analysis, allows for direct analysis of the protein's role in metal transport. Furthermore, *in vivo* and *in vitro* studies can be conducted in this system.

As outlined in Chapter 1, various *ZIP* transporters have been reported to have different metal binding specificities. After ZupT purification, its binding specificities will be evaluated with fluorescence and UV-Visible spectroscopies. Also, to determine the binding stoichiometries, between ZupT and the tested metals, ICP-MS (inductively coupled mass spectrometry) analysis will be conducted.

2.2 Materials

pBAD/mycHis-C plasmid and the *E.coli* strain LMG194 were purchased from Invitrogen.

The pBAD/mycHis-P plasmid was constructed by our collaborator's lab.

2.3 Methods

2.3.1 Construction of ZupT/pBAD/mycHis-P with carboxyl-terminal Precision Protease site

ZupT was subcloned from pBAD/mycHis-C into pBAD/mycHis-P with an addition of a protease site (Figure 2.1). The amplified PCR products were cloned into pBAD/mycHis-P with the help of *Bam*HI and *Eco*RI sites. The creation of the construct was verified with sequencing by GENEWIZ. The final construct was later transformed into TG1 cells and later into LMG194 cells.

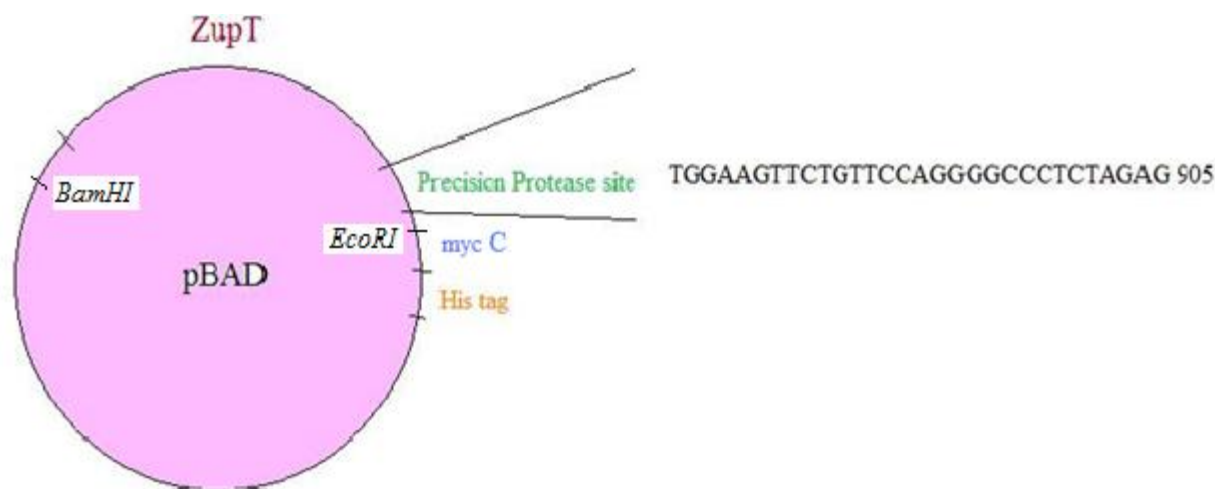


Figure 2.1

ZupT subcloned from pBAD/mycHis-C into pBAD/mycHis-P with an addition of a Precision Protease site

2.3.2 Creation of ZupT/pBAD/mycHis-C mutants

CLUSTALW2 Multiple Sequence Alignment (European Bioinformatics Institute) was used to analyze the ZupT sequence. The sequence analysis revealed two homologically-conserved regions (Figure 2.2), which differed from the previously described conservation found in other *ZIP* family proteins. When compared to the topological model of SLC39 proteins (Figure 1.5), where there is a H-rich region between transmembrane (TM) III and IV, followed by conserved H, S, and E residues, ZupT sequence alignment revealed two repetitive, almost perfectly-conserved, regions (Figure 2.2). With a general sequence of HN-X-PEG, the first region had a 100% conservancy in H, E, and G residues. Second region only had G at the 100% conservancy. In order to evaluate a possible metal-binding role of these two conserved regions, several ZupT mutants were created.

After designing of primers, QuickChange Site-Directed mutagenesis Kit (Stratagene) was utilized in order to create four different mutants. Mutants had a restriction enzyme site inserted into the sequence, *highlighted*, in order to speed up and confirm the mutation creation (Table 2.1). Successful mutants creation was confirmed with sequencing by GENEWIZ.

Table 2.1 ZupT Site-Directed Mutagenesis Primers

H119N	<p>Fwd: 5' CTC GGCATC AGT TTA AAC AAC TTC CCG GAA GGG 3'</p> <p>Rev: 5' CCC TTC CGG GAA GTT GTT TAA ACT GAT GCC GAG 3'</p> <p>(<i>PmeI</i> site)</p>
H148N	<p>Fwd: 5' CTG GCC GTC GCG TTA AAC AAT ATC CCT GAA GG 3'</p> <p>Rev: 5' CC TTC AGG GAT ATT GTT TAA CGC GAC GGC CAG 3'</p>
E123Q	<p>Fwd: 5' CTG CAT AAC TTC CCG CAA GGG ATC GCG ACC TTT GTC 3'</p> <p>Rev: 5' GAC AAA GGT CGC GAT CCC TTG CGG GAA GTT ATG CAG 3'</p> <p>(<i>NruI</i> site)</p>
E152Q	<p>Fwd: 5' GCG TTG CAC AAT ATC CCT CAG G GTT CTG GCA GTG 3'</p> <p>Rev: 5' CAC TGC CAG ACC CTG AGG GAT ATT GTG CAA CGC 3'</p> <p>(<i>Bsu36I</i> site)</p>

2.3.3 Optimization of ZupT expression

Protocol for optimization of ZupT was modified from the reported protocol in reference 133. First, a log phase growth curve was created for ZupT/pBAD/mycHis-C, in LMG194. After a fresh transformation of ZupT/pBAD/mycHis-C into LMG-194 cells 5 colonies were selected and grown in 5-ml LB cultures with Amp, in a 50-ml tube with lids hole-punched 3 times. The OD₆₀₀ of the negative control culture was checked every 30 min in order to construct a log phase growth curve. The remaining colonies # 1-6, plus a negative control colony, were grown to OD₆₀₀ 0.8 at which point 125 ul of the cultures were plated on a LB/ Amp (100 mg/ml) plates and the remainder of the cultures, besides the negative control, were induced with 0.02% Arabinose. The cultures were grown additional 1.5 h at 37°C, at which point 500-ul samples were taken, followed by 18 h growth at 25°C. After overnight growth, 500-ul samples were taken again from all of the cultures and pelleted. The supernatant was discarded and the pellets were treated with 20 ul of SDS loading buffer. The samples were digested at 95°C for 20 min. Samples from 1.5-h of induction and those with additional 18 h of induction at room temperature were compared on a 12% SDS gel. An overall increased protein expression was observed for all the colonies thus longer culturing/induction time was implemented.

The original ZupT expressions of the 7 freshly-transformed colonies were compared on a western blot (Figure 2.5). As a result, colony # 5 was chosen and underwent a 2nd selection as described earlier, again with a negative control and # 1-6 colonies compared. Finally, the results of both selections, colonies # 5 and # 3, were compared on a 12% SDS gel (Figure 2.6). As seen in Figure 2.6, a higher ZupT-expressing colony was isolated.

2.3.4 Purification of ZupT

After the newly made construct ZupT/pBAD/mycHis-P was retransformed into LMG194, as described in the Appendix of this manuscript, an overnight culture was grown with 1 of the colonies resulting from the transformation, to $OD_{600} = 0.10$, followed by growth of a 125-ml overnight culture with 1 ml of the previously grown culture, to $OD_{600} = 1.71$. This culture was used to grow 2-L cultures in a shaker at 37°C for 3.5 h until $OD_{600} = 0.80$. These were induced with 0.4 g of Arabinose, after which the cultures were grown an additional 1.5 h at 37°C. Lastly, the cultures were incubated for 18 h more at 25°C. Final average $OD_{600} = 1.03$ ($n = 3$). The cells were harvested at 7,000 rpm and the average of the obtained pellet was 1.33 g/L ($n = 3$). The combined pellets were resuspended at ~ 7.90 ml/g of cells. The buffer A used for the resuspension included 25 mM Tris, pH 7.0, and 100 mM sucrose. After addition of DNase I the cells were stirred at 4°C for 30 min, after which PMSF was added to a final concentration of 1 mM.

The cells were then lysed twice with a French press at 20,000 p.s.i. and collected immediately into a tube that was kept on ice. 2 mM $MgCl_2$ was added immediately after the French press. The cell suspension was stirred again at 4°C for 30 min. Low speed centrifugation was performed at 8,500 rpm for 40 min. In order to separate the membranes from the soluble fraction of cells, the supernatant from the low speed centrifugation underwent a high speed centrifugation at 45,000 rpm for 1 h. The resulting pellets from high speed centrifugation were resuspended to $OD_{280} = 20$ with the following buffer B: 25 mM Tris, pH 7.0, 100 mM sucrose, 500 mM NaCl, and 1 mM 2-BME. Then at 4°C Triton X-100 was added very slowly, while stirred, to a final concentration of 2%. The suspension was stirred at 4°C for 1 h. The above

underwent ultra-centrifugation at 45,000 rpm for 80 min in order to remove the insoluble fraction. A charged, 5-ml bed, Ni^{2+} - pro-bond column was prepared by successive washes of 50 ml dH_2O and 15 ml of buffer C (25 mM Tris, pH 7.0, 100 mM sucrose, 500 mM NaCl, 1 mM PMSF, 1 mM 2-BME, and 2 mM DDM). The supernatant, resulting from ultra-centrifugation, was loaded onto the column and washed with 50 ml of buffer C, 100 ml of buffer C and 50 mM Imidazole, 50 ml of buffer C and 100 mM Imidazole, and the protein was finally eluted with 20 ml of buffer C and 300 mM Imidazole. 1 ml fractions were collected during the elution step and checked for the presence of protein with a bichinchonic acid assay (Sigma), while using bovine serum albumin as standard. The protein-containing fractions were concentrated with an Ultracel-10 kDa centricon (Millipore), at 3,500 rpm until desired volume was achieved. The Imidazole was removed with a use of a 40-ml Sephadex G-25 column. The protein fractions were concentrated again with an Ultracel-10 kDa centricon. Finally, the aliquots of the protein were stored at -80°C with a final 10% glycerol concentration, which was used as a cryoprotectant.

2.3.5 Characterization of ZupT using Fluorescence Spectroscopy

The samples for the fluorescence spectroscopy analysis were prepared in HPLC H_2O with 10 mM Tris, pH 7.0, and 2 mM DDM. 10 μM protein concentration of ZupT was used for all experiments. Metal solutions utilized for the experiments were made in mqH_2O at 1 mM and 10 mM final concentrations. After each addition of a metal solution, the samples were thoroughly mixed by inversion of the cuvet 20 times, with parafilm used as a stopper. The samples were excited at 290 nm and the emission scans were taken from 300-500 nm.

2.3.6 Characterization of ZupT with UV-Visible spectroscopy

Here, same protein, buffer and metal concentrations were used as for fluorescence studies described above. Scans were taken from 190 nm-900 nm in order to find any changes due to the binding of the metal tested. Later scans were narrowed down to a 190 nm-500 nm range for Fe.

2.3.7 Obtaining metal binding stoichiometry with ICP-MS

The metal concentrations were measured with the use of a PE Sciex Elan 9000 ICP-MS with a cross-flow nebulizer and Scott type spray chamber. The RF power used during the analysis was 1000 W, and the argon flow was optimized at 0.92 L/min. All the metal standards used were obtained from VWR.

10 μ M protein samples were prepared in the buffer (HPLC H_2O with 10 mM Tris, pH 7.0, and 2 mM DDM) along with 150 μ M final metal concentration. All metals were added very slowly with a 10 μ l syringe, after which samples were thoroughly mixed. Samples were then incubated for 20 min and then loaded onto a 1.5-ml Sephadex G-25 column. The column was washed with 15 ml mqH_2O and 4.5 ml of the sample buffer (HPLC H_2O with 10 mM Tris, pH 7.0, and 2 mM DDM). The samples were passed through the column and eluted with the above described buffer. BCA assay was utilized to identify the protein-containing fractions and those were concentrated to a minimum volume at 3,500 rpm using an Ultracel-10 kDa centricon. The washing of the column and eluting the sample were repeated once more for a total of 2 times in order to wash out the excess/unbound metal. BSA assay was performed to measure the exact protein concentration of the samples: duplicate readings were taken at 562 nm.

The samples were then prepared for ICP-MS analysis, using final concentrations of 2% Nitric acid in all samples. At last, the samples were diluted with HPLC water to 2 ml final volume.

Final binding stoichiometry was obtained by first calculating all the metal and protein concentrations to uM units and then dividing the metal concentrations by the protein concentrations.

2.4 Results

2.4.1 ZupT sequence analysis

As a result of CLUSTALW2 Multiple Sequence Alignment (European Bioinformatics Institute) the following 2 conserved regions, inside TM IV and V, were found within *E.coli* ZupT sequence and its homologues throughout the different kingdoms (Figure 2.2).

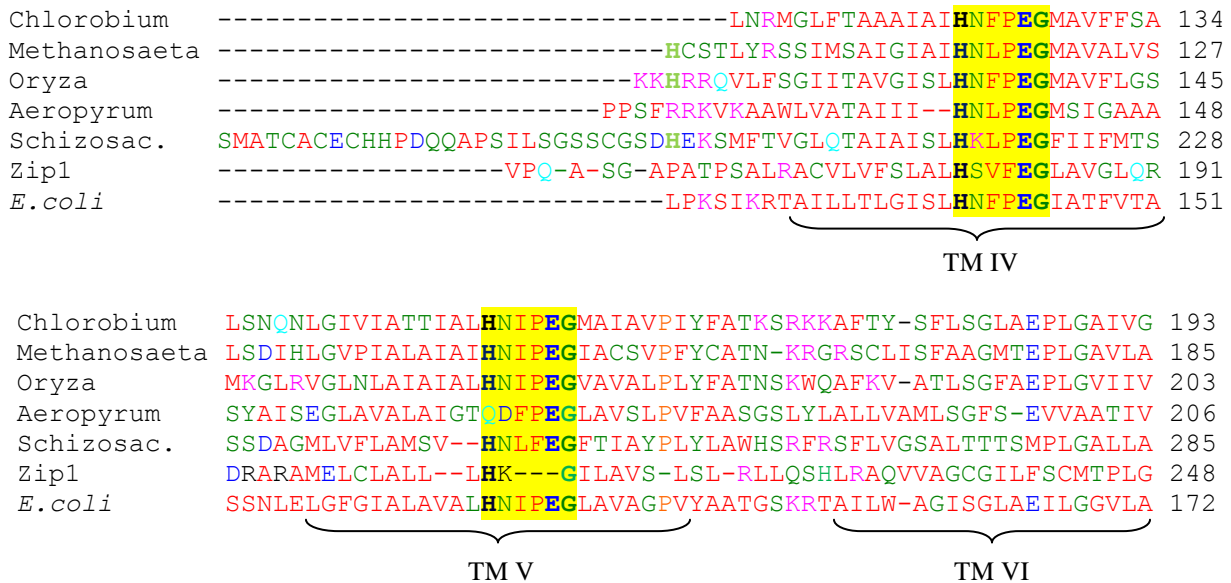


Figure 2.2

Two homologically-conserved regions in ZupT

*Only the conserved regions are presented.

2.4.2 Optimization of ZupT expression

After obtaining a log phase growth curve for ZupT in pBAD/mycHis-C, in LMG194, a double-selection protocol was utilized in order to obtain a high-expressing ZupT colony in LMG194. The original ZupT expressions of 7 freshly-transformed colonies of ZupT in pBAD/mycHis-C, in LMG194, with 1 used as a negative control (uninduced), were compared on a western blot, after which colony # 5* was chosen as the 1st selection (Figure 2.3).



Figure 2.3

Western blot comparison of ZupT expression before 1st selection

Legend:

1. Negative Control (uninduced)
2. Colony 1
3. Colony 2
4. Colony 3
5. Colony 4
6. Colony 5*
7. Colony 6

Colony #5 resulting from the 1st selection was compared to colony #3 resulting from the 2nd selection (Figure 2.4).

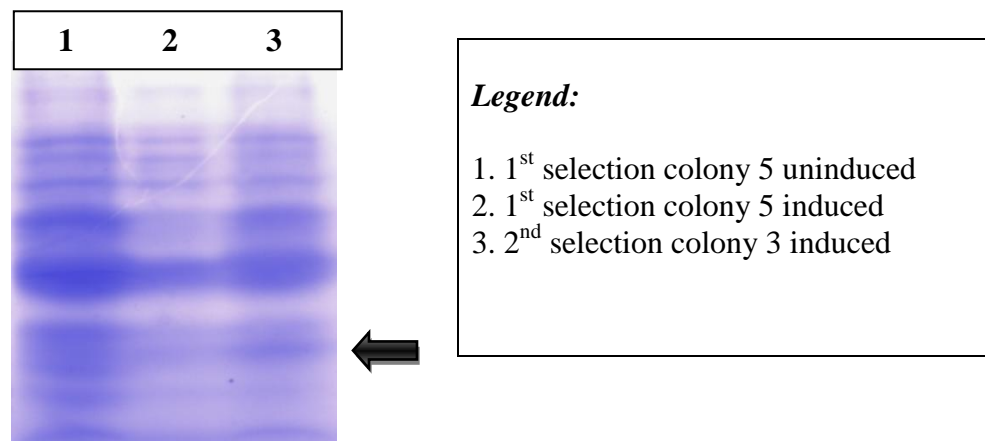


Figure 2.4

Resulting colonies from 1st selection and 2nd selections were compared on a 12% SDS gel

2.4.3 ZupT purification

The fractions collected during ZupT/pBAD/mycHis-P purification were analyzed along with the purified ZupT on a 12% SDS gel Figure 2.5 (A) and a 15% SDS gel Figure 2.5 (B).

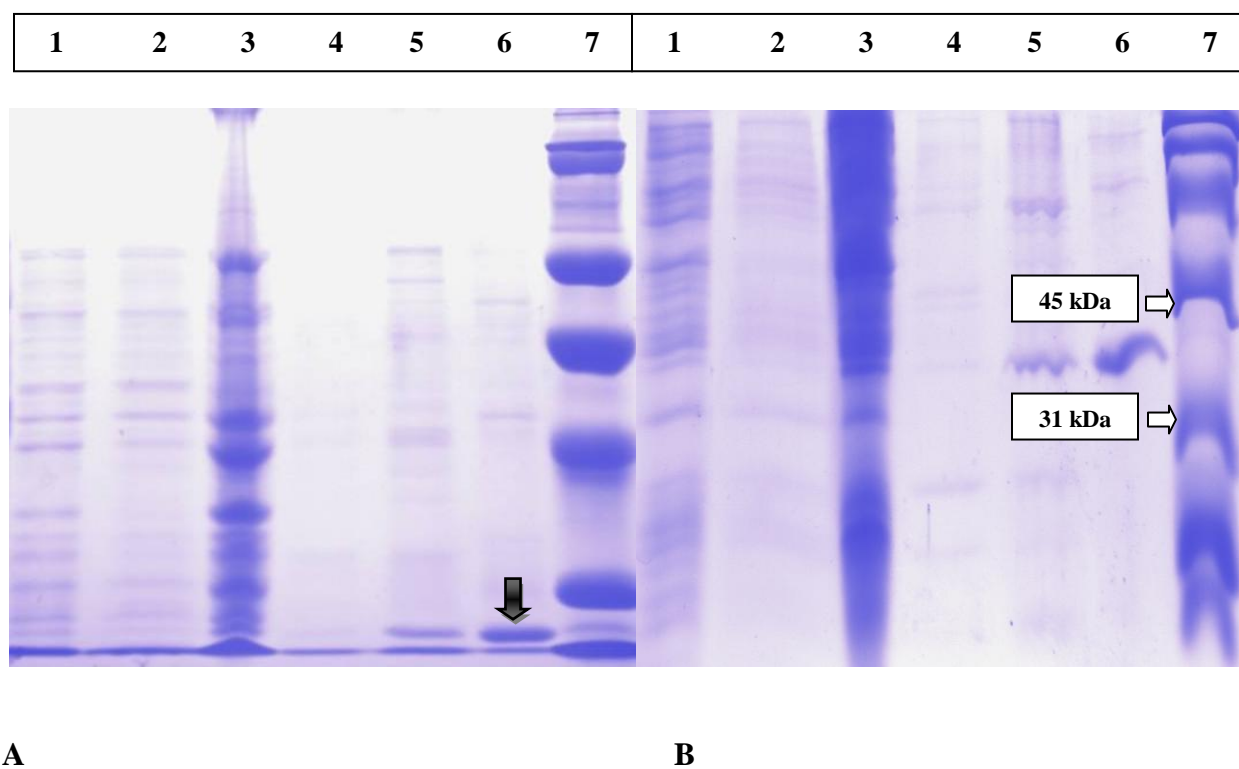


Figure 2.5

SDS gels with fractions obtained during ZupT/pBAD/mycHis-P purification: (A) a 12% SDS gel and (B) a 15% SDS gel.

Legend:

1. HSP1 - 1st high speed pellet
2. HSS2 - 2nd high speed supernatant
3. HSP2 - 2nd high speed pellet
4. 100mM-Imidazole buffer
5. 300mM-Imidazole buffer
6. Purified ZupT concentrated
7. Marker

2.4.4 ZupT characterization

Fluorescence characterization of ZupT/pBAD/mycHis-P was conducted in order to evaluate its metal binding specificities. 10 μ M ZupT/pBAD/mycHis-P was used throughout the characterization experiments along with a neutral pH buffer, which was deemed optimum for ZupT's transport activity (119). All the samples were excited at 290 nm.

2.4.4.1 Titration of fluorescence emission of ZupT with Cd

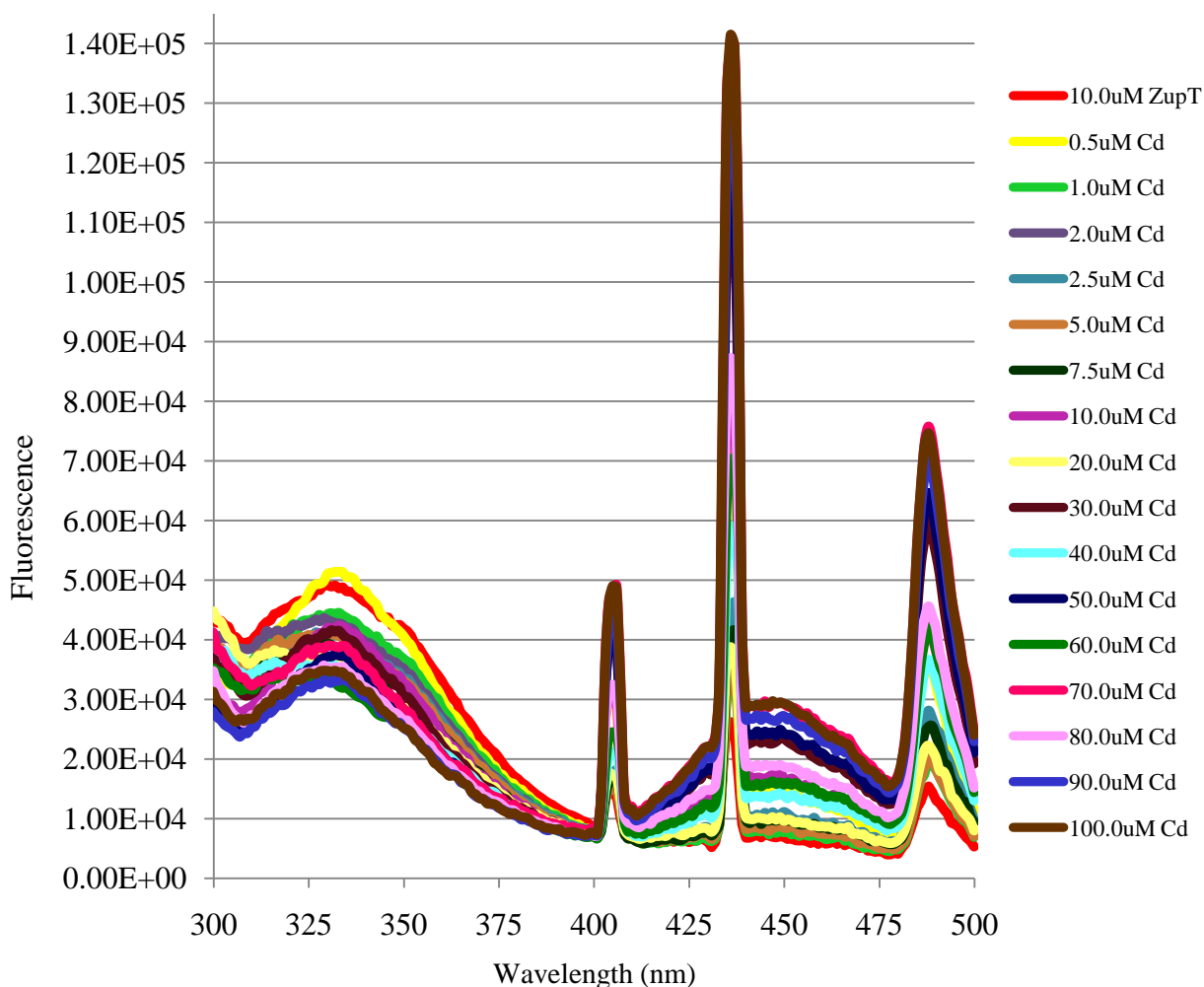


Figure 2.6

300–500 nm emission spectrum of ZupT/pBAD/mycHis-P with Cd

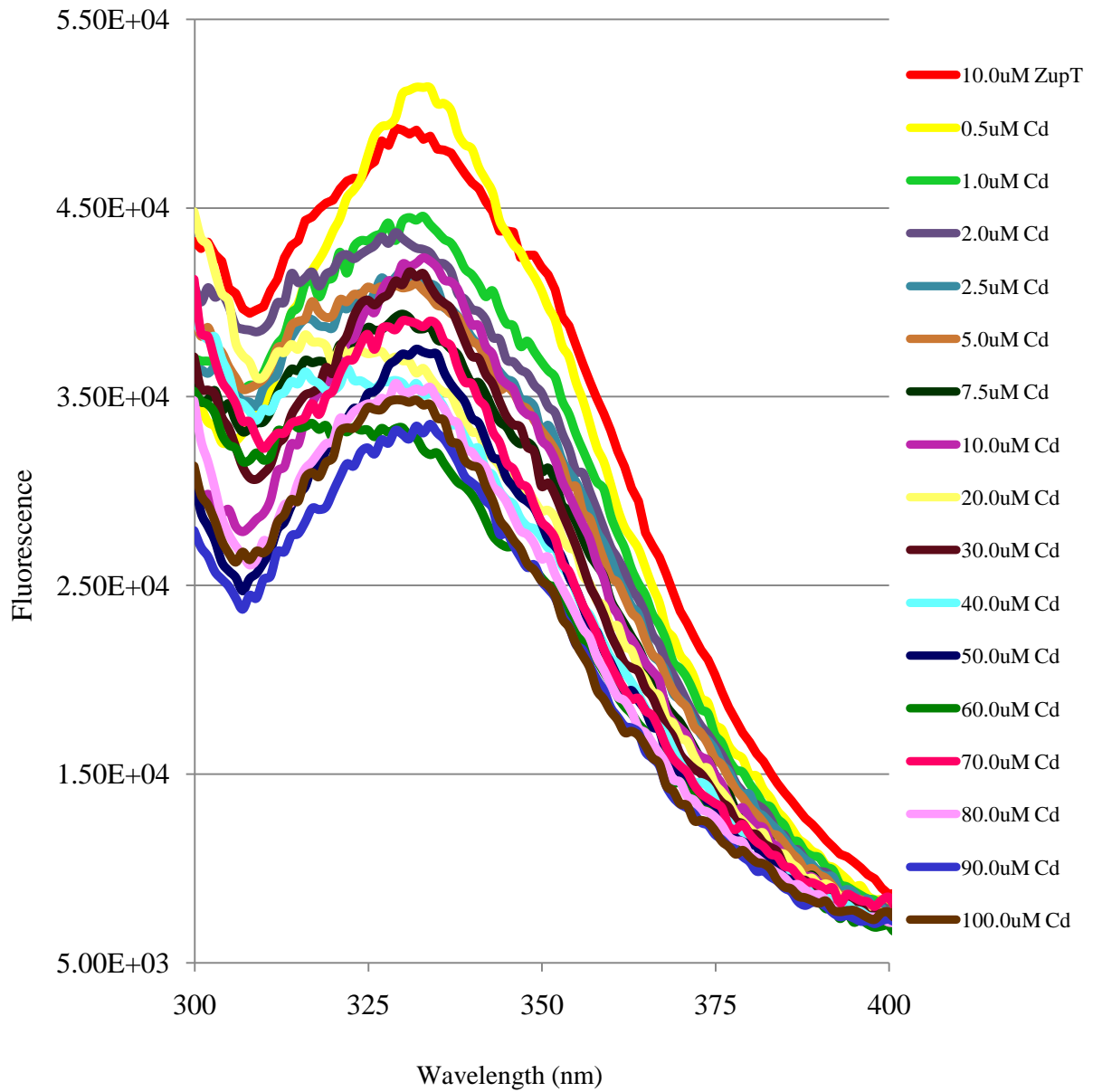


Figure 2.7

300-400 nm emission spectrum of ZupT/pBAD/mycHis-P with Cd

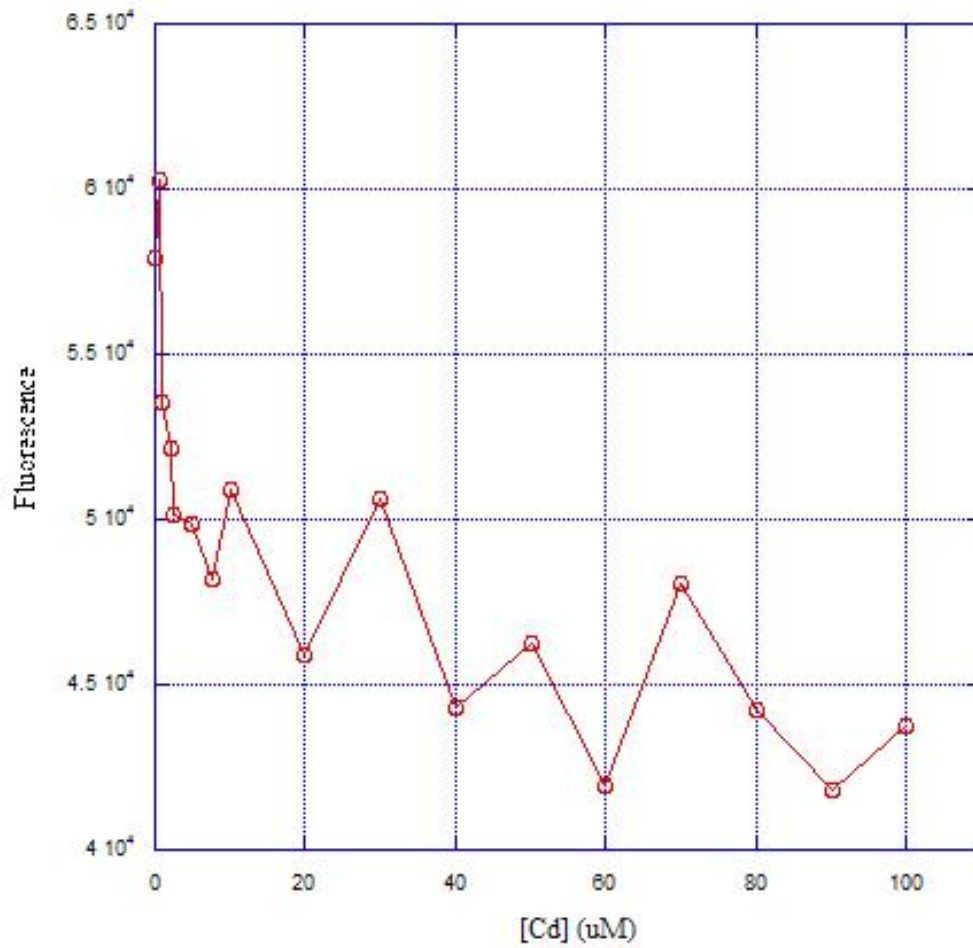


Figure 2.8

Fluorescence study 330.9 nm peak analysis: Fluorescence vs. [Cd] (uM)

2.4.4.2 Titration of fluorescence emission of ZupT with Fe

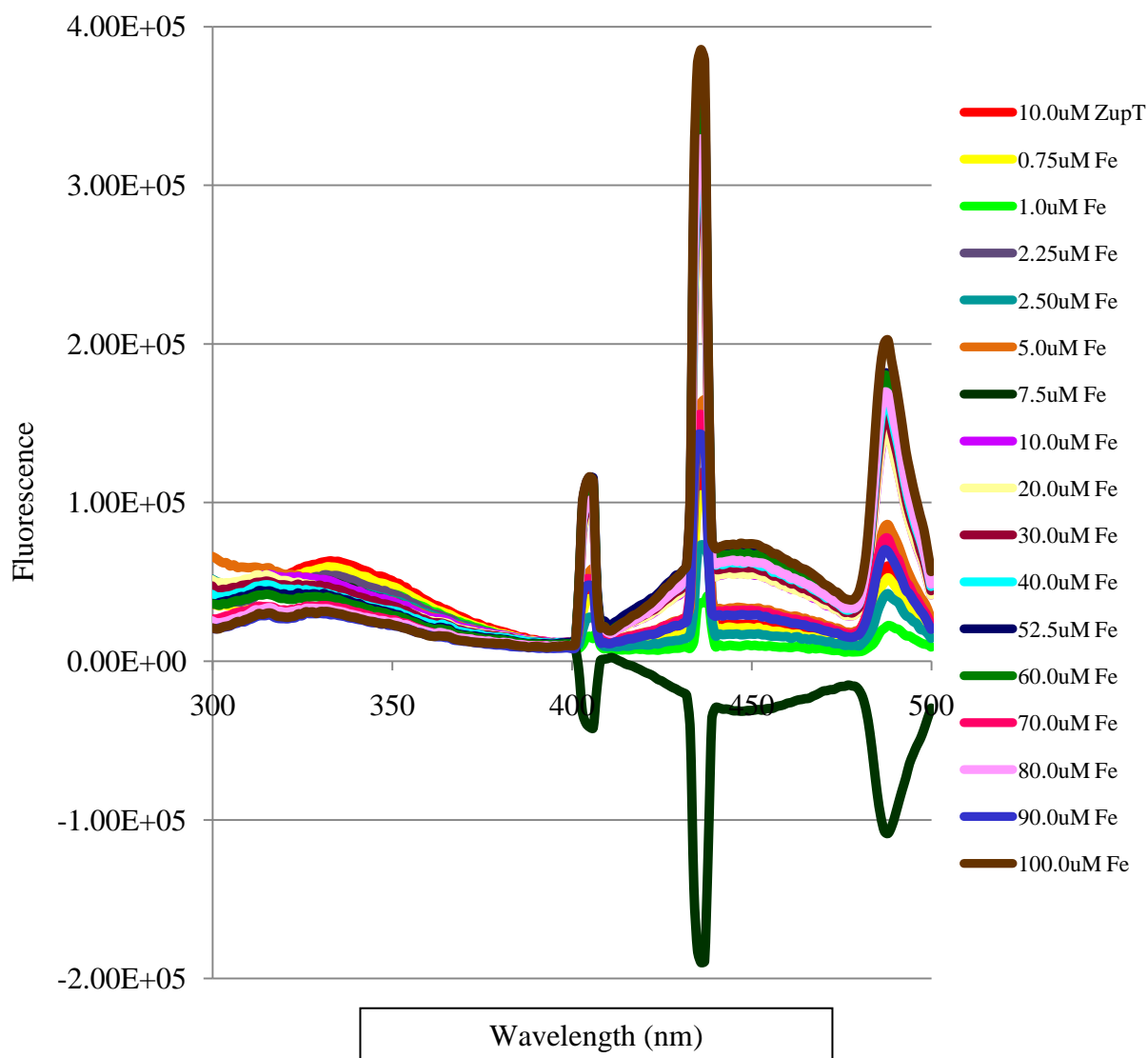


Figure 2.9

300-500 nm emission spectrum of ZupT/pBAD/mycHis-P with Fe

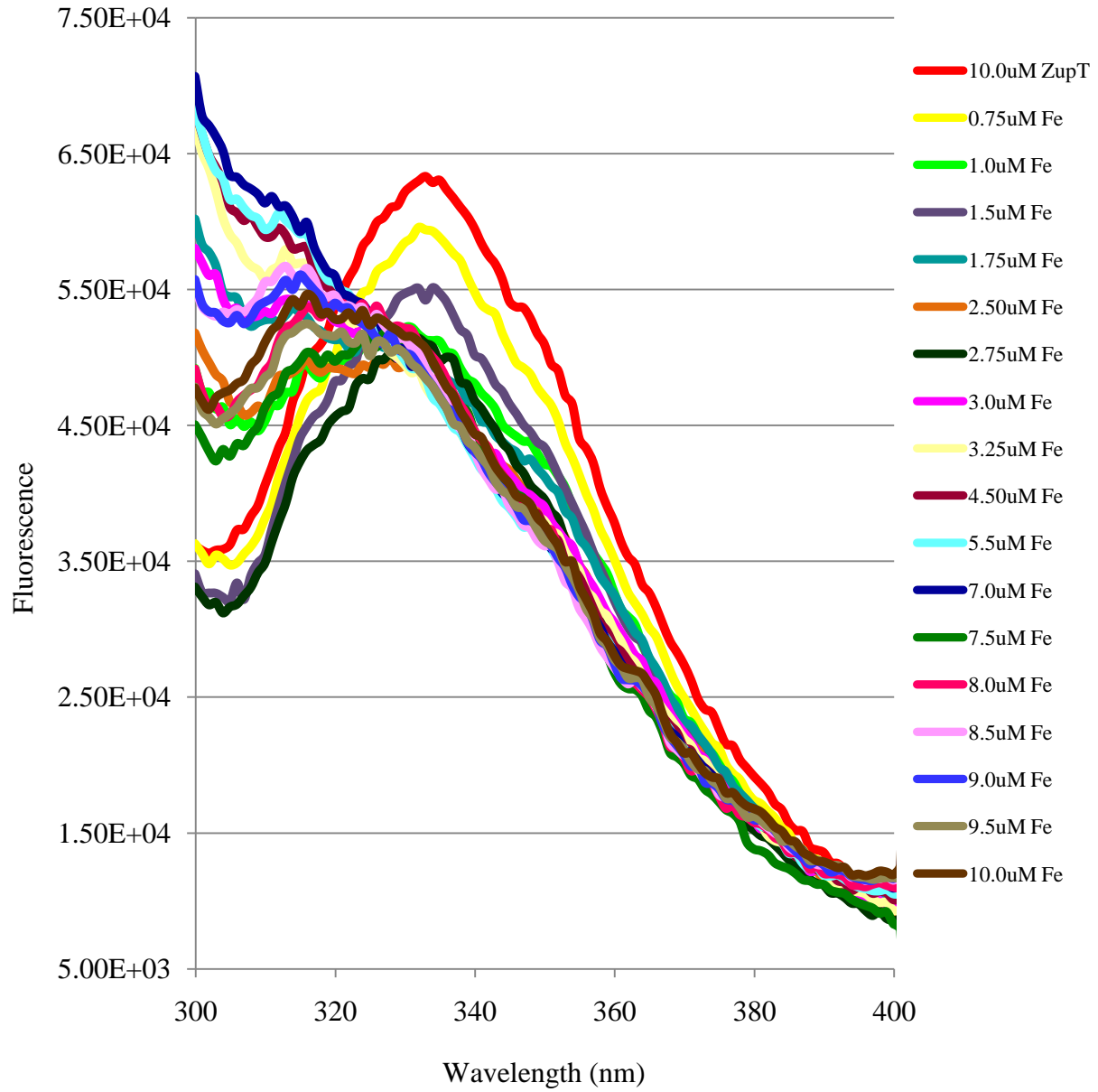


Figure 2.10A

300-400 nm emission spectrum of ZupT/pBAD/mycHis-P with ↓ [Fe]

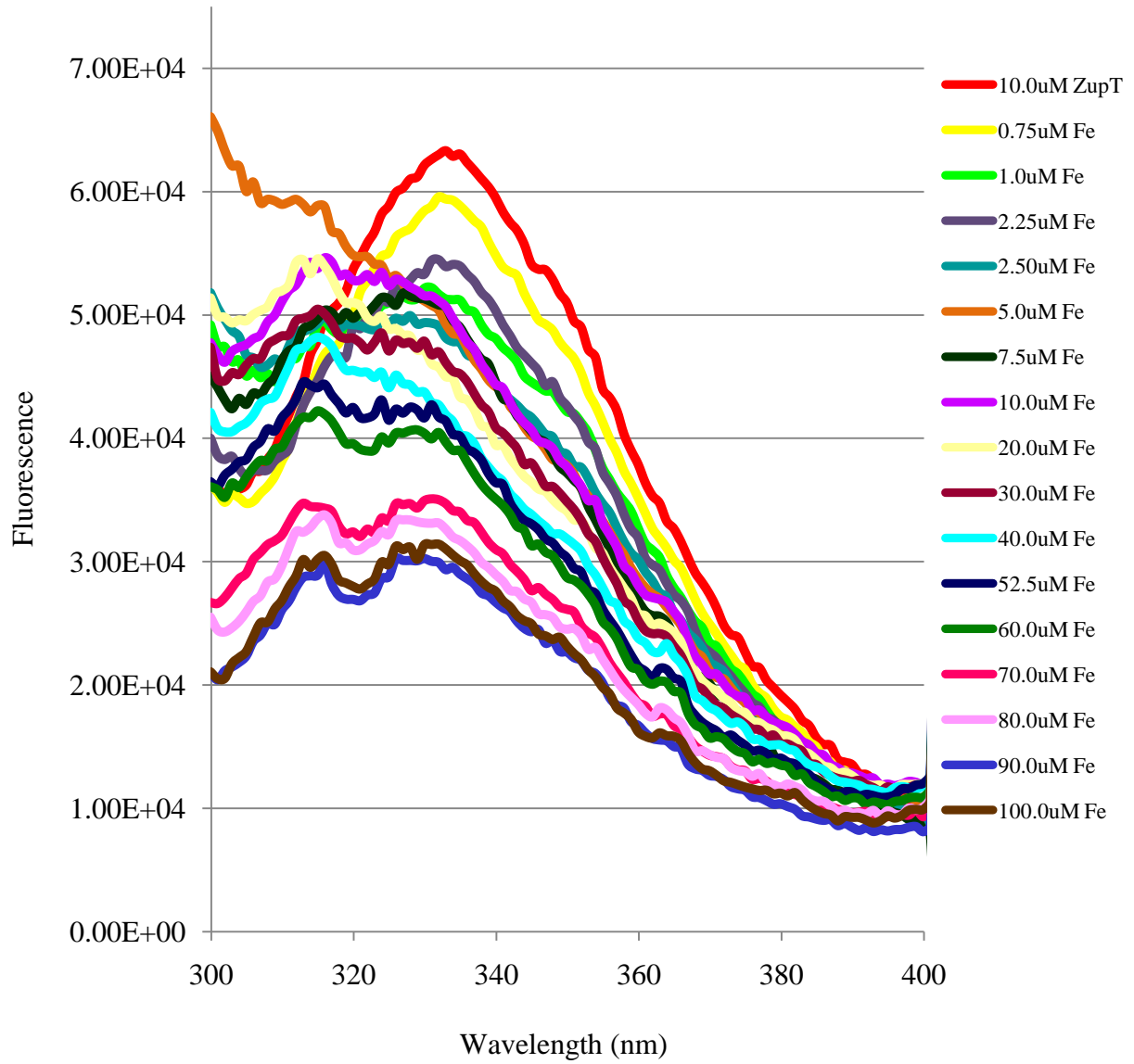


Figure 2.10B

300-400 nm emission spectrum of ZupT/pBAD/mycHis-P with \uparrow [Fe]

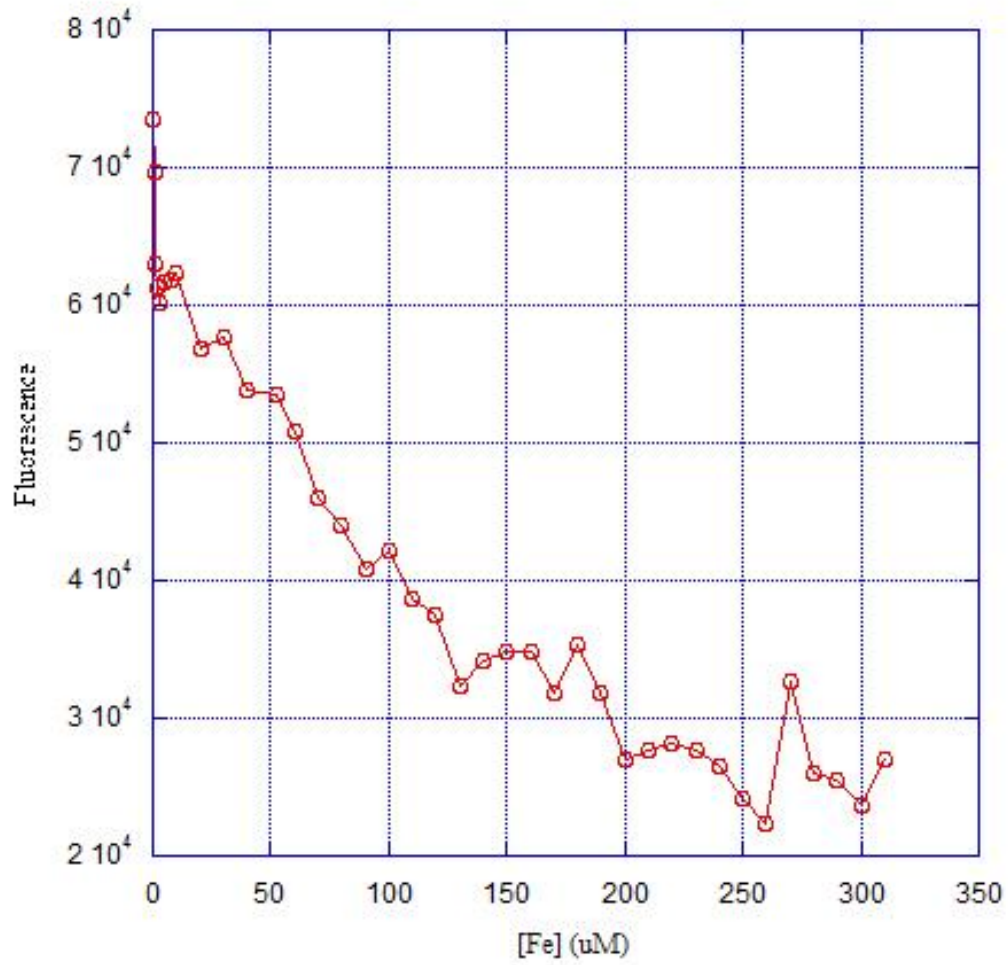


Figure 2.11

Fluorescence study 330.9 nm peak analysis: Fluorescence vs. [Fe] (uM)

2.4.4.3 UV-Visible spectroscopy study with Fe

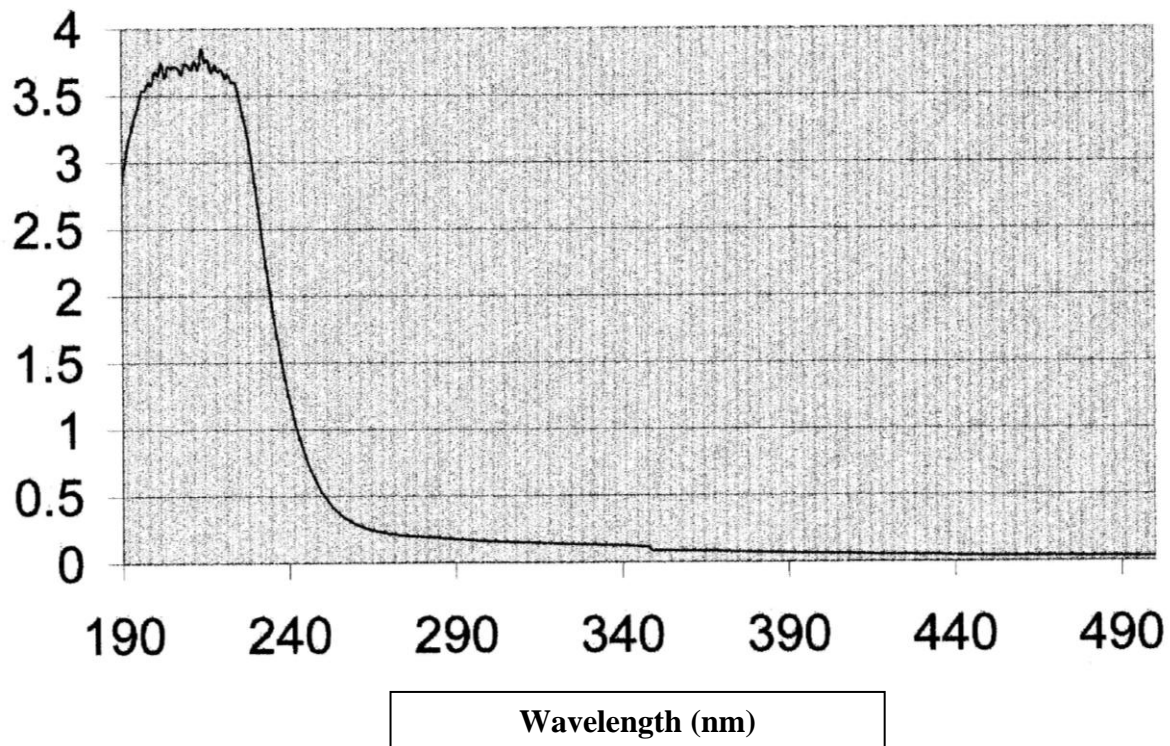


Figure 2.12

10 uM ZupT/pBAD/mycHis-P UV-Vis absorbance peak

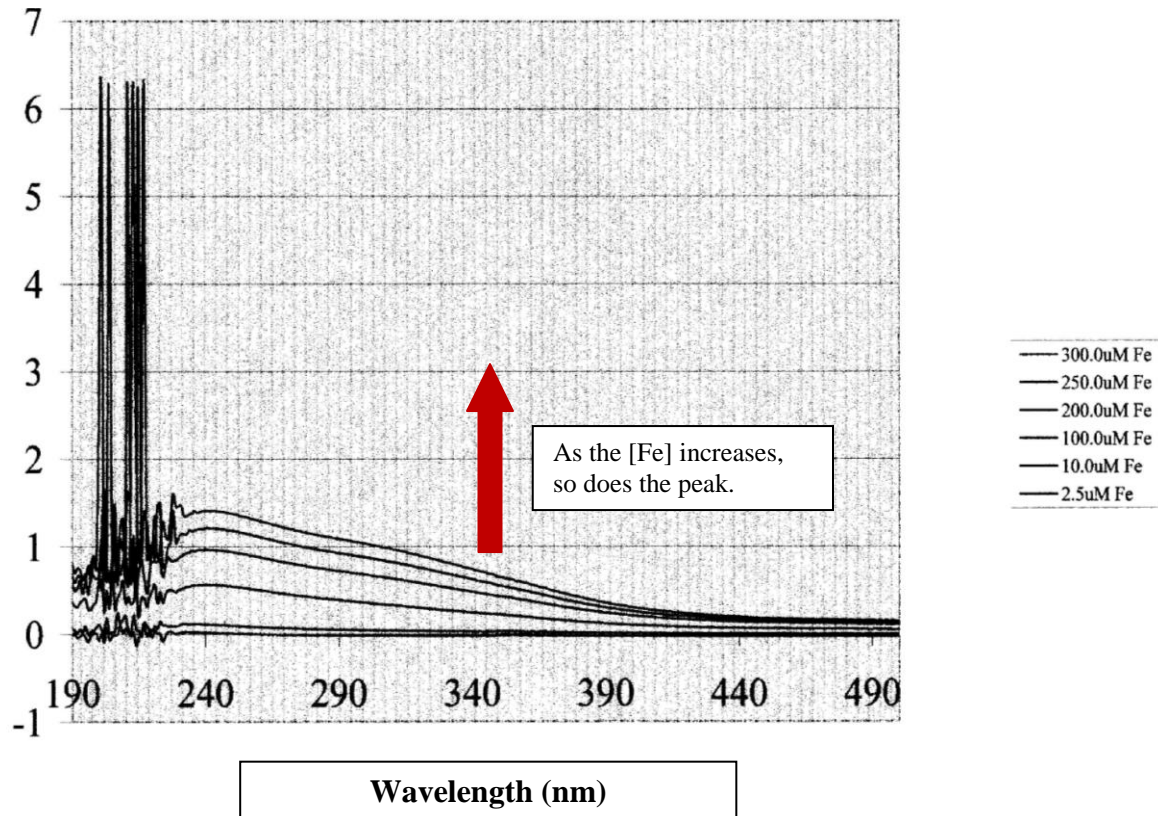


Figure 2.13

Fe UV-Vis peak minus the ZupT/pBAD/mycHis-P absorbance peak

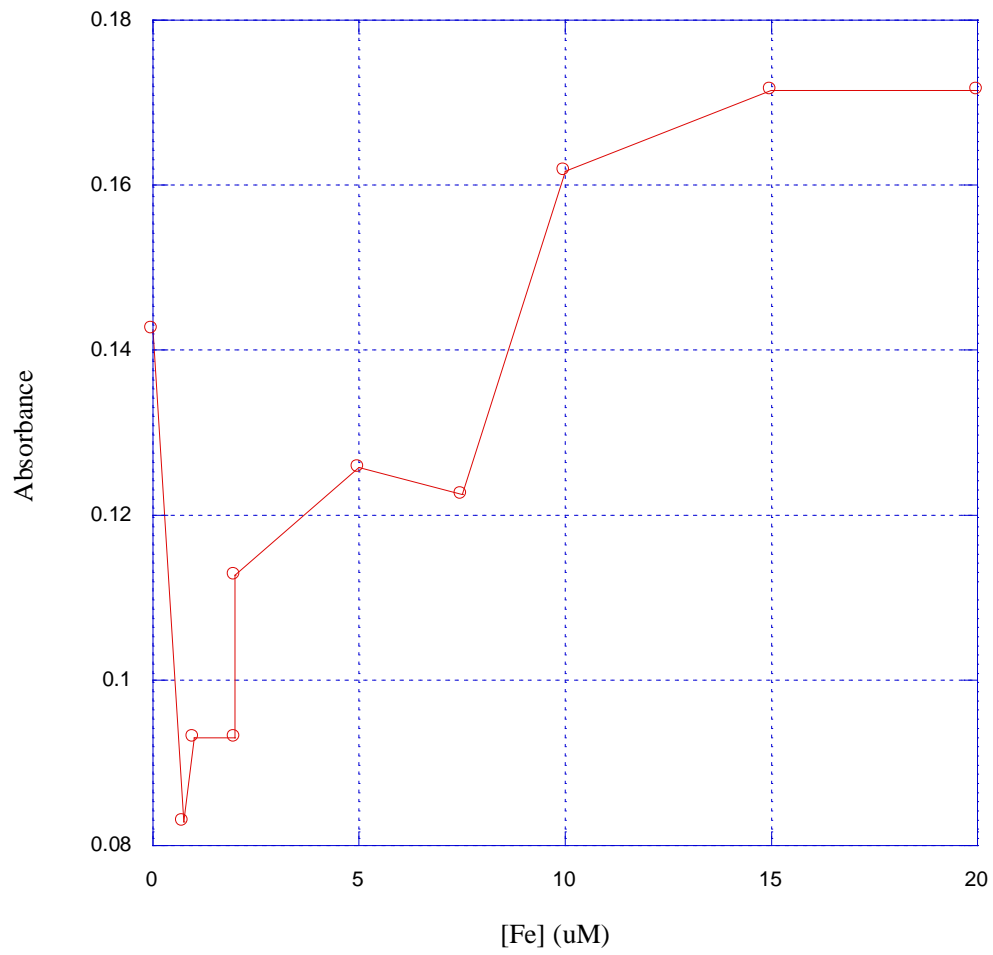


Figure 2.14

UV-Vis 329.6 nm peak analysis: Absorbance vs. [Fe] (uM)

2.4.4.4 Titration of fluorescence emission of ZupT with Pb

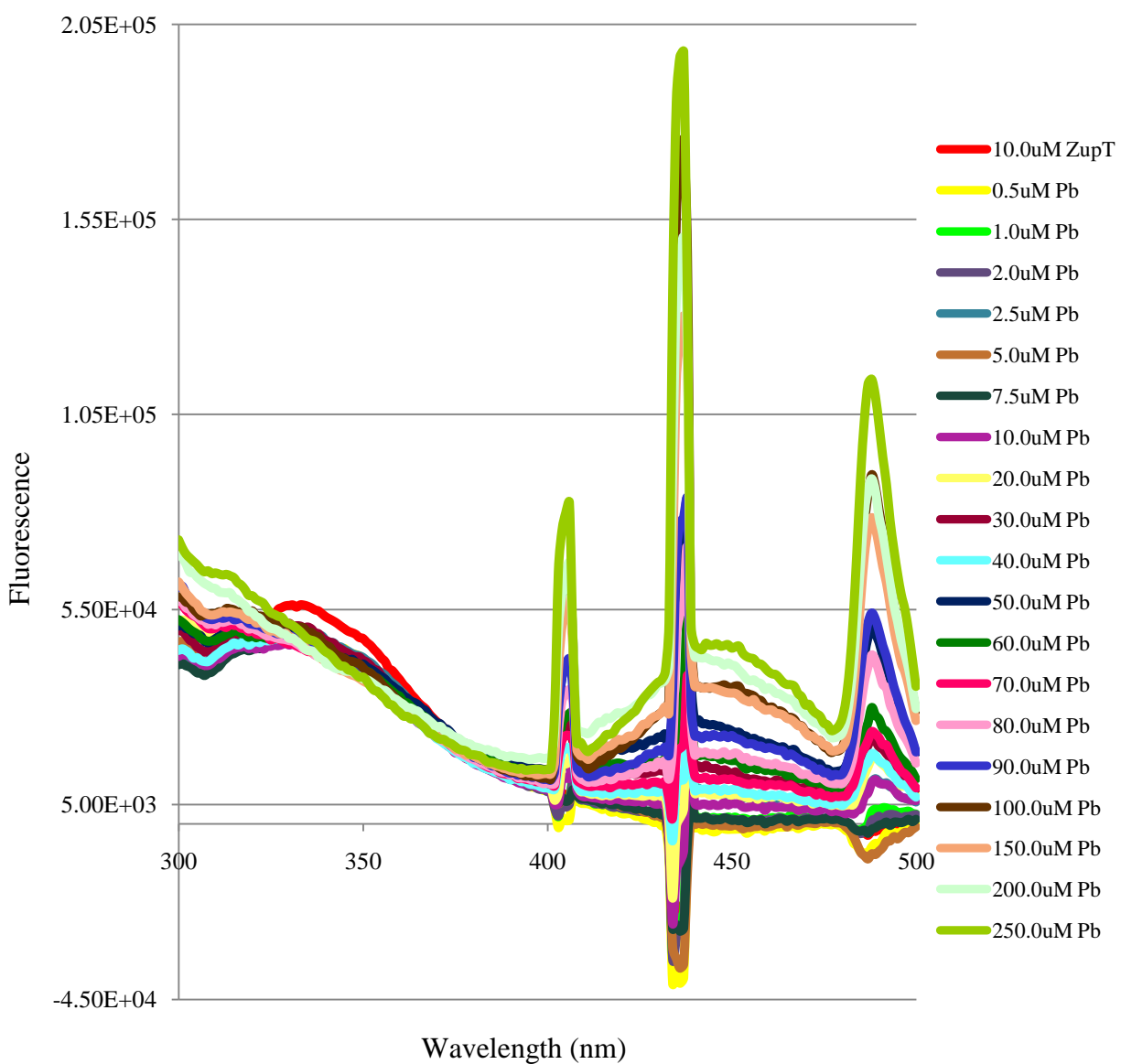


Figure 2.15

300-500 nm emission spectrum of ZupT/pBAD/mycHis-P with Pb

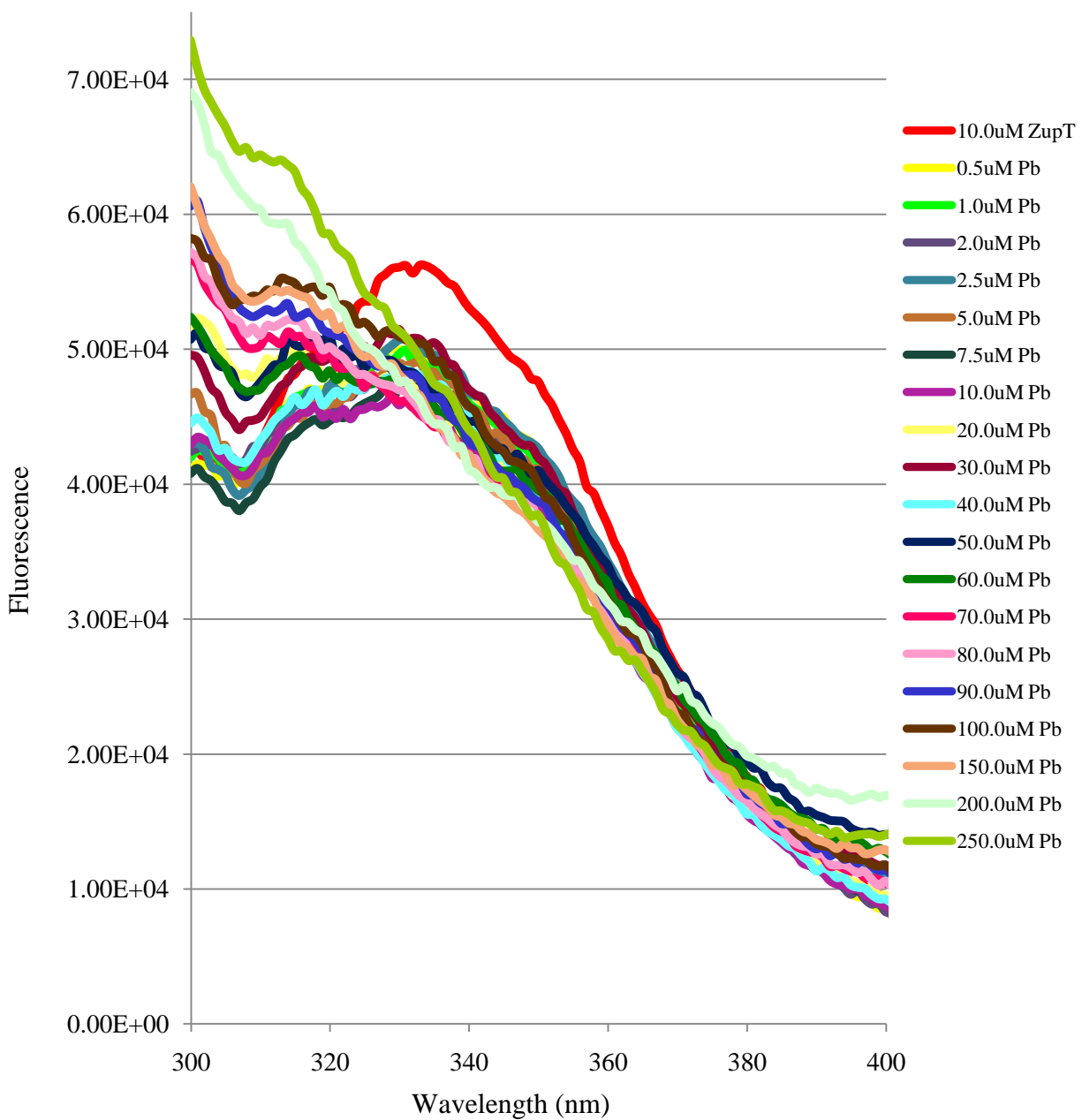


Figure 2.16

300-400 nm emission spectrum of ZupT/pBAD/mycHis-P with Pb

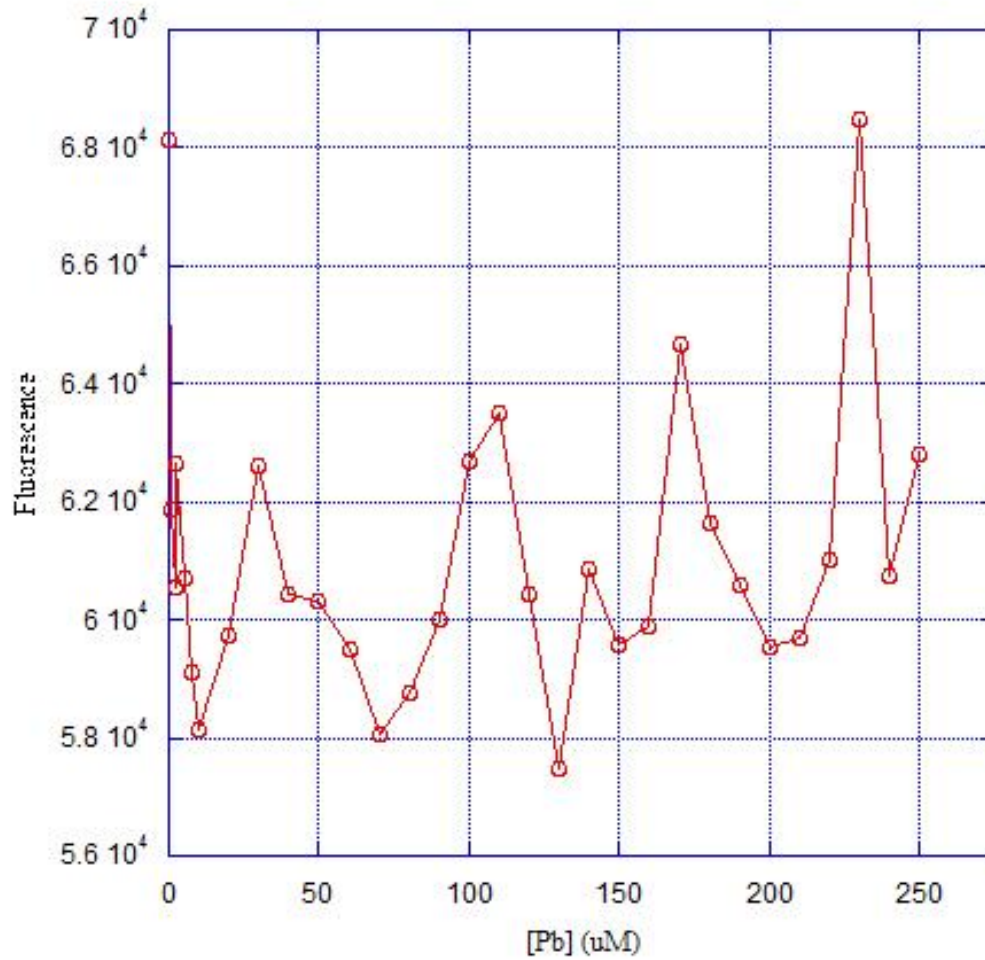


Figure 2.17

Fluorescence study 330.9 nm peak analysis: Fluorescence vs. [Pb] (uM)

2.4.4.5 Titration of fluorescence emission of ZupT with Zn

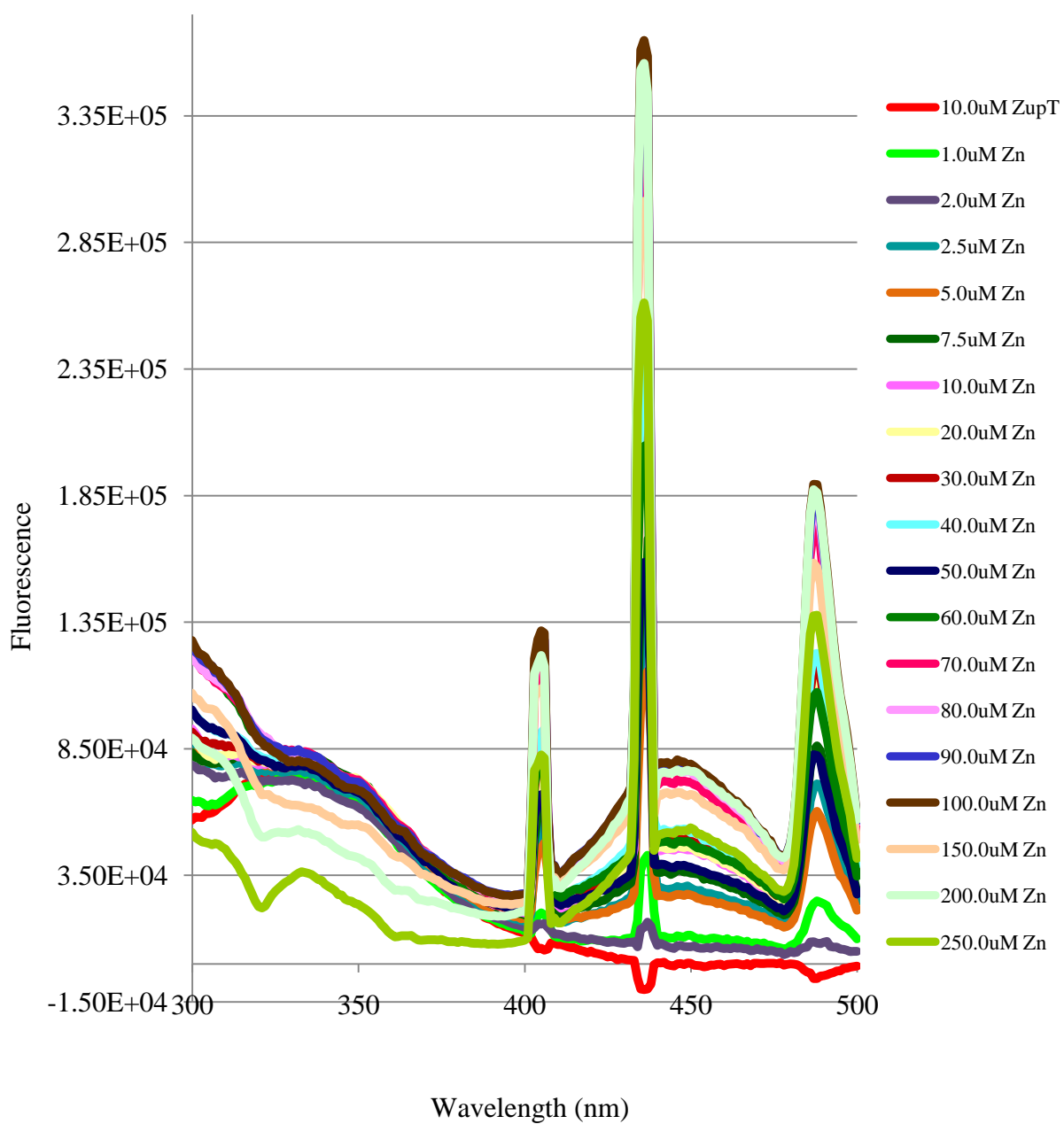


Figure 2.18

300-500 nm emission spectrum of ZupT/pBAD/mycHis-P with Zn

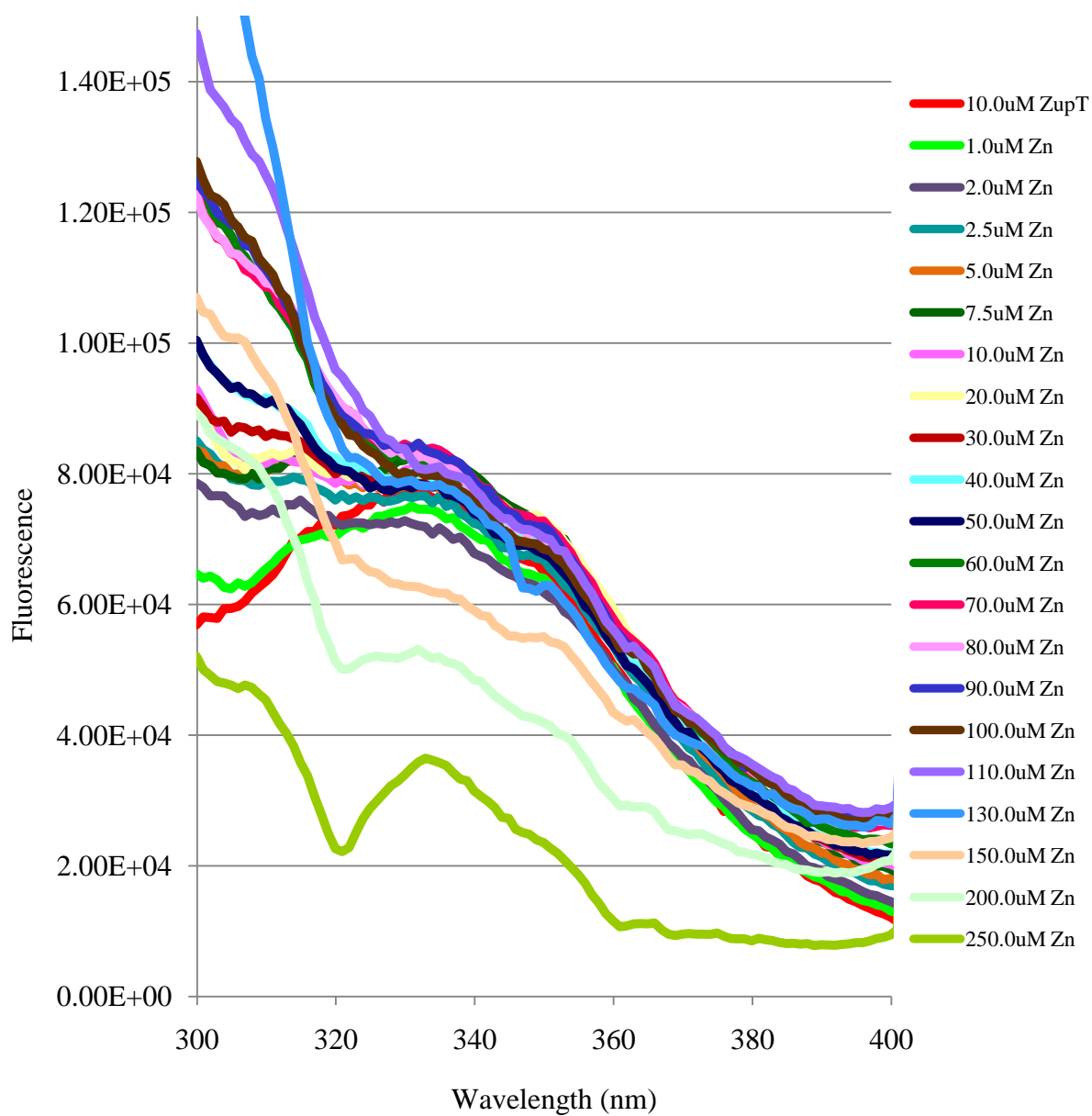


Figure 2.19

300-400 nm emission spectrum of ZupT/pBAD/mycHis-P with Zn

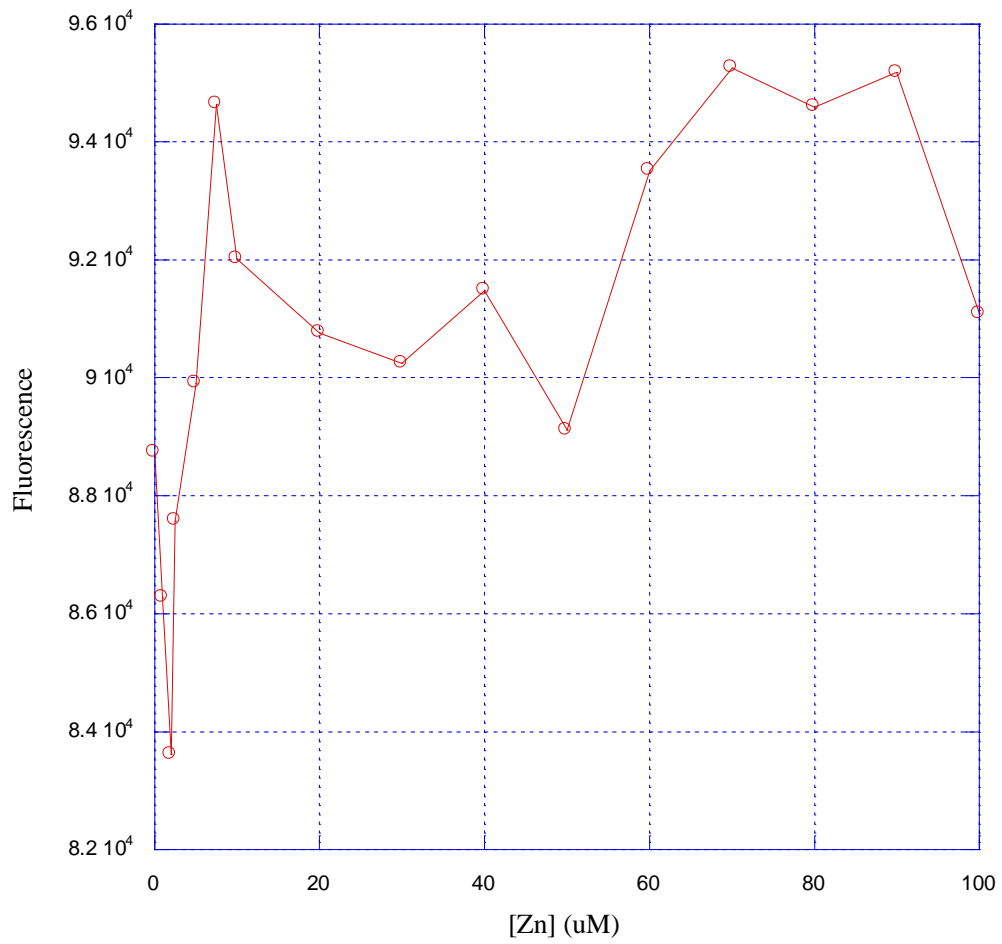


Figure 2.20

Fluorescence study 330.9 nm peak analysis: Fluorescence vs. [Zn] (uM)

2.4.4.6 ICP-MS metal binding stoichiometries

Table 2.2 ICP-MS ZupT/pBAD/mycHis-P metal binding stoichiometries

Metal	ZupT/pBAD/mycHis-P binding stoichiometry
Cd²⁺	32.03 ± 0.03
Pb²⁺	0.07 ± 0.0
Zn²⁺	6.09 ± 0.0

2.5 Discussion

As a result of this study a successful protocol has been established for purification of ZupT. The detailed purification procedure for ZupT is outlined in Appendix (p. 79) of this manuscript. It was found that the lysing of the cells with a French press was more efficient if the resuspended cells were treated with DNase I before the lysing. In addition, while the membrane was solublized with Triton X-100, it was crucial to use DDM and not Triton X-100 in all of the washing/eluting buffers during the ZupT purification. For protein characterization purposes DDM was also a better suited eluting detergent than Triton X-100 because Triton X-100 produces absorbance at 280 nm and below.

Moreover, optimization of ZupT expression was successfully achieved through a double-selection method (Figures 2.3 & 2.4). ZupT, which has been described by others and observed personally as a low-expressing protein, is now expressed enough to be seen from a cell fraction on an SDS gel (Figure 2.4) (55, 119). After utilizing this method, the optimum growth and induction conditions for ZupT were also obtained: with initial growth at 37°C, for 3.5 h, with induction at OD₆₀₀ of 0.8, followed by additional 1.5 h of growth at 37°C, and finally 18 more hours of growth at 25°C.

All the characterization techniques of ZupT were conducted using neutral pH buffers, which were previously mentioned as to be optimum for its binding efficiency (119). The above results of the fluorescence studies showed that the technique itself is a reliable technique for studying metal binding for a transmembrane protein, such as ZupT. The original ZupT/pBAD/mycHis-P fluorescence peak resulted from the presence of 2 Tryptophan residues residing at 173 and 189 amino acid sequence. All four metals showed a notable blue-shifting of

the original peak. The peak shifted from ~330.9 nm to forming a second peak at ~313.9 nm, and then depending on the metal it was binding, increasing metal concentration resulted in the overall peak shifting back to the original one, as seen with Cd, or eventually showed a steady increase at the newly made peak, as apparent with Pb. Blue-shifting is characteristic of the metal-binding environment becoming more non-polar.

Overall ZupT/pBAD/mycHis-P's fluorescence gradually decreased with the increased Cd concentration (Figure 2.8). There was an increase in the fluorescence observed at 0.05 μ M Cd: 1.0 μ M ZupT/pBAD/mycHis-P at ~ 330.9 nm, followed by blue-shifting of the peak to forming a second peak at ~315.0 nm (Figure 2.7). At 1.0 μ M Cd: 1.0 μ M ZupT/pBAD/mycHis-P the peak at ~315.0 nm disappeared and only a peak at 330.9 nm was prominent. The 330.9 nm peak decreased drastically at 2.0 μ M Cd: 1.0 μ M ZupT/pBAD/mycHis-P and blue-shifted again to ~315.0 nm. At 6.0 μ M Cd: 1.0 μ M ZupT/pBAD/mycHis-P both peaks seemed to have reached saturation. Last jump in fluorescence, at 330.9 nm, was observed at 7.0 μ M Cd: 1.0 μ M ZupT/pBAD/mycHis-P after which the fluorescence kept decreasing staying at the original peak range (Figures 2.7, 2.8). Analysis of the 330.9 nm peak suggested two possible binding sites: one with a high affinity and another one with a lower affinity (Figure 2.8). ICP-MS results for Cd binding to ZupT showed a 2-fold higher concentration of Pb in the sample along with Cd, which was deemed unacceptable. Overall, the Cd stoichiometry for the sample was 32.03 Cd to 1 ZupT/pBAD/mycHis-P.

The data obtained from the fluorescence study with Fe revealed possible binding of Fe to ZupT. The original 330.9 nm peak blue-shifted at 0.1 μ M Fe: 1.0 μ M ZupT/pBAD/mycHis-P ratio to ~313.9 nm (Figure 2.10A). At 0.15 μ M Fe: 1.0 μ M ZupT/pBAD/mycHis-P ratio the peak

shifts back to the original peak at ~330.9 nm and an increase in fluorescence is observed (Figure 2.10A). With increased fluorescence intensity, the peak blue-shifted and increased once more at 0.175 μM Fe: 1.0 μM ZupT/pBAD/mycHis-P ratio. There was a decrease of the fluorescence observed, at 313.9 nm peak, when 0.25 μM Fe: 1.0 μM ZupT/pBAD/mycHis-P ratio was reached. Furthermore, there was another shift back to 330.9 nm peak at 0.275 μM Fe: 1.0 μM ZupT/pBAD/mycHis-P ratio. An additional blue-shift was observed at 0.3 μM Fe: 1.0 μM ZupT/pBAD/mycHis-P ratio. This peak kept increasing until 0.7 μM Fe: 1.0 μM ZupT/pBAD/mycHis-P ratio is reached, at which point there was a drastic decrease at 0.75 μM Fe: 1.0 μM ZupT/pBAD/mycHis-P ratio, at which point the peak drastically dropped to the original saturation level (Figure 2.10A). After 0.75 μM Fe: 1.0 μM ZupT/pBAD/mycHis-P ratio, the fluorescence of the 313.9 nm kept increasing until 0.85 μM Fe: 1.0 μM ZupT/pBAD/mycHis-P ratio after which it began decreasing with one last jump in fluorescence at 1.0 μM Fe: 1.0 μM ZupT/pBAD/mycHis-P ratio ratio (Figure 2.10A, 2.10B). UV-Visible spectroscopic studies have also shown possible binding of Fe by the presence of an increasing broad range peak from ~230.0 nm – 390.0 nm (Figure 2.13). Further analysis of absorbance vs. [Fe] (μM) suggested two binding sites with first saturation at 0.25 μM Fe: 1.0 μM ZupT/pBAD/mycHis-P ratio, and a second saturation at 1.0 μM Fe: 1.0 μM ZupT/pBAD/mycHis-P ratio (Figure 2.14). ICP-MS sample with Fe was prepared and is awaiting analysis to shine more light on stoichiometry between Fe and ZupT.

There is a striking resemblance between Cd's and Fe's final fluorescence saturations: 7.0 μM Cd: 1.0 μM ZupT/pBAD/mycHis-P ratio for Cd and 0.7 μM Fe: 1.0 μM ZupT/pBAD/mycHis-P ratio for Fe. According to this fluorescence data there is a possible 10-

fold difference in affinity between these two metals. It is not surprising that there is a similarity in these fluorescence profiles, because according to Frank Thévenod, Cd is believed to be utilizing Fe's uptake pathways for its transport in mammalian cells (48). The same can be expected in *E.coli* cells.

On the other hand, the data obtained from the fluorescence study with Pb showed what could be described as an unspecific binding with an overall increase in fluorescence (Figure 2.17). The original peak at ~330.9 nm saturated at 1.0 uM Pb: 1.0 uM ZupT/pBAD/mycHis-P (Figure 2.16). Then at 2.0 uM Pb: 1.0 uM ZupT/pBAD/mycHis-P the peak blue-shifted from ~330.9 nm to forming a second peak at ~313.9 nm after which it shifted back again to the original peak at 4.0 uM Pb: 1.0 uM ZupT/pBAD/mycHis-P. Finally, the peak blue-shifts one last time at 5.0 uM Pb: 1.0 uM ZupT/pBAD/mycHis-P after which there is a steady increase of fluorescence at ~313.9 nm peak (Figures 2.15, 2.16). ICP-MS data showed a binding stoichiometry of 0.07 Pb 207 to 1 ZupT/pBAD/mycHis-P. This shows that Pb is not bound to ZupT with high affinity; the changes in fluorescence reflect non-specific weak binding.

The data obtained from the fluorescence binding study with Zn showed a possible saturation of 2 metal-binding sites (Figure 2.20). The original peak at ~330.9 nm blue-shifted to ~313.9 nm at 0.2 uM Zn: 1.0 uM ZupT/pBAD/mycHis-P (Figure 2.19). The newly formed peak, along with the original peak, continued to increase up to 5.0 uM Zn: 1.0 uM ZupT/pBAD/mycHis-P ratio. Afterwards, the peak jumped higher and remained there until 10.0 uM Zn: 1.0 uM ZupT/pBAD/mycHis-P ratio is reached (Figure 2.19). Then another jump in fluorescence was observed at 11.0 uM Zn: 1.0 uM ZupT/pBAD/mycHis-P ratio, after which there is a significant decrease in fluorescence which places the peak below the previous level of

saturation. Another increase in fluorescence is observed at 13.0 μM Zn: 1.0 μM ZupT/pBAD/mycHis-P ratio, after which both peaks at 313.9 nm and 330.9 nm decrease steadily (Figure 2.19). ICP-MS data showed a binding stoichiometry of 6.09 Zn to 1 ZupT/pBAD/mycHis-P. Few of these could be coordinating at the two conserved Histidines within ZupT itself, but also there's a possibility of the His tag, found at the end of the sequence, also binding the Zn atoms. However, metal binding to the His tag may or may not affect Trp fluorescence.

2.6 Future Direction

The importance of the *ZIP* family of metal transporters throughout the kingdoms is indisputable. Future investigation is needed in order to elucidate more structural data on one of its more easy to characterize members: ZupT. Fluorescence studies are useful in investigating different metals that ZupT might, and might not bind, as well as their possible affinities. UV-Visible spectroscopy can also be useful in confirming binding of colored metals by ZupT. Although, the number of binding sites, within ZupT, should only be investigated with fluorescence studies while using very tightly-regulated metal titrations. ICP-MS studies have shown to provide most reliable data and should be done for all investigated metals following the procedure utilized during this study. Similar analysis should be performed for all the mutants constructed during this study to further investigate the importance of the proposed metal binding sites within ZupT.

Although these studies were conducted with a His-tagged ZupT, and will be repeated in the future with non-tagged ZupT, they indicate that both fluorescence and UV-Visible absorbance methods can be used to study metal binding to ZupT. Overall, different metals

caused different changes in fluorescence, indicating that these changes were not solely due to the His tag. Additionally, repeating these studies with the non-His-tagged mutant proteins will help to determine whether these residues contribute to metal binding.

APPENDIX A: ZupT purification procedure

1. The new construct ZupT/pBAD/mycHis-P was retransformed into LMG194 strain as follows:
 - 50 ul aliquot of WT-LMG194 competent cells were thawed on ice for 30 min
 - The cells were then transferred to a pre-chilled 15-ml Corning tube
 - Added 1 nanogram, 2 ul, of the plasmid
 - Swirled the mixture and incubated on ice for 30 min
 - Heat-shocked the cells at 42°C for 1 min
 - Incubated again on ice for 2 min
 - Added 500 ul of preheated to 42°C LB media
 - Incubated the tube, in the shaker, at 37°C for 1 h
 - Plated the cells on 2 Amp/LB plates
 - Incubated overnight at 37°C
2. A 5 ml LB/ 5 ul Amp culture was grown with 1 of the colonies, resulting from the transformation, up to $OD_{600} = 0.10$.
3. An overnight culture of 125 ml LB/ 125 ul Amp was grown with 1 ml of the culture from number 2.
4. For each 2-L of culture the following was added:
 - 2 L of autoclaved LB media
 - 0.2 g Amp
 - 25 ml of the overnight culture from 3 above ($OD_{600} = 1.71$).
5. Incubated in a shaker at 37°C for 3.5 h until $OD_{600} = 0.80$.
6. Induced each 2-L culture with 0.4 g of Arabinose.
7. The cultures were grown for an additional 1.5 h at 37°C.
8. Lastly, the cultures incubated for 18 h at 25°C.
9. Final average $OD_{600} = 1.03$ ($n = 3$).
10. Cells were harvested at 7,000 rpm.
11. Average pellet obtained per 2 L of culture was 2.66 g ($n = 3$).
12. The combined pellets were resuspended, approximately 7.90 ml of the buffer per 1 g of cells, with the following **Buffer A** ($V_T = 150$ ml):

- 7.5 ml 0.5 M Tris (pH = 7)
- 15 ml 0.1 M Sucrose
- 127.5 ml dH₂O

13. After addition of DNase I the cells were stirred at 4°C for 30 min.

14. PMSF was added to a final concentration of 1 mM.

15. The cells were French pressed 2 times and collected immediately into a tube that was kept on ice.

16. 2 mM MgCl₂ was added immediately after the French press along with PMSF.

17. The cell suspension was stirred again at 4°C for 30 min.

18. Low speed centrifugation at 8,500 rpm for 40 min.

19. Supernatant from low speed centrifugation underwent a high speed centrifugation at 45,000 rpm for 1 h.

20. The resulting pellets from high speed centrifugation were resuspended to OD₂₈₀ = 20 with the following **Buffer B** (V_T = 300 ml):

- 204.79 ml dH₂O
- 50 ml 3 M NaCl
- 30 ml 1 M Sucrose
- 15 ml 0.5 M Tris (pH = 7)
- 21 µl 2-BME

21. Added 2% Triton X-100: very slowly, at 4°C, while stirred.

22. Stirred at 4°C for 1 h.

23. Ultra-centrifuged the above at 45,000 rpm for 80 min.

24. Prepared **Buffer C** (V_T = 400.0 ml):

- 272.6 ml dH₂O
- 66.6 ml 3 M NaCl
- 40.0 ml 1 M Sucrose
- 20.0 ml 0.5 M Tris (pH = 7)
- 0.800 ml 1 M DDM
- 0.021 ml 2-BME
- 0.068 g PMSF

25. Preparation of Ni^{2+} -*pro-bond column*:

- Added 10 ml of the Ni^{2+} -pro-bond solution to the column to make a 5-ml bed
- Passed 50 ml of dH₂O
- Passed 15 ml of **Buffer C**

26. Loaded the supernatant, resulting from ultra-centrifugation in 23.

27. Washed the column:

- 50 ml of **Buffer C**
- 100 ml 50 mM Imidazole in **Buffer C**
- 50 ml 100 mM Imidazole in **Buffer C**
- 20 ml 300 mM Imidazole in **Buffer C**

28. Collected 1 ml fractions after 300 mM Imidazole in **Buffer C**.

29. Performed BCA assay (Sigma) to locate the protein-containing fractions.

30. Concentrated the fractions using an Ultracel-10 kDa centricon (Millipore), at 3,500 rpm until desired volume was achieved.

31. Prepared **Buffer D** ($V_T = 150$ ml):

- 119.7 ml dH₂O
- 15 ml 1 M Sucrose
- 7.5 ml 1 M KCl
- 7.5 ml 0.5 M Tris (pH=7)
- 0.3 ml 1 M DDM
- 0.026 g PMSF

32. Preparation of **G-25 column**:

- Passed 100 ml of dH₂O
- Passed 50 ml of **Buffer D**

33. With barely any buffer remaining on top of the column, loaded my concentrated fraction from 30 above.

34. Allowed the fraction to go into the column and then added 15 ml of **Buffer D** again to the top of the column in order to elute the protein.

35. Collected 1 ml fractions and located the protein utilizing the BCA assay.

36. Pulled the protein-containing fractions and concentrated maximally at 3,500 rpm using an Ultracel-10 kDa centricon (Millipore) again.
37. Made 75 ul aliquots of the protein with a final 10% glycerol concentration.
38. Stored the protein at -80°C.

APPENDIX B: ZupT characterization with Fluorescence Spectroscopy

1. Used the following **Buffer E** ($V_T = 10.0$ ml):

- 8.995 ml HPLC H_2O
- 1.0 ml 0.1 M Bis-Tris (pH = 7)
- 0.005 ml 1.0 M DDM

2. Final volume of the samples was 400.0 μ l:

- 383.83 μ l of the **Buffer E**
- 16.17 μ l of ZupT, or 10.0 μ M ($[ZupT] = 247.36$ μ M)

3. All of the metal solutions were prepared in the following concentrations with mq H_2O :

- 10.0 mM
- 1.0 mM

4. After each addition of a metal solution, the samples were thoroughly mixed by inversion of the cuvet 20 times, with parafilm used as a stopper.

5. The samples were excited at 290 nm and the emission scans were taken from 300-500 nm.

APPENDIX C: ZupT characterization with UV-Visible spectroscopy

ZupT binding to iron was measured with the use of a spectrophotometer. Same ZupT, *Buffer E*, and metal concentrations were used as for fluorescence studies described above.

Scans were taken from 190 nm-900 nm in order to find a forming peak due to the binding of the metal tested. Later scans were narrowed down to a 190 nm-500 nm range.

APPENDIX D: Obtaining metal binding stoichiometry with ICP-MS

1. Sample preparation:

- 283.37 μ l **Buffer F** (0.1 M Bis-Tris, pH = 7, with 2 mM DDM)
 - 12.13 μ l ZupT/pBAD/mycHis-P [247.36 μ M]: 10 μ M final concentration
 - 4.5 μ l metal [10 mM]: 150 μ M final concentration
- $V_T = 300.0$ μ l

2. All metals were added very slowly with a 10.0 μ l syringe, after which samples were thoroughly mixed. Samples were then incubated for 20 min and then loaded onto a G-25 column.

3. Preparation of G-25 column, with a bed of 1.5 ml:

- 15.0 ml of mqH₂O
- 4.5 ml of **Buffer F**

4. The samples were passed through the column and eluted with the above described **Buffer F**.

5. BCA assay was utilized to identify the protein-containing fractions and those to a minimum volume centrifuging at 3,500 rpm using an Ultracel-10 kDa centricon (Millipore).

6. # 3 above was repeated to wash out the excess metal and the samples were passed through the column again.

7. BSA assay was performed to measure the exact protein concentration of the samples: took duplicate readings at 562 nm.

8. Prepared the samples for ICP-MS analysis:

- used maximum V of all the samples
- added Nitric acid to a final concentration of 2%
- diluted the samples with HPLC water to 2 ml final V

9. Calculated final binding stoichiometry for all metals: first calculated metal and protein concentrations to μ M units, and then divided metal concentrations by protein concentrations.

REFERENCES

1. A.B. Chausmer (1998) Zinc, insulin and diabetes, J. Am. Coll. Nutr. 17, 109–115.
2. Ammendola, S., Pasquali, P., Pistoia, C., Petrucci, P., Petrarca, P., Rotilio, G., and Battistoni, A. (2007) High-affinity Zn^{2+} uptake system ZnuABC is required for bacterial zinc homeostasis in intracellular environments and contributes to the virulence of *Salmonella enteric*, Infect. Immun. 75, 5867–5876.
3. Andreini, C., Banci, L., Bertini, I., and Rosato, A. (2006) Counting the zinc-proteins encoded in the human genome, J. Proteome Res. 5, 196–201.
4. Andreini, C., Banci, L., Bertini, I., and Rosato, A. (2006) Zinc through the three domains of life, J Proteome Res 5, 3173–3178.
5. A. Schützendübel and A. Polle (2002) Plant responses to abiotic stresses: heavy metal-induced oxidative stress and protection by mycorrhization, Journal of Experimental Botany 53, 1351–1365.
6. Assunção, A.G.L., Costa Martins, P.D.A., De Folter, S., Vooijs, R., Schat, H., and Aarts, M.G.M. (2001) Elevated expression of metal transporter genes in three accessions of the metal hyperaccumulator *Thlaspi caerulescens*, Plant, Cell and Environment 24, 217–226.
7. Aydemir, T.B., Liuzzi, J.P., McClellan, S., and Cousins, R.J. (2009) Zinc transporter ZIP8 (SLC39A8) and zinc influence IFN-gamma expression in activated human T cells, J Leukoc Biol 86, 337–348.
8. Begum, N.A., Kobayashi, M., Moriwaki, Y., Matsumoto, M., Toyoshima, K., and Seya, T. (2002) Mycobacterium bovis BCG cell wall and lipopolysaccharide induce a novel gene, BIGM103, encoding a 7-TM protein: identification of a new protein family having Zn-

- transporter and Zn-metalloprotease signatures, *Genomics* 80, 630–645.
9. Bergeron, M.J., Simonin, A., Bhrzle, M., and Hediger, M.A. (2008) Inherited epithelial transporter disorders—an overview, *J Inherit Metab Dis.* 31, 178–187.
 10. Berg, J. M., and Shi, Y. G. (1996) *Science* 271, 1081–1085.
 11. B.L. Vallee and D.S. Auld (1990) Zinc coordination, function, and structure of zinc enzymes and other proteins, *Biochemistry* 29, 5647–5659.
 12. Bughio, N., Yamaguchi, H., Nishizawa, N.K., Nakanishi, H., and Mori, S. (2002) Cloning an iron-regulated metal transporter from rice, *Journal of Experimental Botany* 53, 1677–1682.
 13. Campoy, S., Jara, M., Busquets, N., Perez De Rozas, A.M., Badiola, I., and Barbe, J. (2002) Role of the high-affinity zinc uptake znuABC system in *Salmonella enterica* serovar typhimurium virulence, *Infect Immun* 70, 4721–4725.
 14. Cao, J., Bobo, J. A., Liuzzi, J. P., and Cousins, R. J. (2001) *J. Leukocyte Biol.* 70, 559–566.
 15. Carter, J.E., Truong-Tran, A.Q., Grosser, D., Ho, L., Ruffin, R.E., and Zalewski, P.D. (2002) Involvement of redox events in caspase activation in zinc-depleted airway epithelial cells. Visualization of labile zinc and its role in apoptosis of primary airway epithelial cells and cell lines, *Biochem. Biophys. Res. Commun.* 297, 1062–1070.
 16. C.E. Outten and T.V. O’Halloran (2001) Femtomolar sensitivity of metalloregulatory proteins controlling zinc homeostasis, *Science* 292, 2488–2492.
 17. C.G. Taylor (2005) Zinc, the pancreas, and diabetes: insights from rodent studies and future directions, *Biometals* 18, 305–312.
 18. Cherny, R.A., Atwood, C.S., Xilinas, M.E., Gray, D.N., Jones, W.D., McLean, C.A.,

- Barnham, K.J., Volitakis, I., Fraser, F.W., Kim, Y., Huang, X., Goldstein, L.E., Moir, R.D., Lim, J.T., Beyreuther, K., Zheng, H., Tanzi, R.E., Masters, C.L., and Bush, A.I. (2001) Treatment with a copper-zinc chelator markedly and rapidly inhibits beta-amyloid accumulation in Alzheimer's disease transgenic mice, *Neuron* 30, 665–676.
19. Chimienti, F., Devergnas, S., Favier, A., and Seve, M. (2004) Identification and cloning of a β -cell-specific zinc transporter, ZnT-8, localized into insulin secretory granules, *Diabetes* 53, 2330–2337.
20. Chowanadisai, W., Kelleher, S.L., and Lonnerdal, B. (2005) Zinc deficiency is associated with increased brain zinc import and LIV-1 expression and decreased ZnT-1 expression in neonatal rats, *J. Nutr.* 135, 1002–1007.
21. Connolly, E.L., Fett, J.P., and Guerinot, M.L. (2002) Expression of the IRT1 metal transporter is controlled by metals at the levels of transcript and protein accumulation, *The Plant Cell* 14, 1347–1357.
22. Corbin, B.D., Seeley, E.H., Raab, A., Feldmann, J., Miller, M.R., Torres, V.J., Anderson, K.L., Dattilo, B.M., Dunman, P.M., and Gerads, R., et al. (2008) Metal chelation and inhibition of bacterial growth in tissue abscesses, *Science* 319, 962–965.
23. Costello, L.C., Liu, Y., Zou, J., and Franklin, R.B. (1999) *J. Biol. Chem.* 274, 17499–17504.
24. Courville, P., Urbankova, E., Rensing, C., Chaloupka, R., Quick, M., and Cellier, M.F. (2008) Solute carrier 11 cation symport requires distinct residues in transmembrane helices 1 and 6, *J Biol Chem* 283, 9651–9658.
25. Cousins, R. J., Blanchard, R.K., Popp, M.P., Liu, L., Cao, J., Moore, J.B., and Green, C.L. (2003) *Proc. Natl. Acad. Sci. U.S.A.* 100, 6952–6957.

26. Cousins, R.J., Liuzzi, J.P., and Lichten, L.A. (2006) Mammalian zinc transport, trafficking, and signals, *J. Biol. Chem.* 281, 24085–24089.
27. C.P. Kirschke and L. Huang (2003) ZnT-7, a novel mammalian zinc transporter, accumulates zinc in the Golgi apparatus. *J Biol Chem* 278, 4096–4102.
28. David J. Eide (2004) The SLC39 family of metal ion transporters, *Pflugers Arch - Eur J Physiol* 447, 796–800.
29. Davis, L.M., Kakuda, T., and DiRita, V.J. (2009) A *Campylobacter jejuni* *znuA* orthologue is essential for growth in low-zinc environments and chick colonization, *J Bacteriol* 191, 1631–1640.
30. D. Eide (1997) *Curr. Opin. Cell Biol.* 9, 573–577.
31. de Luis, D.A., Izaola, O., Aller, R., Armentia, A., and Cuellar, L. (2003) Antioxidant and fat intake in patients with polinic asthma, *Med. Clin. (Barc)* 121, 653–654.
32. Devereux, G., Turner, S.W., Craig, L.C., McNeill, G., Martindale, S., Harbour, P.J., Helms, P.J., and Seaton, A. (2006) Low maternal vitamin E intake during pregnancy is associated with asthma in 5-year-old children, *Am. J. Respir. Crit. Care Med.* 174, 499–507.
33. Devirgiliisa, C., Zalewskib, P. D., Perozzia, G., and Murgiaa, C. (2007) Zinc fluxes and zinc transporter genes in chronic diseases, *Mutation Research/Fundamental and Molecular Mechanisms of Mutagenesis*, 622(1-2), 84–93.
34. D.J. Eide (1998) The molecular biology of metal ion transport in *Saccharomyces cerevisiae*, *Annual Review of Nutrition* 18, 441–469.
35. D.J. Eide (2006) Zinc transporters and the cellular trafficking of zinc, *Biochim. Biophys. Acta* 1763, 711–722.

36. Duffy, D.L., Martin, N.G., Battistutta, D., Hopper, J.L., and Mathews, J.D. (1990) Genetics of asthma and hay fever in Australian twins, *Am. Rev. Respir. Dis.* 142, 1351–1358.
37. Dufner-Beattie, J., Langmade, S. J., Wang, F., Eide, D., and Andrews, G. K. (2003) Structure, Function, and Regulation of a Subfamily of Mouse Zinc Transporter Genes, *The Journal of Biological Chemistry* 278(50), 50142–50150.
38. Dufner-Beattie, J., Wang, F., Kuo, Y.-M., Gitschier, J., Eide, D., and Andrews, G. K. (2003) *J. Biol. Chem.* 278, 33474–33481.
39. Dutta, S. J., Liu, J., Stemmler, A. J., and Mitra, B. (2007) Conservative and nonconservative mutations of the transmembrane CPC motif in ZntA: Effect on metal selectivity and activity, *Biochemistry* 46, 3692–3703.
40. Eckhardt, U., Margues, A.M., and Buckhout, T.J. (2001) Two iron-regulated cation transporters from tomato complement metal uptake-deficient yeast mutants, *Plant Molecular Biology* 45, 437–448.
41. E.D. Weinberg (2009) Iron availability and infection, *Biochim Biophys Acta* 1790, 600–605.
42. Eide, D., Broderius, M., Fett, J., and Guerinot, M.L. (1996) A novel iron-regulated metal transporter from plants identified by functional expression in yeast, *Proceedings of the National Academy of Sciences, U.S.A.* 93, 5624–5628.
43. Eng, B. H., Guerinot, M. L., Eide, D., and Saier, M. H., Jr. (1998) *J. Membr. Biol.* 166, 1–7.
44. European Bioinformatics Institute
<<http://www.ebi.ac.uk/Tools/msa/clustalw2/>>
45. Foster, P.S., Hogan, S.P., Ramsay, A.J., Matthaei, K.I., and Young, I.G. (1996) Interleukin 5

- deficiency abolishes eosinophilia, airways hyperreactivity, and lung damage in a mouse asthma model, *J. Exp. Med.* 183, 195–201.
46. Franklin, I., Gromada, J., Gjinovci, A., Theander, A., and Wollheim, C.B. (2005) Beta-cell secretory products activate alpha-cell ATP-dependent potassium channels to inhibit glucagon release, *Diabetes* 54, 1808–1815.
 47. Franklin, R.B., Ma, J., Zou, J., Guan, Z., Kukoyi, B.I., Feng, P., and Costello, L.C. (2003) Human ZIP1 is a major zinc uptake transporter for the accumulation of zinc in prostate cells, *J Inorg Biochem* 96, 435–442.
 48. Frank Thévenod (2010) Catch me if you can! Novel aspects of cadmium transport in mammalian cells, *Biometals* 23(5), 857–875.
 49. Frederickson, C.J., Koh, J.Y., and Bush, A.I. (2005) The neurobiology of zinc in health and disease, *Nat. Rev. Neurosci.* 6, 449–462.
 50. F. Tahan and C. Karakukcu (2006) Zinc status in infantile wheezing, *Pediatr. Pulmonol.* 41, 630–634.
 51. Gaxiola, R.A., Fink, G.R., and Hirschi, K.D. (2002) Genetic manipulation of vacuolar proton pumps and transporters, *Plant Physiology* 129, 967–973.
 52. Giacconi, R., Cipriano, C., Muti, E., Costarelli, L., Maurizio, C., Saba, V., Gasparini, N., Malavolta, M., and Mocchegiani, E. (2005) Novel-209A/G MT2A polymorphism in old patients with type 2 diabetes and atherosclerosis: relationship with inflammation (IL-6) and zinc, *Biogerontology* 6, 407–413.
 53. Girijashanker, K., He, L., Soleimani, M., Reed, J.M., Li, H., Liu, Z., Wang, B., Dalton, T.P.,

- and Nebert, D.W. (2008) *Slc39a14* gene encodes ZIP14, a metal/bicarbonate symporter: similarities to the ZIP8 transporter, *Mol Pharmacol* 73, 1413–1423.
54. Grass, G., Fan, B., Rosen, B.P., Franke, S., Nies, D.H., and Rensing, C. (2001) ZitB, (YbgR), a member of the cation diffusion facilitator family, is an additional zinc transporter in *Escherichia coli*, *J. Bacteriol.* 183, 4664–4667.
55. Grass, G., Franke, S., Taudte, N., Nies, D. H., Kucharski, L. M., Maguire, M. E., and Rensing, C. (2005) The metal permease ZupT from *Escherichia coli* is a transporter with a broad substrate spectrum, *J Bacteriol.* 187(5), 1604–1611.
56. Grass, G., Otto, M., Fricke, B., Haney, C.J., Rensing, C., Nies, D.H., and Munkelt, D. (2005) FieF (YiiP) from *Escherichia coli* mediates decreased cellular accumulation of iron and relieves iron stress, *Arch. Microbiol.* 183, 9–18.
57. Grass, G., Wong, M. D., Rosen, B. P., Smith, R. L., and Rensing, C. (2002) ZupT is a Zn(II) uptake system in *Escherichia coli*, *J Bacteriol.* 184(3), 864–866.
58. Grotz, N., Fox, T., Connolly, E., Park, W., Guerinot, M.L., and Eide, D. (1998) Identification of a family of zinc transporter genes from *Arabidopsis* that respond to zinc deficiency, *Proceedings of the National Academy of Sciences, U.S.A.* 95, 7220–7224.
59. Hazlett, K.R., Rusnak, F., Kehres, D.G., Bearden, S.W., La Vake, C.J., La Vake, M.E., Maguire, M.E., Perry, R.D., and Radolf, J.D. (2003) The *Treponema pallidum* tro operon encodes a multiple metal transporter, a zinc-dependent transcriptional repressor, and a semi-autonomously expressed phosphoglycerate mutase, *J Biol Chem* 278, 20687–20694.
60. He, L., Girijashanker, K., Dalton, T.P., Reed, J., Li, H., Soleimani, M., and Nebert, D.W.

- (2006) ZIP8, member of the solute-carrier-39 (SLC39) metal-transporter family: characterization of transporter properties, *Mol Pharmacol* 70, 171–180.
61. He1, L., Wanga, B., Haya, E. B., and Nebert, D. W. (2009) Discovery of *ZIP* transporters that participate in cadmium damage to testis and kidney, *Toxicol Appl pharmacol* 238(3), 250–257.
62. Henriques, R., Jásik, J., Klein, M., Martinoia, E., Feller, U., Schell, J., Pais, M.S., and Koncz, C. (2002) Knock-out of *Arabidopsis* metal transporter gene IRT1 results in iron deficiency accompanied by cell differentiation defects, *Plant Molecular Biology* 50, 587–597.
63. H. Haase and W. Maret (2005) Protein tyrosine phosphatases as targets of the combined insulinomimetic effects of zinc and oxidants, *Biometals* 18, 333–338.
64. H. Haase and W. Maret (2005) Fluctuations of cellular, available zinc modulate insulin signaling via inhibition of protein tyrosine phosphatases, *J. Trace Elem. Med. Biol.* 19, 37–42.
65. H. Marschner (1995) Mineral nutrition of higher plants, 2nd edn, London: Academic Press.
66. Ho, E., Quan, N., Tsai, Y.H., Lai, W., and Bray, T.M. (2001) Dietary zinc supplementation inhibits NFkappaB activation and protects against chemically induced diabetes in CD1 mice, *Exp. Biol. Med.* (Maywood) 226, 103–111.
67. Hsiao, K., Chapman, P., Nilsen, S., Eckman, C., Harigaya, Y., Younkin, S., Yang, F., and Cole, G. (1996) Correlative memory deficits, Abeta elevation, and amyloid plaques in transgenic mice, *Science* 274, 99–102.
68. <<http://www.ncbi.nlm.nih.gov>>

69. Huang, L., Kirschke, C.P., and Gitschier, J. (2002) Functional characterization of a novel mammalian zinc transporter, ZnT6, *J Biol Chem* 277, 26389–26395.
70. Huang, L., Kirschke, C.P., Zhang, Y., and Yu, Y.Y. (2005) The ZIP7 gene (*Slc39a7*) encodes a zinc transporter involved in zinc homeostasis of the Golgi apparatus, *J Biol Chem* 280, 15456–15463.
71. H. Zhao and D. Eide (1996) The ZRT2 Gene Encodes the Low Affinity Zinc Transporter in *Saccharomyces cerevisiae*, *J. Biol. Chem.* 271, 23203–23210.
72. H. Zhao and D. Eide (1996) The yeast ZRT1 gene encodes the zinc transporter protein of a high-affinity uptake system induced by zinc limitation, *Proc. Natl. Acad. Sci. U.S.A.* 93, 2454–2458.
73. I.E. Dreosti (1993) Recommended dietary intakes of iron, zinc, and other inorganic nutrients and their chemical form and bioavailability, *Nutrition* 9, 542–545.
74. Inoue, K., Takano, H., Yanagisawa, R., Sakurai, M., Ichinose, T., Sadakane, K., Hiyoshi, K., Sato, M., Shimada, A., Inoue, M., and Yoshikawa, T. (2005) Role of metallothionein in antigen-related airway inflammation, *Exp. Biol. Med. (Maywood)* 230, 75–81.
75. Ishihara, H., Maechler, P., Gjinovci, A., Herrera, P.L., and Wollheim, C.B. (2003) Islet beta-cell secretion determines glucagon release from neighbouring alpha-cells, *Nat. Cell Biol.* 5, 330–335.
76. Ishihara, K., Yamazaki, T., Ishida, Y., Suzuki, T., Oda, K., Nagao, M., Yamaguchi-Iwai, Y., and Kambe, T. (2006) Zinc transport complexes contribute to the homeostatic maintenance of secretory pathway function in vertebrate cells, *J. Biol. Chem.* 281, 17743–17750.

77. J. da Silva Jr. and R.J.P. Williams (1991) *The Biological Chemistry of the Elements: The Inorganic Chemistry of Life*, Oxford, Clarendon Press.
78. J.E. Arsenault and K.H. Brown (2003) Zinc intake of US preschool children exceeds new dietary reference intakes, *Am. J. Clin. Nutr.* 78, 1011–1017.
79. J. L. Hall and Lorraine E. Williams (2003) Transition metal transporters in plants, *J. Exp. Bot.* 54 (393), 2601–2613.
80. J.P. Claverys (2001) A new family of high-affinity ABC manganese and zinc permeases, *Res. Microbiol.* 152, 231–243.
81. J.P. Liuzzi and R.J. Cousins (2004) Mammalian zinc transporters, *Annu. Rev. Nutr.* 24, 151–172.
82. Kambe, T., Narita, H., Yamaguchi-Iwai, Y., Hirose, J., Amano, T., Sugiura, N., and Sasaki, R., et al. (2002) Cloning and characterization of a novel mammalian zinc transporter, zinc transporter 5, abundantly expressed in pancreatic β cells, *J Biol Chem* 277, 19049–19055.
83. Karlinsey, J. E., Maguire, M. E., Becker, L. A., Crouch, M.-L. V. and Fang, F. C. (2010) The phage shock protein PspA facilitates divalent metal transport and is required for virulence of *Salmonella enterica* sv. Typhimurium, *Molecular Microbiology* (78), 669–685.
84. K. Hantke (2005) Bacterial zinc uptake and regulators, *Curr. Opin. Microbiol.* 8, 196–202.
85. Kim, B.J., Kim, Y.H., Kim, S., Kim, J.W., Koh, J.Y., Oh, S.H., Lee, M.K., Kim, K.W., and Lee, M.S. (2000) Zinc as a paracrine effector in pancreatic islet cell death, *Diabetes* 49, 367–372.
86. Kim, S., Watanabe, K., Shirahata, T., and Watarai, M. (2004) Zinc uptake system (*znuA* locus) of *Brucella abortus* is essential for intracellular survival and virulence in mice, *J*

- Vet Med Sci 66, 1059–1063.
87. Kitamura, H., Morikawa, H., Kamon, H., Iguchi, M., Hojyo, S., Fukada, T., Yamashita, S., Kaisho, T., Akira, S., and Murakami, M., et al. (2006) Toll-like receptor-mediated regulation of zinc homeostasis influences dendritic cell function, *Nat Immunol* 7, 971–977.
 88. K.J. Waldron and N.J. Robinson (2009) How do bacterial cells ensure that metalloproteins get the correct metal? *Nat Rev Microbiol* 7, 25–35.
 89. Koh, J.Y., Suh, S.W., Gwag, B.J., He, Y.Y., Hsu, C.Y., and Choi, D.W. (1996) The role of zinc in selective neuronal death after transient global cerebral ischemia, *Science* 272, 1013–1016.
 90. Korshunova, Y. O., Eide, D., Clark, W. G., Guerinot, M. L., and Pakrasi, H. B. (1999) The IRT1 protein from *Arabidopsis thaliana* is a metal transporter with broad specificity, *Plant Molecular Biology* 40, 37–44.
 91. Krishna, S. S., Majumdar, I., and Grishin, N. V. (2003) *Nucleic Acids Res.* 31, 532–550.
 92. Kristiansen, L.H., Rungby, J., Sondergaard, L.G., Stoltenberg, M., and Danscher, G. (2001) Autometallography allows ultrastructural monitoring of Zinc in the endocrine pancreas, *Histochem. Cell Biol.* 115, 125–129.
 93. L.A. Gaither and D.J. Eide (2001) Eukaryotic zinc transporters and their regulation, *Biometals* 14, 251–270.
 94. L.A. Gaither and D.J. Eide (2000) Functional expression of the human hZIP2 zinc transporter, *J. Biol. Chem.* 275, 5560–5564.
 95. L.A. Gaither and D.J. Eide (2001) The human ZIP1 transporter mediates zinc uptake in

- human K562 erythroleukemia cells, *J Biol. Chem.* 276, 22258–22264.
96. Lang, C.J., Murgia, C., Leong, M., Tan, L.W., Perozzi, G., Knight, D., Ruffin, R.E., and Zalewski, P.E. (2006) Anti-inflammatory effects of zinc and alterations in zinc transporter mRNA in mouse models of allergic inflammation, *Am. J. Physiol. Lung Cell Mol. Physiol.*
97. Langmade, S. J., Ravindra, R., Daniels, P. J., and Andrews, G. K. (2000) The Transcription Factor MTF-1 Mediates Metal Regulation of the Mouse ZnT1 Gene, *J. Biol. Chem.* 275, 34803–34809.
98. Lawrence, M.C., Pilling, P.A., Epa, V.C., Berry, A.M., Ogunniyi, A.D., and Paton, J.C. (1998) The crystal structure of pneumococcal surface antigen PsaA reveals a metal-binding site and a novel structure for a putative ABC-type binding protein, *Structure* 6, 1553–1561.
99. Lee, J.Y., Cole, T.B., Palmiter, R.D., Suh, S.W., and Koh, J.Y. (2002) Contribution by synaptic zinc to the gender-disparate plaque formation in human Swedish mutant APP transgenic mice, *Proc. Natl. Acad. Sci. U.S.A.* 99, 7705–7710.
100. Lee, J.Y., Kim, J.H., Hong, S.H., Cherny, R.A., Bush, A.I., Palmiter, R.D., and Koh, J.Y. (2004) Estrogen decreases zinc transporter 3 expression and synaptic vesicle zinc levels in mouse brain, *J. Biol. Chem.* 279, 8602–8607.
101. Lee, Y.H., Dorwart, M.R., Hazlett, K.R., Deka, R.K., Norgard, M.V., Radolf, J.D., and Hasemann, C.A. (2002) The crystal structure of Zn(II)-free *Treponema pallidum* TroA, a periplasmic metal-binding protein, reveals a closed conformation, *J Bacteriol* 184, 2300–2304.

102. Leung, K. W., Liu, M., Xu, X., Seiler, M. J., Barnstable, C. J., and Tombran-Tink, J.
Expression of ZnT and ZIP Zinc Transporters in the Human RPE and Their Regulation
by Neurotrophic Factors, *Invest Ophthalmol Vis Sci.* 49(3), 1221–1231.
103. Lewis, D.A., Klesney-Tait, J., Lumbley, S.R., Ward, C.K., Latimer, J.L., Ison, C.A., and
Hansen, E.J. (1999) Identification of the *znuA*-encoded periplasmic zinc transport protein
of *Haemophilus ducreyi*, *Infect Immun* 67, 5060–5068.
104. L. Huang and J. Gitschier (1997) A novel gene involved in zinc transport is deficient in the
lethal milk mouse, *Nat Genet* 17, 292–297.
105. Lioumi, M., Ferguson, C.A., Sharpe, P.T., Freeman, T., Marenholz, I., Mischke, D.,
Heizmann, C., and Ragoussis, J. (1999) Isolation and characterization of human and
mouse ZIRT1, a member of the IRT1 family of transporters, mapping within the
epidermal differentiation complex, *Genomics* 62, 272–280.
106. Liu, J., Stemmler, A. J., Fatima, J., and Mitra, B. (2005) Metal-binding characteristics of the
amino-terminal domain of ZntA: binding of lead is different compared to cadmium and
zinc, *Biochemistry* 44, 5159–5167.
107. Liu, Z., Li, H., Soleimani, M., Girijashanker, K., Reed, J.M., He, L., Dalton, T.P., and
Nebert, D.W. (2008) Cd^{2+} versus Zn^{2+} uptake by the ZIP8 HCO_3^- -dependent symporter:
kinetics, electrogenicity and trafficking, *Biochem Biophys Res Commun* 365, 814–820.
108. Liuzzi, J. P., Blanchard, R. K., and Cousins, R. J. (2001) Differential regulation of zinc
transporter 1, 2, and 4 mRNA expression by dietary zinc in rats, *J. Nutr.* 131, 46–52.
109. Liuzzi, J. P., Lichten, L. A., Rivera, S., Blanchard, R. K., Aydemir, T. B., Knutson, M. D.,
Ganz, T., and Cousins, R. J. (2005) Interleukin-6 regulates the zinc transporter Zip14 in

- liver and contributes to the hypozincemia of the acute-phase response, Proc. Natl. Acad. Sci. U.S.A. 102, 6843–6848.
110. Lombi, E., Tearall, K.L., Howarth, J.R., Zhao, F.-J., Hawkesford, M.J., and McGrath, S.P. (2002) Influence of iron status on cadmium and zinc uptake by different ecotypes of the hyperaccumulator *Thlaspi caerulescens*, Plant Physiology 128, 1359–1367.
111. L. Rink and H. Haase (2007) Zinc homeostasis and immunity, Trends Immunol. 28, 1–4.
112. MacDiarmid, C.W., Gaither, L.A., and Eide, D.J. (2000) Zinc transporters that regulate vacuolar zinc storage in *Saccharomyces cerevisiae*, EMBO Journal 19, 2845–2955.
113. Mäser, P., Thomine, S., and Schroeder, J.I., *et al.* (2001) Phylogenetic relationships within cation transporter families of *Arabidopsis*, Plant Physiology 126, 1646–1667.
114. Milon, B., Wu, Q., Zou, J., Costello, L.C., and Franklin, R.B. (2006) Histidine residues in the region between transmembrane domains III and IV of hZip1 are required for zinc transport across the plasma membrane in PC-3 cells, Biochim Biophys Acta 1758, 1696–1701.
115. M.L. Guerinot (2000) The ZIP family of metal transporters, Biochimica et Biophysica Acta 1465, 190–198.
116. M. Murakami and T. Hirano (2008) Intracellular zinc homeostasis and zinc signaling, Cancer Sci 99, 1515–1522.
117. Moreau, S., Thomson, R.M., Kaiser, B.N., Trevaskis, B., Guerinot, M.L., Udvardi, M.K., Puppo, A., and Day, D.A. (2002) GmZIP1 encodes a symbiosis-specific zinc transporter in soybean, Journal of Biological Chemistry 277, 4738–4746.
118. Murgia, C., Lang, C.J., Truong-Tran, A.Q., Grosser, D., Jayaram, L., Ruffin, R.E., Perozzi,

- G., and Zalewski, P.D. (2006) Zinc and its specific transporters as potential targets in airway disease, *Curr. Drug Targets* 7, 607–627.
119. Nadine Taudte and Gregor Grass (2010) Point mutations change specificity and kinetics of metal uptake by ZupT from *Escherichia coli*, *Biometals* 23(4), 643–656.
120. N. Grotz and M.L. Guerinot (2002) Limiting nutrients: an old problem with new solutions? *Current Opinion in Plant Biology* 5, 158–163.
121. Palmiter, R.D., Cole, T.B., and Findley, S.D. (1996) ZnT-2, a mammalian protein that confers resistance to zinc by facilitating vesicular sequestration, *EMBO J* 15, 1784–1791.
122. Palmiter, R.D., Cole, T.B., Quaife, C.J., and Findley, S.D. (1996) ZnT-3, a putative transporter of zinc into synaptic vesicles, *Proc Natl Acad Sci U.S.A.* 93, 14934–14939.
123. Pence, N.S., Larsen, P.B., Ebbs, S.D., Letham, D.L.D., Lasat, M.M., Garvin, D.F., Eide, D., and Kochian, L.V. (2000) The molecular physiology of heavy metal transport in the Zn Cd hyperaccumulator *Thlaspi caerulescens*, *Proceedings of the National Academy of Sciences, U.S.A.* 97, 4956–4960.
124. R. Balasubramanian and A.C. Rosenzweig (2008) Copper methanobactin: a molecule whose time has come, *Curr Opin Chem Biol* 12, 245–249.
125. R.D. Palmiter and L. Huang (2004) Efflux and compartmentalization of zinc by members of the SLC30 family of solute carriers, *Pflugers Arch.* 447, 744–751.
126. R.D. Palmiter (2004) Protection against zinc toxicity by metallothionein and zinc transporter 1, *Proc Natl Acad Sci USA* 101, 4918–4923.
127. Rensing, C., Mitra, B., and Rosen, B.P. (1997) The *zntA* gene of *Escherichia coli* encodes a Zn(II)-translocating P-type ATPase, *Proc. Natl. Acad. Sci. USA* 94, 14326–14331.

128. Ritchie, C.W., Bush, A.I., Mackinnon, A., Macfarlane, S., Mastwyk, M., MacGregor, L., Kiers, L., Cherny, R., Li, Q.X., Tammer, A., Carrington, D., Mavros, C., Volitakis, I., Xilinas, M., Ames, D., Davis, S., Beyreuther, K., Tanzi, R.E., and Masters, C.L. (2003) Metal-protein attenuation with iodochlorhydroxyquin (clioquinol) targeting Abeta amyloid deposition and toxicity in Alzheimer disease: a pilot phase 2 clinical trial, Arch. Neurol. 60, 1685–1691.
129. Rogers, E. E., Eide, D. J., and Gueriot, M. L. (2000) Altered selectivity in an *Arabidopsis* metal transporter. Proceedings of the National Academy of Sciences, U.S.A. 97, 12356–12360.
130. Sabri, M., Houle, S., and Dozois, C. M. (2009) Roles of the extraintestinal pathogenic *Escherichia coli* ZnuACB and ZupT zinc transporters during urinary tract infection, Infect Immun. 77(3), 1155–1164.
131. S.L. Bao and D.L. Knoell (2006) Zinc modulates cytokine-induced lung epithelial cell barrier permeability, Am. J. Physiol. Lung Cell Mol. Physiol.
132. S.I. Patzer and K. Hantke (1998) The ZnuABC high-affinity zinc uptake system and its regulator Zur in *Escherichia coli*, Mol. Microbiol. 28, 1199–1210.
133. Sivashanmugam, A., Murray, V., Cui, C., Zhang, Y., Wang, J., and Li, Q. (2009) Practical protocols for production of very high yields of recombinant proteins using *Escherichia coli*, Protein Science 18, 936–948.
134. S.L. Kelleher and B. Lonnerdal (2005) Zip3 plays a major role in zinc uptake into mammary epithelial cells and is regulated by prolactin, Am J Physiol Cell Physiol 288, C1042–1047.

135. Soutar, A., Seaton, A., and Brown, K. (1997) Bronchial reactivity and dietary antioxidants, *Thorax* 52, 166–170.
136. Taylor, K.M., Morgan, H.E., Johnson, A., and Nicholson, R.I. (2004) Structure-function analysis of HKE4, a member of the new LIV-1 subfamily of zinc transporters, *Biochem J* 377, 131–139.
137. Taylor, K.M., Morgan, H.E., Johnson, A., Hadley, L.J., and Nicholson, R.I. (2003) Structure-function analysis of LIV-1, the breast cancer-associated protein that belongs to a new subfamily of zinc transporters, *Biochem J* 375, 51–59.
138. T.C. Fox and M.L. Guerinot (1998) Molecular biology of cation transport in plants, *Annual Review of Plant Physiology and Plant Molecular Biology* 49, 669–696.
139. Terres-Martos, C., Navarro-Alarcon, M., Martin-Lagos, F., Lopez, G.d.l.S.H., Perez-Valero, V., and Lopez-Martinez, M.C. (1998) Serum zinc and copper concentrations and Cu/Zn ratios in patients with hepatopathies or diabetes, *J. Trace Elem. Med. Biol.* 12, 44–49.
140. Thomas E. Kehl-Fiea and Eric P. Skaara (2010) Nutritional immunity beyond iron: a role for manganese and zinc, *Current Opinion in Chemical Biology* 14(2), 218–224.
141. Tonder, N., Johansen, F.F., Frederickson, C.J., Zimmer, J., and Diemer, N.H. (1990) Possible role of zinc in the selective degeneration of dentate hilar neurons after cerebral ischemia in the adult rat, *Neurosci. Lett.* 109, 247–252.
142. Truong-Tran, A.Q., Ruffin, R.E., and Zalewski, P.D. (2000) Visualization of labile zinc and its role in apoptosis of primary airway epithelial cells and cell lines, *Am. J. Physiol.* 279, L1172–L1183.
143. Truong-Tran, A.Q., Ruffin, R.E., Foster, P.S., Koskinen, A.M., Coyle, P., Philcox, J.C.,

- Rofe, A.M., and Zalewski, P.D. (2002) Altered zinc homeostasis and caspase-3 activity in murine allergic airway inflammation, *Am. J. Respir. Cell Mol. Biol.* 27, 286–296.
144. U.E. Schaible and S.H. Kaufmann (2004) Iron and microbial infection, *Nat Rev Microbiol* 2, 946–953.
145. Vallee, B. L., and D. S. Auld (1990) Zinc coordination, function, and structure of zinc enzymes and other proteins, *Biochemistry* 29, 5647–5659.
146. Van Eerdewegh, P., Little, R.D., Dupuis, J., Del Mastro, R.G., Falls, K., Simon, J., Torrey, D., Pandit, S., McKenny, J., Braunschweiger, K., Walsh, A., Liu, Z., Hayward, B., Folz, C., Manning, S.P., Bawa, A., Saracino, L., Thackston, M., Benchekroun, Y., Capparell, N., Wang, M., Adair, R., Feng, Y., Dubois, J., FitzGerald, M.G., Huang, H., Gibson, R., Allen, K.M. Pedan, A., Danzig, M.R., Umland, S.P., Egan, R.W., Cuss, F.M., Rorke, S., Clough, J.B., Holloway, J.W., Holgate, S.T., and Keith, T.P. (2002) Association of the ADAM33 gene with asthma and bronchial hyperresponsiveness, *Nature* 418, 426–430.
147. Van Ho, A., Ward, D.M., and Kaplan, J. (2002) Transition metal transport in yeast, *Annual Review of Microbiology* 56, 237–261.
148. Varotto, C., Maiwald, D., Pesaresi, P., Jahns, P., Salamini, F., and Leister, D. (2002) The metal ion transporter IRT1 is necessary for iron homeostasis and efficient photosynthesis in *Arabidopsis thaliana*, *The Plant Journal* 31, 589–599.
149. Vert, G., Briatt, J.-F., and Curie, C. (2001) *Arabidopsis* IRT2 gene encodes a root periphery iron transporter, *The Plant Journal* 26, 181–189.
150. Vert, G., Grotz, N., Dédaldéchamp, F., Gaymard, F., Guerinot, M.L., Briat, J.-F., and Curie, C. (2002) IRT1, an *Arabidopsis* transporter essential for iron uptake from the soil and for

- plant growth, *The Plant Cell* 14, 1223–1233.
151. Wang, F., Kim, B.E., Petris, M.J., and Eide, D.J. (2004) The mammalian Zip5 protein is a zinc transporter that localizes to the basolateral surface of polarized cells, *J Biol Chem* 279, 51433–51441.
 152. Wang, K., Zhou, B., Kuo, Y.M., Zemansky, J., and Gitschier, J. (2002) A novel member of a zinc transporter family is defective in acrodermatitis enteropathica, *Am J Hum Genet* 71, 66–73.
 153. Wang, Y.-H., Garvin, D.F., and Kochian, L.V. (2002) Rapid induction of regulatory and transporter genes in response to phosphorus, potassium, and iron deficiencies in tomato roots. Evidence for cross talk and root/rhizosphere-mediated signals, *Plant Physiology* 130, 1361–1370.
 154. Weston, B.F., Brenot, A., and Caparon, M.G. (2009) The metal homeostasis protein, Lsp, of *Streptococcus pyogenes* is necessary for acquisition of zinc and virulence, *Infect Immun* 77, 2840–2848.
 155. Williams, L.E., Pittman, J.K., and Hall, J.L. (2000) Emerging mechanisms for heavy metal transport in plants, *Biochimica et Biophysica Acta* 1465, 104–126.
 156. Wintergerst, E.S., Maggini, S., and Hornig, D.H. (2007) Contribution of selected vitamins and trace elements to immune function, *Ann Nutr Metab* 51, 301–323.
 157. W. Maret and H.H. Sandstead (2006) Zinc requirements and the risks and benefits of zinc supplementation, *J. Trace Elem. Med. Biol.* 20, 3–18.
 158. Yu, Y. Y., Kirschke, C. P., and Huang, L. (2006) Immunohistochemical analysis of ZnT1, 4, 5, 6, and 7 in the mouse gastrointestinal tract, *Journal of Histochemistry and*

- Cytochemistry 55(3), 223–234.
159. Zalewski, P.D., Millard, S.H., Forbes, I.J., Kapaniris, O., Slavotinek, A., Betts, W.H., Ward, A.D., Lincoln, S.F., and Mahadevan, I. (1994) Video image analysis of labile zinc in viable pancreatic islet cells using a specific fluorescent probe for zinc, J. Histochem. Cytochem. 42, 877–884.
160. Zalewski, P.D., Truong-Tran, A.Q., Grosser, D., Jayaram, L., Murgia, C., and Ruffin, R.E. (2005) Zinc metabolism in airway epithelium and airway inflammation: basic mechanisms and clinical targets, A review, Pharmacol. Ther. 105, 127–149.

ABSTRACT**THE ROLE OF ZIP SUPERFAMILY OF METAL TRANSPORTERS
IN CHRONIC DISEASES,
PURIFICATION & CHARACTERIZATION
OF ITS MEMBER:
ZUPT**

by

IRYNA KING**May 2011****Advisor:** Dr. Bharati Mitra**Major:** Biochemistry and Molecular Biology**Degree:** Master of Science

In mammals zinc is the second most abundant essential trace metal. Since Zn^{2+} is a small, hydrophilic, and a highly charged ion, it cannot be transported across the plasma or intracellular organelle membrane by passive diffusion. Different types of cells require a different constant concentration of zinc at all times. Presence of excess free Zn ions can be toxic to the cell. All cells must have tightly regulated homeostatic mechanisms in order to preserve healthy levels and proper compartmentalization of zinc. This is accomplished through the actions of specialized proteins that facilitate zinc uptake, efflux and compartmentalization. If the integrity of genes responsible for maintenance of zinc homeostasis is compromised by mutations or polymorphisms, this will likely result in complex genetic variations and even sensitivity to dietary zinc in health and disease.

In *E.coli*, the uptake of zinc is mediated by two major types of transporters: *ZnuACB*, which belongs to the cluster C9 family of (TroA-like) ATP-binding cassette (ABC) transporters,

and ZupT, which is a member of the ZRT/IRT-related proteins (*ZIP*) family of transporters. *ZIPs* are expressed amongst different organisms in order to maintain their metal homeostasis and thus contribute greatly to their growth and development. *ZIPs* have also been found to play key roles in bacterial infections, as well as the onset and progression of chronic diseases in humans.

In comparison with mammalian cells, *E.coli*'s lack of complex organelles, and ease of genetic analysis, allows for direct analysis of the protein's role in metal transport. In this study *E.coli*'s ZupT was purified and characterized, and its expression was optimized with double-selection method. The binding specificity for ZupT with Cd^{2+} , Fe^{2+} , Pb^{2+} , and Zn^{2+} were evaluated with fluorescence spectroscopy. Furthermore, UV-Visible spectroscopy was used to further explore the binding of ZupT with Fe^{2+} . The binding stoichiometry between ZupT and Cd^{2+} , Pb^{2+} , and Zn^{2+} were determined utilizing ICP-MS (inductively coupled mass spectrometry) analysis. Finally, based on the results of sequence analysis of ZupT, four mutants were successfully created within transmembrane (TM) regions IV and V, which have been shown in other *ZIP* family members to be crucial for metal binding.

AUTOBIOGRAPHICAL STATEMENT

I was born in Lviv, Ukraine. I was raised there until I was 14, at which point I moved with my family to Michigan, United States. I completed my undergraduate studies at the University of Michigan-Flint, following which I was employed by the American Red Cross Detroit-NTL. My mother was an aerophoto geodesist, at the Lviv Polytechnic National University, and my father was a reanimatologist at the Danylo Halytsky Lviv National Medical Academy.

EDUCATION

M.S., Biochemistry & Molecular Biology, Wayne State University School of Medicine, Detroit, Michigan (2011)

B.S., Molecular Biology/Biotechnology, University of Michigan-Flint, Flint, Michigan (2007)

AFFILIATIONS

Member of the American Society for Clinical Pathology, Molecular Biology (2010-2011)

PUBLICATIONS

Yong Yang, Deborah Cochran, Mary D. Gargano, **Iryna King**, Benjamin P. Burger, Nayef K. Samhat, Katherine R. Sabourin, Yuqing Hou, Junya Awata, David A.D. Parry, Wallace F. Marshall, George B. Witman and Xiangyi Lu (2011) Regulation of flagellar motility by the conserved flagellar protein CG34110/Ccdc135/FAP50, Molecular Biology of the Cell. (Manuscript under revision)